Molecular Design and Self-assembly of Polydiacetylene for Biosensors and Sensor
Arrays

by

Ji Seok Lee

A dissertation submitted in partial fulfillment
of the requirements for the degree of
Doctor of Philosophy
(Macromolecular Science and Engineering)
in The University of Michigan
2011

Doctoral Committee:

    Professor Jinsang Kim, Chair
    Professor L. Jay Guo
    Professor Kenichi Kuroda
    Professor David C. Martin

ACKNOWLEDGMENTS

enjoyable. Lastly, but most importantly, I thank my family. Seongsoo Jung, my precious wife, made my life as a real one. I could not have accomplished all of my works without her sacrifice. Also I thanks to my lovely son. He encouraged me and we are expecting to meet him on August 2011. Kyungrae Shin, my mother, and Myunggoon Lee, my farther, have always supported and prayed for me with great care. Their great support helped me to focus on my research. I thank God that I could have such a great opportunity to live with my precious people.

TABLE OF CONTENTS

LIST OF SCHEMES

Scheme

LIST OF FIGURES

Figure

LIST OF TABLES

Table

CHAPTER 1

Introduction

1.1 Motivation of biosensor development

Chemo/Biosensors are defined in different ways, but all of the definitions recognize that any chemo/biosensor involves a sensor and an *analyte* or chemical that is defined in an analytical procedure. Chemo/biosensors are analytical tools for the analysis of bio-material samples. They are used to gain an understanding of bio-composition, structure and function by converting a biological response into a signal. Chemo/bio sensors can be divided into several types according to their detection mode such as electrochemical, optical, mass sensitive and thermal. Recent mainstream research has been conducted by using bioNMES[1], quantum dots[2], nanoparticles[3], nanocantilevers, nanowires and nanotubes.[4] Biosensor research has provided a lot of additional studies including those of biomolecule interactions, drug development, crime investigation, quality control in food factories, home medical diagnostics etc. The global market size of biosensors has expanded to more than $10 billion and it is believed that the market is forecasted to reach $12 billion by the year 2015. Therefore, there have been increasing needs of rapid, cheap and low tech biomedical diagnostics that can be carried by technicians or patients. The most well-known biosensor is a glucose-based sensor which was invented by Clark in 1962 and conveniently used by diabetic patients to monitor blood glucose at home. Rapid analysis is possible from just single drop of blood.

The fundamental requirement of a biosensor is good linearity, sensitivity, selectivity and response time. First, linearity of a sensor device should be high to easily

quantify the target amount. Second, sensitivity must be high enough to detect a slight change from the physiological condition and a trace amount of analyte. Third, interference of other chemicals should be minimized to achieve highly selective and guaranteed results. Finally the response time should short for fast detection. A lot of protocols and materials have been investigated to realize an efficient chemo/biosensor system. Nanotechnology has enabled us to design chemo/biosensor systems that are much smaller, more energy efficient and more sensitive than typical micro or macro chemo/biosensors. Nanomaterials such as carbon nanotubes, nanoparticles, nanorods, nanowires and quantum dots have been used to make electrochemical sensors. Furthermore BioNano/Micro-Electro-Mechanical Systems (N/MEMS)[1], lab-on-Chip[5] systems, microfluidic systems[6], and micro-array based sensor fabrication methods have been competitively developed and applied to real clinical use. However, most approaches of nano-technology based sensor development require delicate control from well-trained persons and are commonly not suitable for cheap and low tech chemo/biosensor system development. In this regard, conjugated polymer-based chemo/biosensor systems are very attractive because of their easy signal analysis; most conjugated polymers have very unique optical properties such as color transitions and also fluorescence emission change upon external stimuli.[7]

Polydiacetylenes (PDAs), among conjugated polymers, have many advantages as a sensor material by their easy preparation and the fabrication feasibility of sensor device.[8] Also PDA based sensor systems can provide dual signals through optical color transitions and fluorescence emission. Furthermore PDA liposomes consist of bi-layered lipid-like membranes, and the structural study of PDA membranes with target materials will provide a decent analogue to build understanding the cell membrane interactions with biological target materials. During the past decade, variety of studies for PDA sensory systems was carried by many research groups. Many researchers have developed, through their research efforts, newer PDA biosensor systems that can provide highly

2

accurate, sensitive, rapid and convenient detection. The advantages of easy preparation protocols and the superior dual signaling properties of PDA molecules resulted in growing attention to PDA based biosensor development. In this thesis work we established a molecular design principle of highly sensitive and selective PDA sensory molecules and identified important intra- and intermolecular mechanisms for sensitive colorimetric signal production. We also developed an efficient protocol for a rapid and convenient PDA sensor device fabrication.

1.2 Conjugated Polymer

Polymers containing alternating saturated/unsaturated bond and delocalized π-electrons through their backbones, often referred as a conjugated polymer (CP) or conducting polymers. Conjugated polymers are very unique polymers because they have a backbone with an extended π-conjugated system. Their extended π-bonds contain continuous delocalized electrons which gives rise to the unique optical and electronic properties. As a result these electro-active polymers are used in a variety of applications including field-effect transistors, polymer actuators, light-emitting materials, sensors and solar cells. The practical value of conjugated polymers was recognized by Nobel Prize in chemistry in 2000. Numerous CPs have been investigated and some examples of typical CPs are represented in Figure 1.1. Conjugated polymer (CP) systems are very attractive in a sensor design because their absorption and emission properties are very sensitive to environmental perturbations.[7, 9] CPs-based sensor systems typically compared to conventional small molecular sensors systems by their potentials for signal amplification when subjected to external stimuli.[10] Accordignly, a variety of conjugated polymers such as polythiophenes,[11] polyanilines,[12] poly(phenylene ethynylenes),[13] polyacetylenes,[14] and polydiacetylenes,[15] have been studied as sensor matrices.

3

Unsubstituted CPs are mostly insoluble in aqueous solutions. However, biological targets exist in aqueous solutions in many cases. For this reason, conjugated polyelectrolytes (CPEs) have been designed with water-soluble side chains on the polymer backbone to improve their solubility in aqueous solutions. As a water-soluble side chain, sulfonate (SO_3^-), carboxylic acid (COOH), phosphate (PO_4^{3-}), and ethylene oxide have been commonly used to increase the water solubility and avoid aggregation of CPEs in aqueous solution. The addition of side chains also alters the electronic and other physical properties of the polymer besides solubility. Therefore, a CPE should be carefully designed and developed to have desired optimum physical properties. However, this is not an easy task.

Polyaniline   Polypyrrole   Polythiophene   Polyacetylene

Poly(p-phenylene vinylene)s   Poly(p-phenylene ethynylene)s   Polydiacetylene
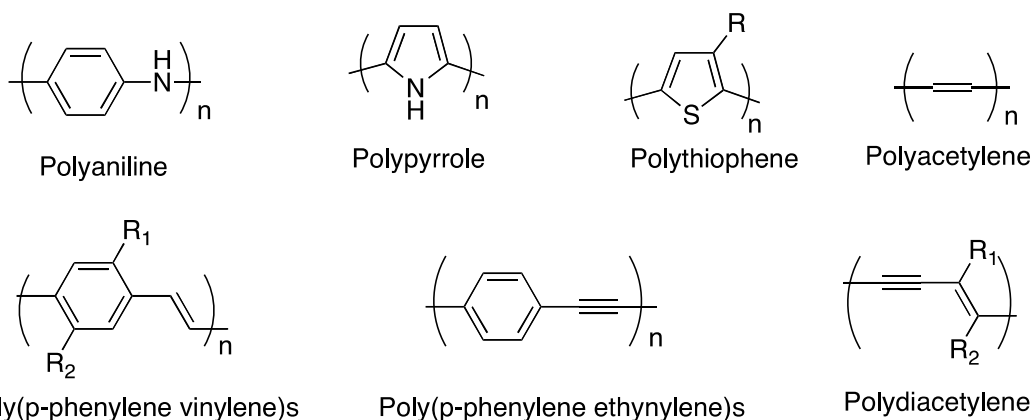
Figure 1.1. Chemical structure of various conjugated polymers.

1.3 Polydiacetylene Polymer

Among CPs, polydiacetylene (PDA) is one of the most attractive CPs for biosensor application because PDA can be conveniently prepared by photopolymerization after self-assembly of diacetylene molecules. When diacetylene molecules are properly ordered to form crystalline structures they undergo photo-polymerization via a 1,4-addition reaction to form an ene-yne conjugated back-bone upon exposure to 254 nm light. In addition, PDAs generally consisted of amphiphilic lipid

monomer showing good dispersion property in aqueous solution. Accordingly, PDA molecules can be easily prepared in forms of liposomes in aqueous solutions through colloidal dispersion,[16] solid film by means of Langmuir-Blodgett (LB)/Langmuir-Schaefer (LS) method[17] and immobilized liposomes on solid substrates thorugh chemical reaction,[18] or embedded liposomes in polymer matrices.[19] Therefore, multiple steps of synthetic chemistry and molecular design for water-solubility are not necessary.

PDAs have interesting optical properties including a color transition and red fluorescence emission that enable their application in sensor devices.[8] PDA typically shows blue color when they are photo-polymerized. Interestingly, PDAs change their optical color from blue to red when they are exposed to a variety of environmental perturbations due to the induced backbone twisting. This phenomenon is named as mechanochromism, a very attractive self-signaling property for sensor applications. PDA based sensor systems have been studied a lot in the form of PDA films and liposomes functionalized with specific probe molecules. Those PDA sensors have proven to be effective as selective and sensitive biosensors for the detection of biological targets such as the cholera toxin and *E. Coli.*.[20] Colorimetric detection of glucose, selective detection of metal ions,[21] ligands,[22] and antigen detection based on specific antibody-antigen interactions also have been successfully developed.[23]

1.4 Self-assembly of Diacetylene Molecules

Self-assembled PDAs have been prepared in a variety of forms through Langmuir-Blodgett (LB)/ Langmuir-Schaefer (LS) methods, layer-by-layer thin films, and colloidal dispersion and assembly of liposomes.
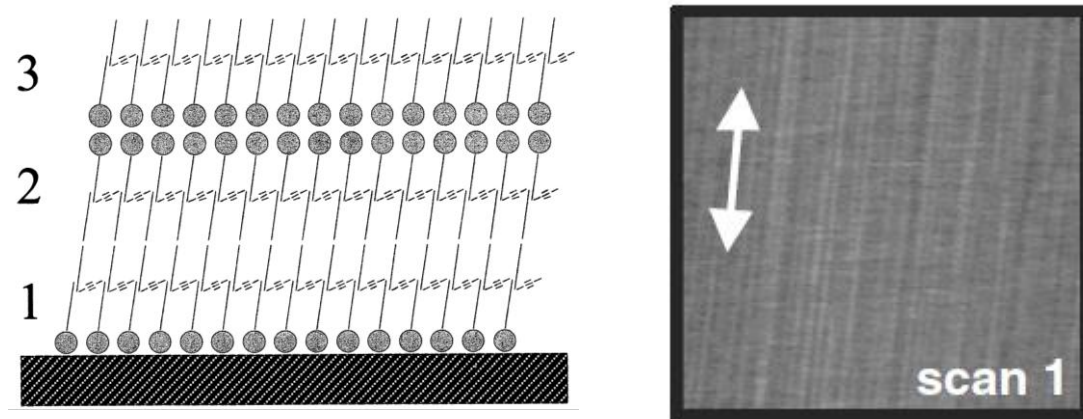
Figure 1.2. a) Illustration of the trilayer stacking of PCDA molecules. The circles represent the COOH headgroups which are expected to hydrogen bond to the silicon substrate (silicon−layer 1 interface) or with each other (layer 2−layer 3 interface).[17b] The polymer backbones (thick lines), which lie parallel to the surface, are aligned in all three layers within a given domain of the film. b) Topographic AFM images of blue PCDA showing the progressive growth of the tip-induced red domains. Striations indicative of the polymer backbone direction are observed.[24]

1.4.1 Langmuir-Blodgett (LB)/ Langmuir-Schaefer (LS) Method

A Langmuir–Blodgett film (LB) has mono or multi layers of an amphiphilic molecules, deposited from the surface of aqueous solution onto a solid substrate by immersion or emersion the solid substrate into or from the aqueous solution. A monolayer is accurately deposited with each immersion or emersion step and therefore films with very homogeneous thickness can be achieved. The thickness of mono or multi layer is very accurate in that the length of each monomer is known and can be used to calculate the total thickness of a LB Film. The mono or multi layers are usually deposited vertically and typically consisted of amphiphilic molecules with a hydrophilic head and a hydrophobic tail. LB films can be used to study the biological membranes. Lipid molecules with amphiphilic property have gathered great attention because they can be readily assembled by the Langmuir method. This kind of biological membranes can be studied for the investigation of drug action upon cell membrane, the chemistry of biologically functionalized molecules, and the modeling of biological systems.

Diacetylene is one of the amphiphilic molecules and was deposited onto solid substrate using LB method.[17b] Self-assembled diacetylene monolayers were readily polymerized onto solid substrate and generated highly ordered thin film. Such ultrathin films of PDA are very attractive because they provide potentials as colorimetric sensing device as well as fundamental studies of PDA structure.

Also it is possible to propose field effect devices for observing the immunological response and enzyme-substrate reactions by collecting biological molecules such as antibodies and enzymes in insulating LB films. Langmuir layers are formed by spreading diacetylene monomers onto an air/water interface and applying compression to the densely packed diacetylene monomers at the surface. These mono and multi-layered diacetylene molecules were studied at the surface of water or they were transferred onto solid substrates to make LB or LS films[24] (Figure 2). PDA LB/LS films have been used to study the spectroscopic properties of PDAs. In sensor applications, mono and multi layered PDA Langmuir films have been used for the detection of biological analytes such as streptavidin protein[17a] (Figure 1.3).
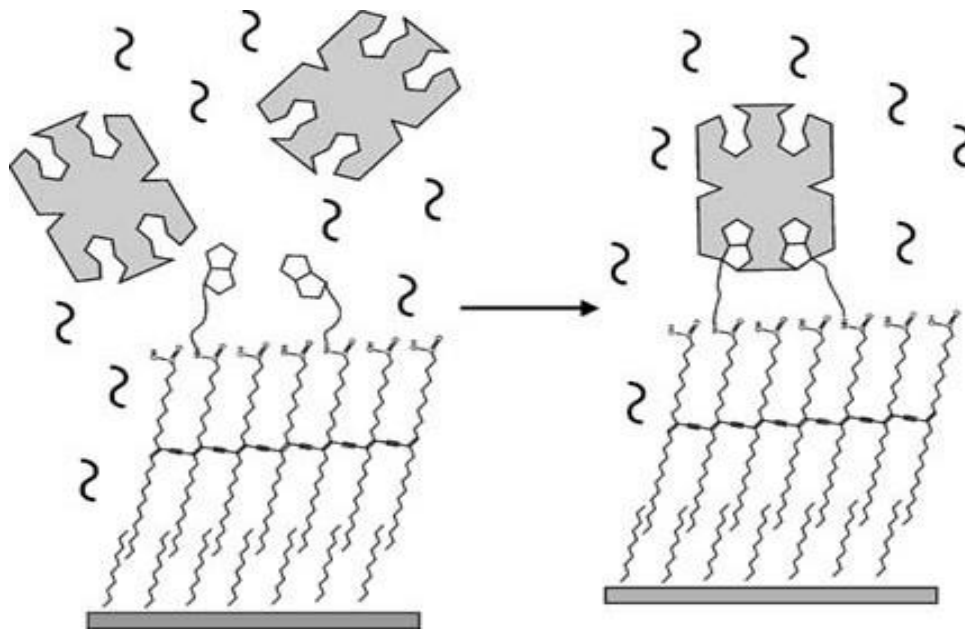
Figure 1.3. Schematic drawing of the noncovalent affinity interaction between streptavidin and the surface-immobilized biotin-PDA LB film.[17a]

However, the relatively low quantity of PDA present in a mono/multi-layer makes it hard to perform a spectroscopic detection of biological targets, exacerbated by the fact that these homogeneous PDA films are relatively complicated to prepare. Furthermore it was reported that at least three layers are required to generate an observable chromatic signal.[17a, 25] Although the sensitivity as a sensor device is relatively lower, LB method provided probability of decent fundamental studies because diacetylene monomers were able to be deposited onto solid substrate with maintaining their highly self-assembled structures and accurate thickness.

1.4.2 Layer-by-Layer Thin Film

Layer-by-Layer (LbL) deposition method is one of the thin film fabrication techniques. The films are generated by deposition of oppositely charged materials. Each layer having positive and negative charge was deposited through charge-charge interaction. The deposition can be performed in many different ways such as dip coating, spin-coating, spray-coating and flow based techniques.[26] LbL provides several advantages compared to other thin film deposition methods in that the protocol is extremely simple and low cost. There are a variety of materials that can be deposited by LbL method including metals, ceramics, nanoparticles, and biological molecules. Another advantage of LbL is the high degree of thickness control that is resulted from the linear growth of the films with the number of layers. By the fact that each layer can be controlled as thin as 1 nm, LBL deposition method provides convenient control of the thickness with 1 nm resolution. In this reason, LbL method has been used in a variety of field such as corrosion control of coated material[27] and biomedical applications.[28]
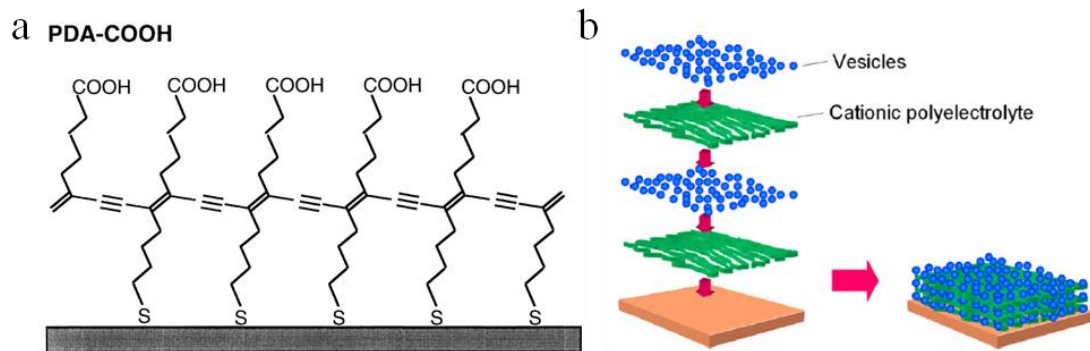
Figure 1.4. Illustration of layer-by-layer assembly on glass substrate using a) thiol modified polydiacetylene monomer[29] and b) cationic polyelectrolyte.[30]

The self-assembly of PDAs can be achieved with a layer-by-layer (LbL) deposition method, as reported by Crooks and Evans. Crook and co-workers modified diacetylene monomers with a thiol unit at the tail group, and they deposited the self-assembled diacetylene onto a gold substrate. They demonstrated that the self-assembled diacetylene structure from this method is more stable than the traditional alkane self-assembled structure, such as LB/LS films, upon heating and exposure to solvents.[29, 31] Evan's group further investigated the characteristics of the thiol modified diacetylene self-assembled structure with normal akane monolayers through the variation of substrate preparation. They investigated the crystallinity of the diacetylene self-assembled structures by changing the chain length as well as the position of diacetylene unit.[32]

Recently Sukwattanasinitt and Kim provided the LbL assembly of polydiacetylene vesicles with retained chromic properties.[30] Sukwattanasinitt and co-workers assembled the photopolymerized vesicles of PDAs into polyelectrolyte multilayer thin films using chitosan and poly(ethyleneimine) as a polycation. They studied the structural property of PDA vesicles and their optical properties upon solvent, pH, and temperature. The PDA vesicles in the polyelectrolyte film represented the more stability upon aging. Kim and co-workers also reported a preparation of layered PDA systems by alternative deposition of positively charged PDA vesicles and negatively charged linear polymers.[33] They deposited the positively charged PDA vesicles

9

alternatively with poly(styrenesulfonate) or poly(vinyl sulfate). They further characterized the surface morphology of LBL structure of PDA vesicles. Interestingly PDA vesicles deposited by LbL method showed reversible optical color change upon heating. It is well known that the reversible thermochromism is due to strong hydrogen bonding at the headgroup.[34] They proposed another issue that bidiacetylenic structures restrict the structural mobility of the headgroup, and therefore help the PDA structure back to original conformation after removing the heating. LbL method has been studied a lot to increase the structural property of self-assembled PDA vesicles and provided a convenient means to prepare colorimetric sensor systems having extended stability.

1.4.3 Colloidal Dispersion

Liposomes/Vesicles
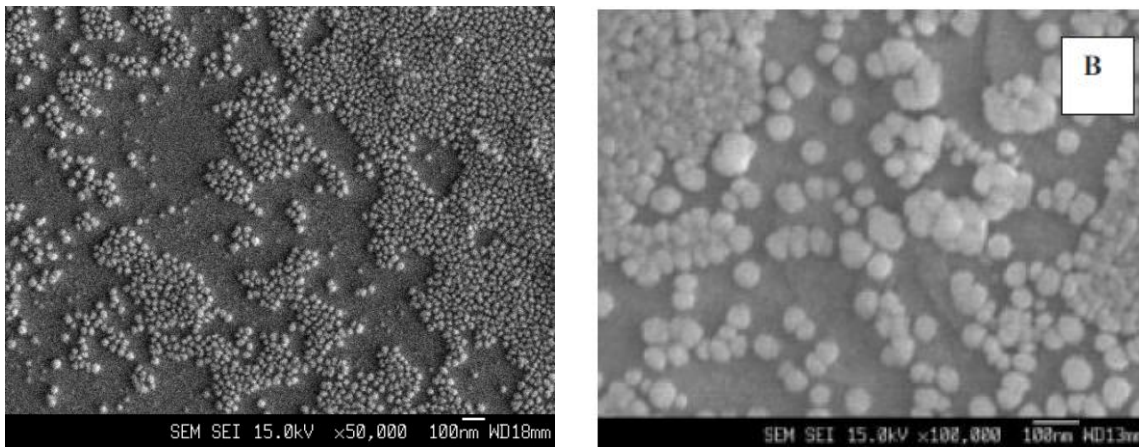
Figure 1.5. Scanning electron microscope (SEM) images of PDA liposomes.[34-35]

Amphiphilic diacetylene monomers can be readily dispersed into water by sonication to form self-assembled bi-layered liposomes. These types of colloidal dispersed liposomes can form films through chemical immobilization. Their preparation method is relatively easier than LBL and the LB/LS method, and is more preferable for large volume production. The formation of PDA liposomes has been discussed a lot as a model system for biosensor application.[36] The initial studies of PDA liposomes were

focused on the creation of stable biomimetic membranes using diacetylenes and phospholipids with the diacetylene unit. Ringsdorf and co-workers have shown that the size and the stability of PDA liposomes can be affected by additives such as structural stability agents of cholesterol.[16, 37] Jelinek and Charych have published TEM images of PDA liposomes in demonstration of the importance of preparation conditions.[38] According to their researches, variation of the preparation method resulted in changes to the PDA structure from vesicles to sheets. The variation of structures also significantly affected the chromatic response upon external stimuli.

PDA liposomes have potential for biosensor application but they have the intrinsic disadvantages of aggregation and photopolymerization in ambient conditions after long time storage. Another important issue is that liposomes require a delicate purification process after probe modification, such as column chromatography and membrane dialysis to remove unreacted probe materials. The unreacted probe materials of PDA liposomes provide a possible decrease of response of the PDA liposomes after probe-target interaction because unreacted probes induces competitive binding to targets. These disadvantages can be addressed by attaching the probes molecules to the surface of PDA colloids. Recently Kim and co-workers embedded the PDA molecules into a polymer structure to prevent their aggregation and demonstrated the chromatic transition of the PDA liposomes.[19, 39] In addition PDA liposomes were immobilized onto a solid substrate using a layer-by-layer method providing a convenient fabrication route for a colorimetric sensor device. PDA liposomes in solution have been used to understand the interaction of biologically important materials with membranes because liposomes are basically a biomimetic membrane structure.

Non-spherical structures

Numerous diacetylene lipids mononers have also been self-assembled into a variety of non-spherical structures such as tubules,[40] helices,[41] ribbons,[42] and sheets.[43] The initial studies for tubule structures were generally conducted with bis-(10,12-TRCDA)-sn-glycero-3-phosphocholine.[40a] Additional work conducted to investigate the formation of tubules using asymmetric diacetylene bolaamphiphiles in forms of fibers, ribbons and sheets.[44] This research issued that strongly H-bonding symmetric bolaamphiphiles, and asymmetric bolaamphiphiles with one head group capable of π–π stacking and resulted in the formation of ribbon.
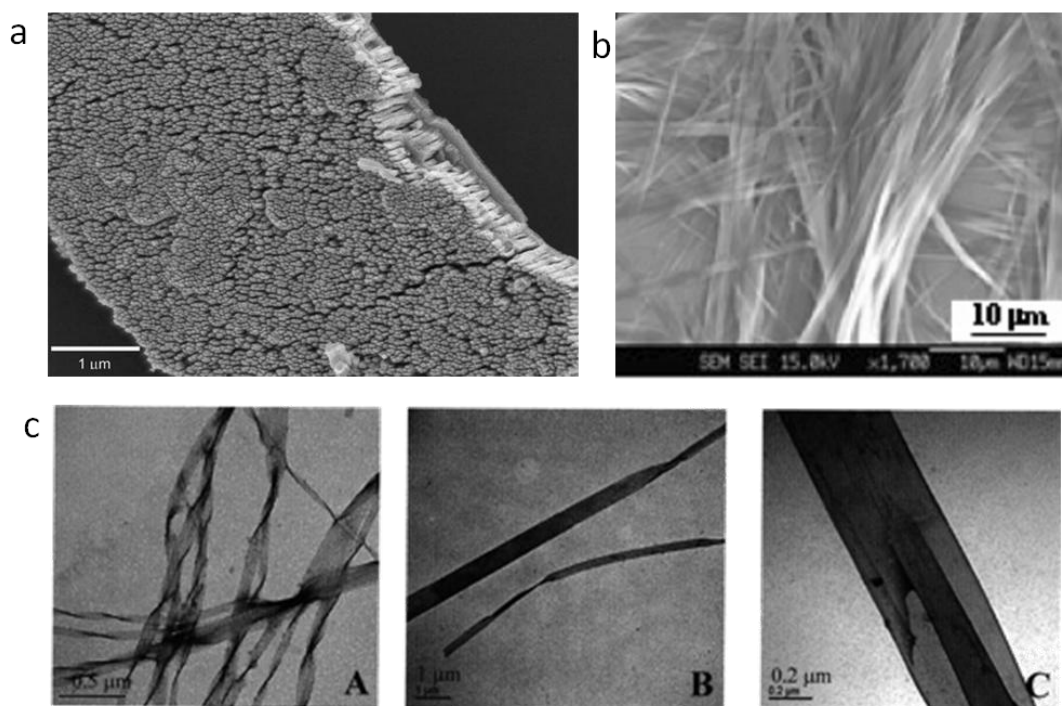
Figure 1.6. Scanning electron microscope (SEM) images of a) PDA tubules,[45] b) sheet[42] and c) ribbon.[44a]

Interestingly, most of the diacetylene monomers that were known to induce non-spherical structures had chiral moiety and it was believed as the origin of structural chirality.[40b] However, Thomas and co-workers prepared achiral PDA molecules and

showed that molecular chirality is not essential for the chiral tubule structures.[46] In this research they showed that the achiral molecules still formed helical tubules with left- and right-handed geometry. Recently, tubules were formed from the hydrobromide salt of an achiral diacetylene.[45, 47] Authors described the remarkable ability of an achiral lipid diacetylene with a secondary amine salt headgroup to form uniform nanotuble structures. These tubules were observed to be monodisperse and have a distinct CD spectrum, despite lacking any chirality in the monomer. The authors hypothesized that the intermolecular interaction between the bromide ion and the hydrogen atoms of the headgroup induced chirality and resulted in chiral tubular structures. These tubules were readily deposited onto the glass substrate and polymerized. Recently Kim and co-workers provided the reversible ribbon-sphere microstructural transformation of dipeptide-containing diacetylene supramolecules by specific ligand–receptor interactions.[42] This study has shown that ribbon-sphere formation can be reversible. The investigated microstructural transformation of the D-Ala-D-Ala dipeptide-containing PDA assembly provided possible sensor platform because of their enormous conformational change.

1.4.4 Conclusion of Self-assembled Structure

PDA can be formed in a variety of self-assembled structures when the diacetylene monomers are highly ordered in the correct geometry for the topochemical polymerization. PDA LB/LS films, liposomes and non-spherical type of PDAs have been studied extensively. Recently new formats such as multilayer LBL coatings and immobilized liposomes have been prepared. Variety of material form offers specific advantages for different biosensor applications. For instance, PDA liposomes are proper for assay applications such as high throughput screening in drug discovery. On the contrary, PDA sensory systems on the solid substrate are proper for the devices where

ease use are design concerns. The variety of PDA structures has also provided platforms

for studying the colorimetric and fluorometric properties of this interesting polymer.

1.5 Topochemical Polymerization

PDAs are formed from 1,4-addition photo-polymerization of self-assembled

diacetylenes, resulting in a highly ordered conjugated backbone as shown in Scheme 1.

The photo-polymerization only happens when the diacetylene monomers are densely

arranged in the appropriate crystalline structure with 4.7-5.2 Å intermolecular

distance.[32a] The topochemically polymerized PDA structures demonstrate stable features

upon external stimulation with temperature and mechanical strain.[48]

(R$_1$ = functionalized alkyl chain, R$_2$ = alkyl chain)
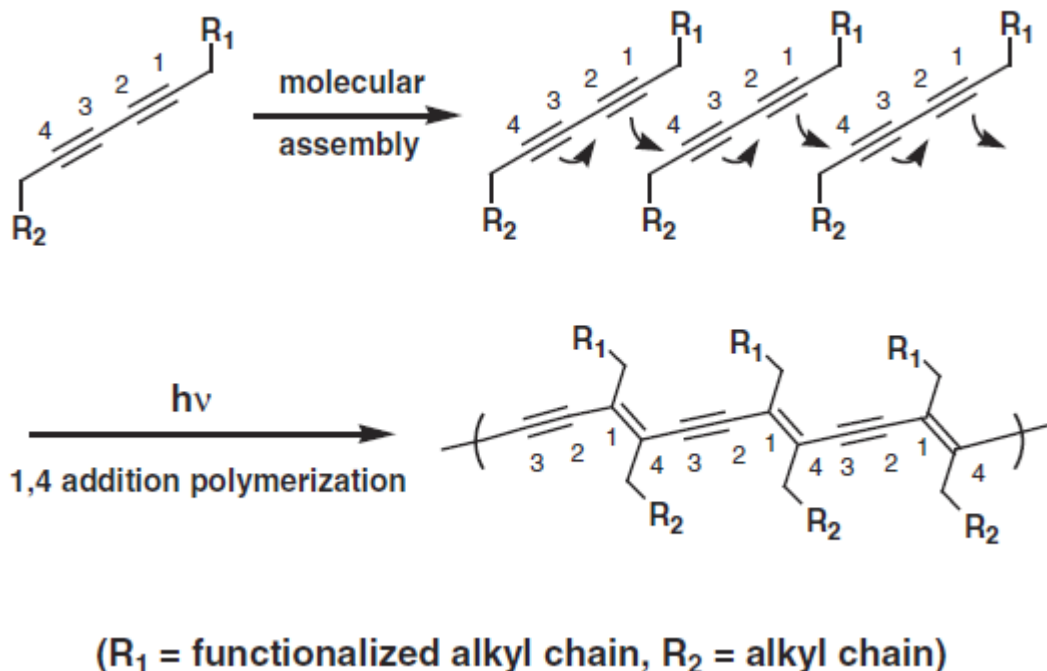
Figure 1.7 Schematic representation of topochemical photopolymerization of diacetylenes by UV
light.[35]

PDA typically usually develops a blue color upon exposure to 254 nm UV light.

Extended exposure of UV light induces a blue to red color transition and causes breakage

of the polymerization and chain distortion. The polymerization rate of PDA molecules

can be changed upon rearrangement of the diacetylene monomers. When the diacetylene units are not properly located in the crystalline lattice their weak blue polymerization color indicates a lower polymerization yield. Much research effort was devoted to investigate how the position of diacetylene (within the monomer) affects the crystalline structure and polymerization rate of the monomer and its assemblies. Evans and co-workers proved that the polymerization rate was reduced as the total chain length decreased and as the diacetylene unit was moved closer to the head group.[32] Interestingly they found out that diacetylene molecules with an odd number of alkyl spacers did not generate the intense blue color and only the evenly spaced molecules produced a significant blue color through photo-polymerization. They concluded that the shorter spacer is good for enhancing the crystalline structure but poor for polymerization and they also concluded that the even number spacer provides a better blue optical property. In addition, Tieke and Tachibana investigated the location effect of the diacetylene unit on the formation and polymerization of PDA LB films. Their research showed that the structure was more stabilized as the diacetylene unit was moved closer to the head group but that the polymerization rate was decreased and also the PDA showed red color rather than blue.[49]

1.6 Optical Properties of Polydiacetylene

1.6.1 Colorimetric Property

The optical property of PDAs results from the conjugated backbone. PDA molecules typically have maxima in the absorption spectra at 630 and, 550 nm. These peaks correspond to blue (630 nm) and red (550 nm) color by naked eyes. An interesting research report showed that PDA can be made green and yellow in color as well.[50] Also, absorption above 700 nm was observed in films and liposomes. These results are very

unusual but are closely related with the stability of the self-assembled structure of PDAs. According to the literature, the side chain length of PDA, the polymerization rate, the type of the PDA formation (such as film and liposome) and the external strain upon PDA are the reasons for the various kinds of absorption spectra. An optical color transition of PDAs has been observed upon external stimuli such as temperature,[34, 51] pH,[52] ions,[21, 53] solvent,[39b, 54] stress,[55] or ligand interactions.[22] Typically, absorption in the (blue form) red wavelengths (650 nm) was reduced and the absorption in the (red form) blue wavelengths (550 nm) increased upon exposure to those external stimuli. The colorimetric transition can be observed by naked eyes and the transition of color from the environmental perturbation has been used to develop PDA based colorimetric sensor systems.

1.6.2 Mechanism of Color Change

Much effort was devoted to investigate the mechanism of color change property in PDA molecules. However, this turned out to be one of the most challenging takes and the origin of chromism has not been fully understood yet. It is believed that multiple mechanisms caused the chromic transition and the responsible mechanisms are prevalent is dependent on the nature of environmental stimuli. Vast range of studies has shown that the self-assembled chain structure and the hydrogen bond among the head groups affect the optical property change of PDA molecules. Rotation of the single bonds in PDA backbone without side chains was predicted to require less energy and can be thermally accessible at room temperature.[56] However, such rotations in real PDA materials involve changes in the packing and inter-chain interactions of side-chains. Conformational changes of the conjugated backbone, changes of the side chains assembly, and hydrogen bonding interactions at the side chain are interrelated each other.

Polymerization of diacetylene molecules changes the alkyne carbons from sp to sp^2 and therefore changes the bond angle from 180° to 120°. However, the packing of the side chains prevents the polymer backbone from rearrangement and therefore resulted in accumulation of stress in the self-assembled structure as polymerization rate increases.[56] Another possible explanation of the PDA chromic change is that external stimuli increase the mobility of the side chains overcoming the barrier to rearrangement of the conjugated backbone created by the packing of the side chains, and therefore induced structural changes in the packing of the chains. UV exposure increased the conjugated backbone length of PDA and also increased the overall stress of the polymer system which efficiently reduced the energy required for backbone rearrangement. Additionally pH changes the hydrogen bonding in headgroups enables the linker unit between the headgroup and the backbone to be rearranged.

A rising question is that the color transition mechanisms of PDAs caused by biological recognitions such as analytes binding to targets, interactions with membrane inserting biomolecules can be different from the mechanisms caused by simple environmental stress. It has been generally hypothesized that interactions with biological targets makes large bulky complex and cause repulsion between complexes.[21a, 57] Those repulsion from bulky complex changes the hydrogen bonding in the headgroup and alkyl chain packing which is similar to those of thermochromic and pH based changes, permitting release of accumulated strain. However, the covering the surface of PDA structures with microorganism such as bacteria or virus might affect the optical properties of the polymer through different mechanisms than the insertion or bulky complex formation of a target protein. Understanding the fundamental basis of the optical changes of PDA molecules under a variety of conditions is essential to the design of sensitive, selective and stable sensing PDA systems.

17

1.6.3 Emissive Property

PDAs show weak red fluorescence in the red phase while the blue phase is not emissive. The emissive properties of PDA molecules were studied with urethane modified PDA molecules.[58] According to the research, the quantum yield of blue phase PDA is less than 10^{-5} implying fast non-radiative relaxation of the excited state. The quantum yield of the red phase at 15K was $0.3^{[59]}$ and the quantum yield at ambient temperature was $0.02.^{[60]}$ This implies that the lower quantum yield was induced by the increased temperature and also by the possible quenching through inter-chain energy transfer.[17b] Optical properties of PDA molecules provide the basic principle for PDA biosensor development. The colorimetric transition provides a convenient detection signal and the fluorescent property has potential as a sensitive detection system. Although the optical color change is relatively less intense than a conventional dye labeled sensor system, PDAs are very convenient and effective systems in that they can be used for a label free sensor system because of their dual signaling and self-signaling capability.
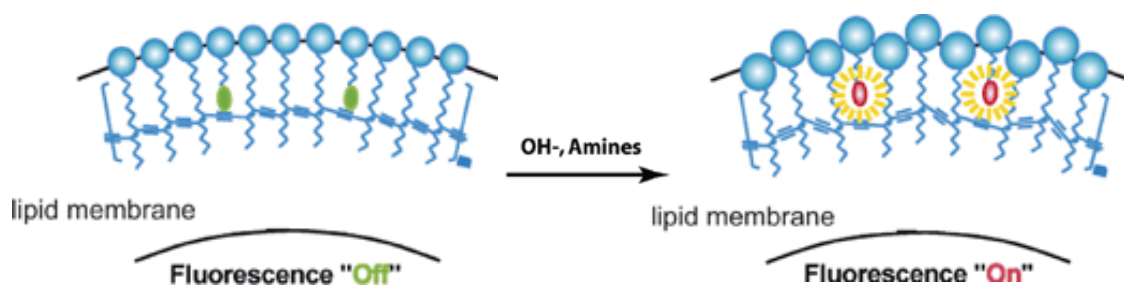
Figure 1.8. A schematic illustration of the fluorescence "turn-on" mechanism. Only one leaflet of the vesicle membrane is shown for better demonstration of the dye position.[61]

PDA has also been used to quench fluorophores. Cheng and co-workers developed reversible turn "on-off" PDA sensor using reversible quenching of 4,4-difluoro-5-(2-thienyl)-4-bora-3a,4a-diaza-s-indacene-3-dodecanoic acid (BO558) in PDA liposomes upon exposure to amines.[61] After addition of a HCl solution the distance between fluorophores and polydiacetylene was close enough for forming Forster energy transfer and the fluorescent of BO558 was quenched. However, the fluorescence intensity

of BO558 showed an enormous increase exceeding the original intensity before UV polymerization when a NaOH solution was added. This mechanism of quenching is important to understand and investigate an FRET based PDA sensor system (Figure 1.8.)

1.6.4 Conclusion for Optical Property of Polydiacetylene

The colorimetric and fluorometric transition is the basic signal generation of PDA based biosensor system. Developing full understanding on the fundamental mechanism of optical change and how these changes happen through the biological circumstances remains challenging. Colorimetric detection has been considered as an efficient approach for biosensor developments and also the emissive property of PDA molecules renders great potentials as an ultra sensitive detection/visualization mechanism of biological targets. Although the fluorescent intensity of PDA molecules in red phase is relatively lower than that of conventional dye-based sensor systems, a lot of effort has been made to increase the emission intensity through energy transfer theory but more systematic studies should be carried out to understand the low quantum yield of PDA molecules.[62]

1.7 PDA Sensors in the Literature

Optical properties of PDA molecules have been widely used to develop a sensory system because they are very sensitive in response to environmental stimuli as discussed above. For the initial work, Charych reported that PDA liposomes and thin films having sialic acid functionalization changed their color from blue to red upon exposure to the influenza virus.[63] Another interesting work was performed by Jiang and Li. They prepared glucoside tethered PDA liposomes and exposed them to *E. coli* and investigated the effect of the linker length on the sensitivity of PDA liposomes.[64] Much detection studies have been conducted with analytes such as microorganisms,[65] proteins[23a, 23b, 66] and biologically relevant molecules[53, 67] using PDA liposomes or LB/LS films. Most

PDA molecule based research utilizes modification of the head group to enable tethering of the specified probe material to the surface of PDA liposomes. However, PDA aqueous sensors have fundamental limitations such as aggregation and undesired photo polymerization in ambient conditions after long-term storage.
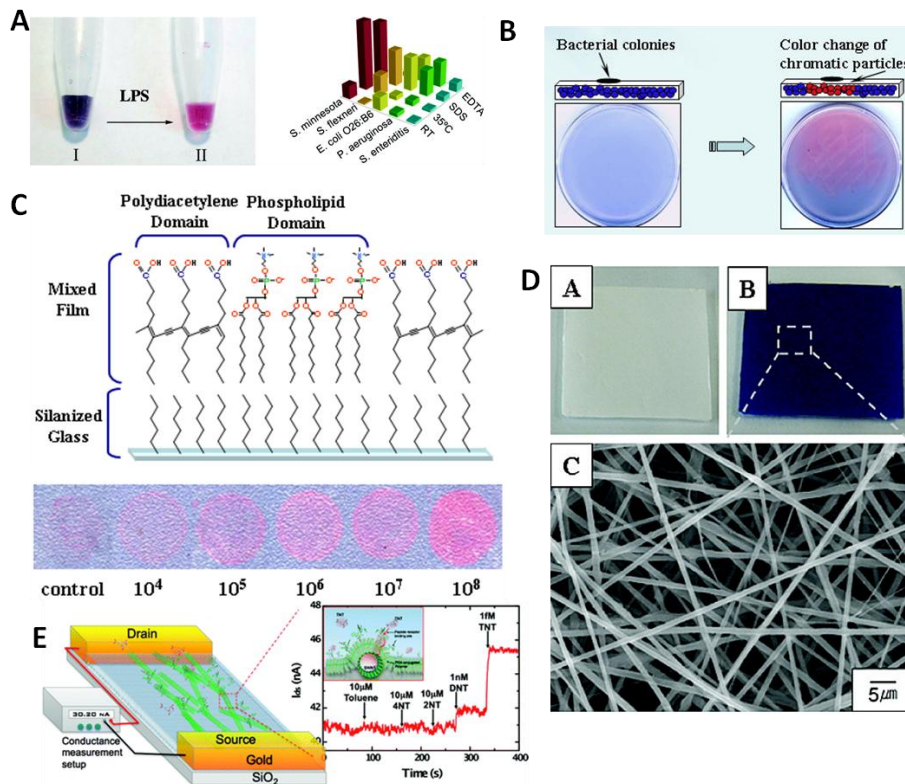
Figure 1.9 Illustration of various kinds of PDA based sensory system. a) polysaccharide sensor using PDA liposomes solution.[67c] b) bacteria detection system using PDA embedded agarose gel[68] and c) film.[57b] d) PDA electronspun polymer patch for VOC detection.[39b] e) PDA coated SWNT-FET sensor system for sensitive detection of TNT.[69]

Recently Kim and co-workers prepared polymer supported sensory systems to remove the intrinsic aggregation and undesired photopolymerization problems of PDA molecules. They showed the colorimetric transition property of PDA molecules upon exposure to volatile organic solvents (VOC).[39b] In this research the PDA molecules were mixed with poly(ethylene oxide) and teraethlyl orthosilicate (TEOS) during an

electrospinning process. PEO and TEOS were used as a stability enhancer for the sensor device. Typically PDA films and liposomes are not able to maintain their structure when they are exposed to organic solvents. Polymer matrices support the PDA sensor system and enhance the versatility of the PDA liposome sensor by enhancing the stability of the PDA molecules. In this way PDA molecules have been used to study biosensor fabrication through variation of their sensitivity in response to external stimuli. Additionally, they have been used for the study of cell membrane transactions as a model for understanding peptide interaction with and through a liposome membrane.[68a] PDA liposomes having biomimetic membrane structures have been considered as a good model for the study of the interaction between viruses and proteins. Recently Majumdar and Lee developed PDA based trinitrotoluene sensor.[69] At the initial study, they explored the PDA sensor system by the recognition event between peptide (Trp-His-Trp) and TNT. They observed colorimetric transition upon the addition of TNT vapor. They identified the role of end-group composition, surface density and side chain length. However, this system has a potential limitation in terms of sensitivity. Therefore they developed PDA based sensor system using carbon nanotube-based field-effect transistors to increase the sensitivity. They developed selective combined trinitrotoluene (TNT) receptors to conjugated polydiacetylene (PDA) polymers with single-walled carbon nanotube field-effect transistors (SWNT-FET). Selective recognition between the TNT molecules and TNT receptors effectively generated a sensitive SWNT-FET conductance sensor through the PDA coating layers. These studies of FET based PDA sensor system have provided a novel principle for ultra sensitive biosensor device development.

1.8 References

[1] a)A. Abbas, A. Treizebre, P. Supiot, N.-E. Bourzgui, D. Guillochon, D. Vercaigne-Marko, B. Bocquet, *Biosensors and Bioelectronics* **2009**, *25*, 154; b)M. Madou, J. Florkey, *Chemical Reviews* **2000**, *100*, 2679.

[2] I. L. Medintz, A. R. Clapp, H. Mattoussi, E. R. Goldman, B. Fisher, J. M. Mauro, *Nat Mater* **2003**, *2*, 630.

[3] L. Soleymani, Z. Fang, E. H. Sargent, S. O. Kelley, *Nat Nano* **2009**, *4*, 844.

[4] J. Wang, G. Liu, Y. Lin, *Nanotubes, Nanowires, and Nanocantilevers in Biosensor Development*, Wiley-VCH Verlag GmbH & Co. KGaA, **2007**.

[5] P. S. Dittrich, A. Manz, *Nat Rev Drug Discov* **2006**, *5*, 210.

[6] N. V. Zaytseva, V. N. Goral, R. A. Montagna, A. J. Baeumner, *Lab on a Chip* **2005**, *5*, 805.

[7] K. Lee, L. K. Povlich, J. Kim, *Analyst* **2010**, *135*, 2179.

[8] a)B. Yoon, S. Lee, J.-M. Kim, *Chemical Society Reviews* **2009**, *38*, 1958; b)M. A. Reppy, B. A. Pindzola, *Chemical Communications* **2007**, 4317.

[9] a)R. Langer, D. A. Tirrell, *Nature* **2004**, *428*, 487; b)J. J. Storhoff, C. A. Mirkin, *Chemical Reviews* **1999**, *99*, 1849; c)A. B. Sanghvi, K. P. H. Miller, A. M. Belcher, C. E. Schmidt, *Nat Mater* **2005**, *4*, 496.

[10] a)S. Wang, B. S. Gaylord, G. C. Bazan, *Journal of the American Chemical Society* **2004**, *126*, 5446; b)K. Lee, J.-M. Rouillard, T. Pham, E. Gulari, J. Kim, *Angewandte Chemie International Edition* **2007**, *46*, 4667; c)S. Wang, B. S. Gaylord, G. C. Bazan, *Advanced Materials* **2004**, *16*, 2127; d)Q.-H. Xu, S. Wang, D. Korystov, A. Mikhailovsky, G. C. Bazan, D. Moses, A. J. Heeger, *Proceedings of the National Academy of Sciences of the United States of America* **2005**, *102*, 530.

[11] a)T. Cassagneau, F. Caruso, *Advanced Materials* **2002**, *14*, 1629; b)P. Bäuerle, A. Emge, *Advanced Materials* **1998**, *10*, 324; c)S. S. Zhu, P. J. Carroll, T. M. Swager, *Journal of the American Chemical Society* **1996**, *118*, 8713; d)E. Shoji, M. S. Freund, *Journal of the American Chemical Society* **2002**, *124*, 12486.

[12] a)J. Huang, S. Virji, B. H. Weiller, R. B. Kaner, *Journal of the American Chemical Society* **2002**, *125*, 314; b)H. Korri-Youssoufi, A. Yassar, *Biomacromolecules* **2001**, *2*, 58.

[13] a)M. R. Pinto, B. M. Kristal, K. S. Schanze, *Langmuir* **2003**, *19*, 6523; b)B. Wang, M. R. Wasielewski, *Journal of the American Chemical Society* **1997**, *119*, 12.

[14] Y. Liu, R. C. Mills, J. M. Boncella, K. S. Schanze, *Langmuir* **2001**, *17*, 7452.

[15] S. Y. Okada, R. Jelinek, D. Charych, *Angewandte Chemie International Edition* **1999**, *38*, 655.

[16] a)H. Bader, K. Dorn, B. Hupfer, H. Ringsdorf, in *Polymer Membranes, Vol. 64* (Ed.: M. Gordon), Springer Berlin / Heidelberg, **1985**, pp. 1; b)B. Hupfer, H. Ringsdorf, H. Schupp, *Chemistry and Physics of Lipids* **1983**, *33*, 355.

[17] a)E. Geiger, P. Hug, B. A. Keller, *Macromolecular Chemistry and Physics* **2002**, *203*, 2422; b)R. W. Carpick, T. M. Mayer, D. Y. Sasaki, A. R. Burns, *Langmuir* **2000**, *16*, 4639.

[18] J.-M. Kim, Y. B. Lee, D. H. Yang, J.-S. Lee, G. S. Lee, D. J. Ahn, *Journal of the American Chemical Society* **2005**, *127*, 17580.

[19] J. M. Kim, Y. B. Lee, S. K. Chae, D. J. Ahn, *Advanced Functional Materials* **2006**, *16*, 2103.

[20] Y. Li, B. Ma, Y. Fan, X. Kong, J. Li, *Analytical Chemistry* **2002**, *74*, 6349.

[21] a)J. Lee, H.-J. Kim, J. Kim, *Journal of the American Chemical Society* **2008**, *130*, 5010; b)J. Lee, H. Jun, J. Kim, *Advanced Materials* **2009**, *21*, n/a.

[22]   S. Kolusheva, O. Molt, M. Herm, T. Schrader, R. Jelinek, *Journal of the American Chemical Society* **2005**, *127*, 10000.

[23]   a)Y.-l. Su, J.-r. Li, L. Jiang, *Colloids and Surfaces B: Biointerfaces* **2004**, *38*, 29; b)S. W. Lee, C. D. Kang, D. H. Yang, J. S. Lee, J. M. Kim, D. J. Ahn, S. J. Sim, *Advanced Functional Materials* **2007**, *17*, 2038; c)S. Kolusheva, R. Kafri, M. Katz, R. Jelinek, *Journal of the American Chemical Society* **2000**, *123*, 417; d)R. Jelinek, *Drug Development Research* **2000**, *50*, 497.

[24]   R. W. Carpick, et al., *Journal of Physics: Condensed Matter* **2004**, *16*, R679.

[25]   F. Gaboriaud, R. Volinsky, A. Berman, R. Jelinek, *Journal of Colloid and Interface Science* **2005**, *287*, 191.

[26]   D. Cranston Emily, G. Gray Derek, in *Model Cellulosic Surfaces, Vol. 1019*, American Chemical Society, **2009**, pp. 95.

[27]   T. R. Farhat, J. B. Schlenoff, *Electrochemical and Solid-State Letters* **2002**, *5*, B13.

[28]   H. Ai, S. Jones, Y. Lvov, *Cell Biochemistry and Biophysics* **2003**, *39*, 23.

[29]   T. Kim, K. C. Chan, R. M. Crooks, *Journal of the American Chemical Society* **1997**, *119*, 189.

[30]   A. Potisatityuenyong, G. Tumcharern, S. T. Dubas, M. Sukwattanasinitt, *Journal of Colloid and Interface Science* **2006**, *304*, 45.

[31]   T. Kim, Q. Ye, L. Sun, K. C. Chan, R. M. Crooks, *Langmuir* **1996**, *12*, 6065.

[32]   a)H. Menzel, M. D. Mowery, M. Cai, C. E. Evans, *The Journal of Physical Chemistry B* **1998**, *102*, 9550; b)H. Menzel, S. Horstmann, M. D. Mowery, M. Cai, C. E. Evans, *Polymer* **2000**, *41*, 8113.

[33]   J. Kim, J. M. Kim, D. J. Ahn, *Macromolecular Research* **2006**, *14*, 478.

[34]   J.-M. Kim, J.-S. Lee, H. Choi, D. Sohn, D. J. Ahn, *Macromolecules* **2005**, *38*, 9366.

[35] J. M. Kim, E. K. Ji, S. M. Woo, H. Lee, D. J. Ahn, *Advanced Materials* **2003**, *15*, 1118.

[36] K. Morigaki, T. Baumgart, U. Jonas, A. Offenhäusser, W. Knoll, *Langmuir* **2002**, *18*, 4082.

[37] a)H.-H. Hub, B. Hupfer, H. Koch, H. Ringsdorf, *Angewandte Chemie International Edition in English* **1980**, *19*, 938; b)N. Wagner, K. Dose, H. Koch, H. Ringsdorf, *FEBS Letters* **1981**, *132*, 313.

[38] a)S. Kolusheva, E. Wachtel, R. Jelinek, *Journal of Lipid Research* **2003**, *44*, 65; b)R. Volinsky, F. Gaboriaud, A. Berman, R. Jelinek, *The Journal of Physical Chemistry B* **2002**, *106*, 9231.

[39] a)J. Yoon, J.-M. Kim, *Macromolecular Chemistry and Physics* **2008**, *209*, 2194; b)J. Yoon, S. K. Chae, J.-M. Kim, *Journal of the American Chemical Society* **2007**, *129*, 3038.

[40] a)J. M. Schnur, R. Price, P. Schoen, P. Yager, J. M. Calvert, J. Georger, A. Singh, *Thin Solid Films* **1987**, *152*, 181; b)J. M. Schnur, B. R. Ratna, J. V. Selinger, A. Singh, G. Jyothi, K. R. K. Easwaran, *Science* **1994**, *264*, 945.

[41] D. A. Frankel, D. F. O'Brien, *Journal of the American Chemical Society* **1994**, *116*, 10057.

[42] K. H. Park, J.-S. Lee, H. Park, E.-H. Oh, J.-M. Kim, *Chemical Communications* **2007**, 410.

[43] H. Park, J. S. Lee, H. Choi, D. J. Ahn, J. M. Kim, *Advanced Functional Materials* **2007**, *17*, 3447.

[44] a)J. Song, Q. Cheng, S. Kopta, R. C. Stevens, *Journal of the American Chemical Society* **2001**, *123*, 3205; b)J. Song, Q. Cheng, R. C. Stevens, *Chemistry and Physics of Lipids* **2002**, *114*, 203.

[45] S. B. Lee, R. Koepsel, D. B. Stolz, H. E. Warriner, A. J. Russell, *Journal of the American Chemical Society* **2004**, *126*, 13400.

[46]   S. Pakhomov, R. P. Hammer, B. K. Mishra, B. N. Thomas, *Proceedings of the National Academy of Sciences of the United States of America* **2003**, *100*, 3040.

[47]   S. B. Lee, R. R. Koepsel, A. J. Russell, *Nano Letters* **2005**, *5*, 2202.

[48]   S. R. Sheth, D. E. Leckband, *Langmuir* **1997**, *13*, 5652.

[49]   a)B. Tieke, G. Lieser, *Journal of Colloid and Interface Science* **1982**, *88*, 471; b)H. Tachibana, Y. Yamanaka, H. Sakai, M. Abe, M. Matsumoto, *Macromolecules* **1999**, *32*, 8306.

[50]   a)B. Chu, R. Xu, *Accounts of Chemical Research* **1991**, *24*, 384; b)H. Oikawa, T. Korenaga, S. Okada, H. Nakanishi, *Polymer* **1999**, *40*, 5993.

[51]   a)D. J. Ahn, E.-H. Chae, G. S. Lee, H.-Y. Shim, T.-E. Chang, K.-D. Ahn, J.-M. Kim, *Journal of the American Chemical Society* **2003**, *125*, 8976; b)Y. Lu, Y. Yang, A. Sellinger, M. Lu, J. Huang, H. Fan, R. Haddad, G. Lopez, A. R. Burns, D. Y. Sasaki, J. Shelnutt, C. J. Brinker, *Nature* **2001**, *410*, 913.

[52]   Q. Cheng, R. C. Stevens, *Langmuir* **1998**, *14*, 1974.

[53]   S. Kolusheva, T. Shahal, R. Jelinek, *Journal of the American Chemical Society* **2000**, *122*, 776.

[54]   R. R. Chance, *Macromolecules* **1980**, *13*, 396.

[55]   a)K. Tashiro, H. Nishimura, M. Kobayashi, *Macromolecules* **1996**, *29*, 8188; b)R. W. Carpick, D. Y. Sasaki, A. R. Burns, *Langmuir* **2000**, *16*, 1270.

[56]   V. Dobrosavljevicacute, R. M. Stratt, *Physical Review B* **1987**, *35*, 2781.

[57]   a)J. Lee, H. Jun, J. Kim, *Advanced Materials* **2009**, *21*, 3674; b)Y. Scindia, L. Silbert, R. Volinsky, S. Kolusheva, R. Jelinek, *Langmuir* **2007**, *23*, 4682.

[58]   a)A. Yasuda, M. Yoshizawa, T. Kobayashi, *Chemical Physics Letters* **1993**, *209*, 281; b)T. Kobayashi, M. Yasuda, S. Okada, H. Matsuda, H. Nakanishi, *Chemical Physics Letters* **1997**, *267*, 472.

[59]   R. Lécuiller, J. Berréhar, C. Lapersonne-Meyer, M. Schott, J. D. Ganière, *Chemical Physics Letters* **1999**, *314*, 255.

[60]   J. Olmsted, M. Strand, *The Journal of Physical Chemistry* **1983**, *87*, 4790.

[61]   G. Ma, A. M. Müller, C. J. Bardeen, Q. Cheng, *Advanced Materials* **2006**, *18*, 55.

[62]   X. Li, S. Matthews, P. Kohli, *The Journal of Physical Chemistry B* **2008**, *112*, 13263.

[63]   D. Charych, J. Nagy, W. Spevak, M. Bednarski, *Science* **1993**, *261*, 585.

[64]   a)Y. Zhang, Y. Fan, C. Sun, D. Shen, Y. Li, J. Li, *Colloids and Surfaces B: Biointerfaces* **2005**, *40*, 137; b)Z. Ma, J. Li, L. Jiang, J. Cao, P. Boullanger, *Langmuir* **2000**, *16*, 7801.

[65]   B. A. Pindzola, A. T. Nguyen, M. A. Reppy, *Chemical Communications* **2006**, 906.

[66]   a)D. Charych, Q. Cheng, A. Reichert, G. Kuziemko, M. Stroh, J. O. Nagy, W. Spevak, R. C. Stevens, *Chemistry & Biology* **1996**, *3*, 113; b)J. J. Pan, D. Charych, *Langmuir* **1997**, *13*, 1365; c)J. Song, Q. Cheng, S. Zhu, R. C. Stevens, *Biomedical Microdevices* **2002**, *4*, 213; d)R. Jelinek, S. Okada, S. Norvez, D. Charych, *Chemistry & Biology* **1998**, *5*, 619; e)G. Ma, Q. Cheng, *Langmuir* **2005**, *21*, 6123; f)S. Kolusheva, R. Zadmard, T. Schrader, R. Jelinek, *Journal of the American Chemical Society* **2006**, *128*, 13592.

[67]   a)S. Rozner, S. Kolusheva, Z. Cohen, W. Dowhan, J. Eichler, R. Jelinek, *Analytical Biochemistry* **2003**, *319*, 96; b)Q. Cheng, R. C. Stevens, *Advanced Materials* **1997**, *9*, 481; c)M. Rangin, A. Basu, *Journal of the American Chemical Society* **2004**, *126*, 5038; d)M. Katz, I. Ben-Shlush, S. Kolusheva, R. Jelinek, *Pharmaceutical Research* **2006**, *23*, 580; e)X. Chen, J. Lee, M. J. Jou, J.-M. Kim, J. Yoon, *Chemical Communications* **2009**, 3434.

[68]   a)D. Meir, L. Silbert, R. Volinsky, S. Kolusheva, I. Weiser, R. Jelinek, *Journal of Applied Microbiology* **2008**, *104*, 787; b)L. Silbert, I. B. Shlush, E. Israel, A.

Porgador, S. Kolusheva, R. Jelinek, *Appl. Environ. Microbiol.* **2006**, AEM.01324.

[69]   T. H. Kim, B. Y. Lee, J. Jaworski, K. Yokoyama, W.-J. Chung, E. Wang, S. Hong, A. Majumdar, S.-W. Lee, *ACS Nano* **2011**, *5*, 2824.

CHAPTER 2

Polydiacetylene–Liposome Arrays for Selective Potassium Detection

Published in **J. Am. Chem. Soc. 2008,** *130*, 5010-5011

2.1 Introduction

Conjugated polymer-based biosensor systems have gained much interest from both academia and industry.[1] This is because an environmental change at a single site along the conjugated polymer chain can affect the properties of the collective system, producing large signal amplification.[2] [3] [4] [5] If biological materials are uniquely combined as a receptor with synthetic conjugated polymers having the tunable signal amplification property, the specificity of the biosystems will provide the ultimate selectivity in a sensor design. In this respect, developing biological and synthetic conjugated polymer hybrid biosensors through rational design, organic and bioconjugated synthesis, and molecular assembly is a promising direction to realize high sensitivity and high selectivity. Polydiacetylene-based sensor systems are unique in terms of the sensitive colorimetric/fluorescence dual detection capability and the convenient preparation method through self-assembly and subsequent photopolymerization.[6] [7] It has been well-known that polydiacetylene in the blue phase is not emissive but produces red fluorescence when it transformsto the red phase by external stimuli including temperature,[8] pH,[9] ions,[10] solvent,[11] stress,[12] or ligand interactions.[13]
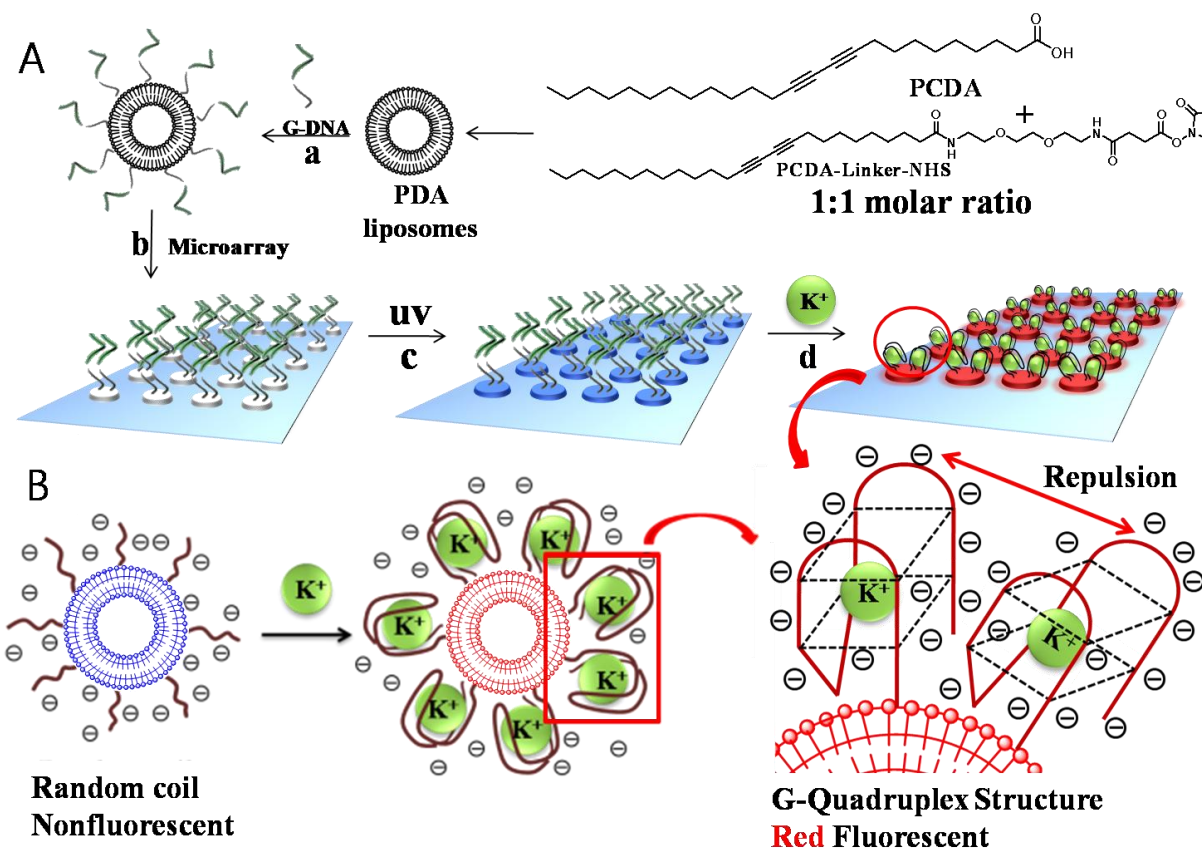
Scheme 2.1. A. The chemical structure of the diacetylene monomers investigated and a schematic representation of the PDA liposome-based microarray for potassium detection. (a) Surface modification of the diacetylene liposome with the amine-functionalized G-rich ssDNA. (b) Microarray of G-rich ssDNA-tethered PDA liposomes onto an amine glass. (c) Photopolymerization of the G-rich ssDNA-tethered PDA liposomes using a 254 nm UV lamp. (d) Recognition of target potassium ions via the quadruplex formation results in red fluorescent emission. B. Schematic representation of the G-quadruplex formation and the resulting steric repulsion.

2.2 Results and Discussion

We describe the development of practical polydiacetylene (PDA) liposome-based microarrays to selectively detect potassium even in the presence of sodium. Potassium is an important cation in biology and quantitative detection of the extracellular potassium level in the blood stream is also important.[14] The typical physiological concentration of potassium and sodium in the blood stream is 3.5–5.3 and 135–145 mM, respectively.[15] However, selective detection of physiological potassium is a challenging task due to the presence of sodium in a much higher concentration. Our PDA liposome sensor has ssDNAs having a guanine-rich

sequence (5´- GGTTGGTGTGGTTGG-3´) as a selective probe for potassium detection. We utilize the fact that the G-rich ssDNA can fold into a G-quadruplex via intramolecular hydrogen bonding by wrapping around a potassium ion exclusively.[16] We rationally design the PDA liposome in such a way that the G-rich ssDNA probes are presented densely at the liposome surface, and upon binding with K^+, the resulting bulky quadruplexes repulse each other as illustrated in Scheme 1. The steric repulsion of the quadruplexes will induce the perturbation of the ene-yne backbone of PDA liposomes and produce the color change from blue to red and red fluorescence, as well.

We synthesized the NHS-activated carboxylic-acid-containing diacetylene in Scheme 2.1A (PCDA-linker-NHS). The selfassembled diacetylene liposomes were prepared by using a 1:1 mixture of the PCDA-linker-NHS and 10,12-pentacosadiynoic acid (PCDA). The G-rich ssDNA was covalently linked to the liposome surface by means of conventional amide chemistry betweenthe amine-modified G-rich ssDNA and the PCDA-linker-NHS. The self-assembled and functionalized liposomes were then printed onto an amine-modified glass substrate by using a manual microarrayer in a humidity chamber and photopolymerized.

Scheme 2.1B schematically illustrates the steric repulsion and the resulting conformational change of the PDA liposome, which is induced by G-quadruplex formation with K^+ selectively. Weconfirmed the selective G-quadruplex formation of the PDA liposomes with K^+ by using CD analysis as shown in Figure 2.1a. The characteristic absorption bands at 270 and 290 nm of the quadruplex were observed only when K + was added to the solution of the PDA liposomes.[17] The CD analysis also shows that the presence of Na^+ does not interfere with the selective K+ recognition. Even more than 30 times more concentrated Na^+ (100 mM) essentially did not hinder the quadruplex formation of the G-rich ssDNA probe with K^+ (3 mM). Figure 2.1 panels b and c show the UV–vis absorption and PL emission spectra of the G-rich ssDNA-tethered PDA liposome solution upon addition of KCl solution in various concentrations. The solution was incubated at 25 °C for 3 h. As the concentration of K^+ increases, the absorption

31

band at 650 nm (blue phase) decreases and the new absorption band at 550 nm (red phase) increases. The detection limit shown in Figure 2.1b is 0.1 mM, and that is suitable for the detection of the physiological potassium level (3.50–5.30 mM). The same liposome solution did not show any change upon addition of even 100 times higher concentration of Na^+, providing excellent selectivity (Figure 2.2.). The fluorescence intensity of the liposome also increased gradually with the increasing concentration of K^+ (Figure 2.1c). As the incubation time at 25 ℃ increases, the PL intensity also increases (Figure 2.1d).
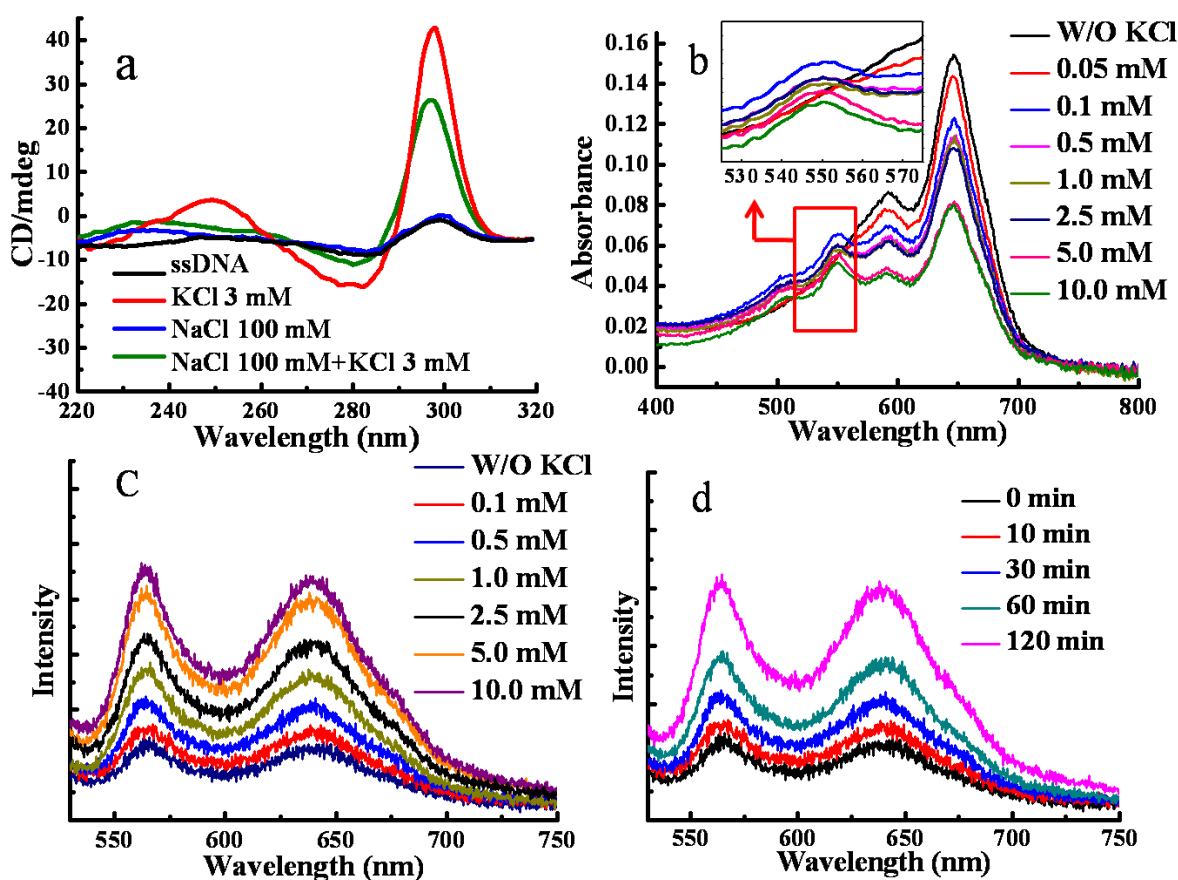
Figure 2.**1.** (a) CD spectra of the G-quadruplex at 6 ℃ before and after adding K^+ and Na^+. (b) UV–vis spectrum and (c) PL spectrum change of G-rich ssDNA-tethered PDA liposome solution (1 mM) upon addition of KCl. The concentration of KCl ranges from 0 to 10.0 mM. (d) PL spectrum change of the G-rich ssDNA-modified PDA liposome solution (1 mM) upon addition of 1 mM KCl (excitation at 503 nm).

We further developed practically useful solid-state liposome arrays for selective potassium detection. The G-rich ssDNAmodified liposome solution was spotted onto amine-modified glass substrates using a manual microarrayer followed by incubation at 30 ℃ for 3 h under 90% humidity condition to prevent the liposomes from drying out and subsequently photopolymerized with a 1 mW/cm^2 254 nm UV lamp for 2 min. Twenty milliliters of 5 mM NaCl solution and 20 mL of 5 mM KCl solution were then added onto the glass substrate, respectively. As shown in Figure 2.3a, no fluorescence was observed after adding the NaCl solution and before adding the KCl, while the red fluorescence emission was turned on as an indication of the K$^+$ detection after adding the KCl solution followed by 30 min of incubation at room temperature (Figure 2.3b). The results demonstrate that the immobilized liposomes having G-rich ssDNA selectively detect K$^+$ even in the presence of Na$^+$ because the presence of Na$^+$ does not interfere with the selective K$^+$ detection.
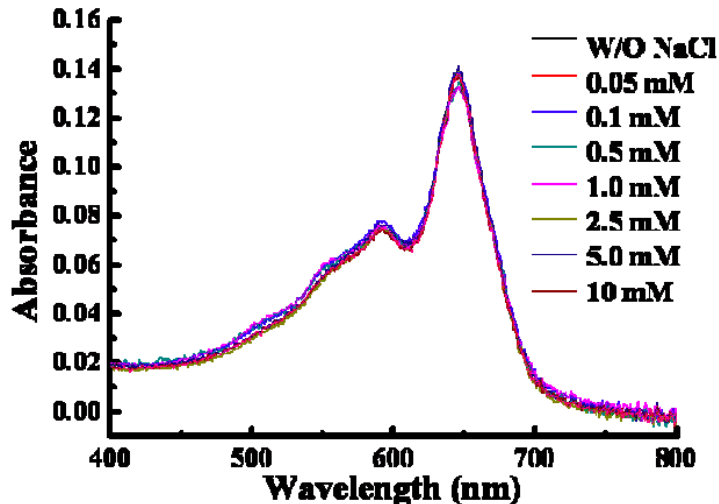
Figure 2.2. UV–vis spectrum change of G-rich ssDNA-tethered PDA liposome solution upon addition of NaCl.
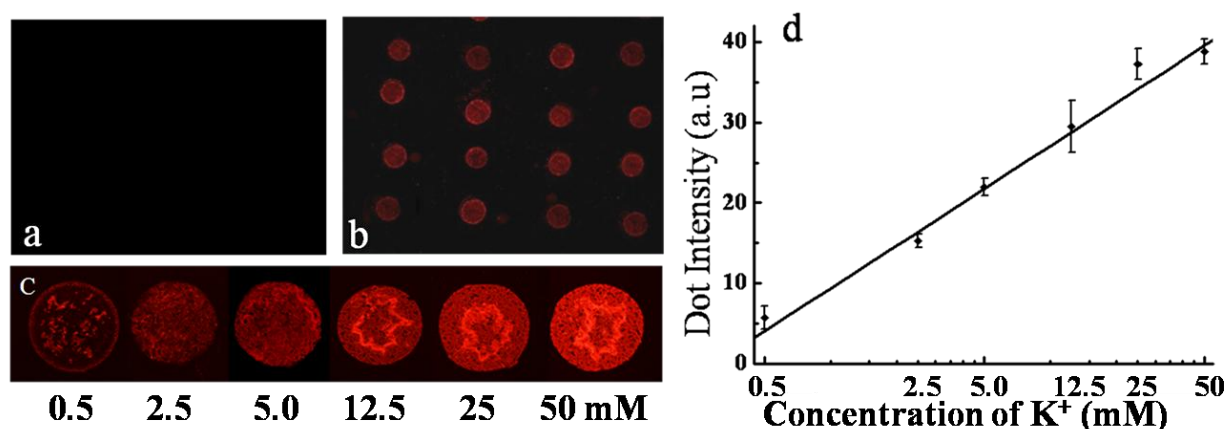
Figure 2.3. Fluorescent microscope images of the microarrayed PDA liposomes (excitation at 600 nm and a long-pass emission filter with 550 nm cutoff were used) (a) after adding NaCl (5 mM) and before KCl (5 mM) addition, and (b) after adding the KCl solution and 30 min of incubation at room temperature. (c) Fluorescent images of the PDA liposome arrays with KCl solutions at various concentrations (20 mL each). (d) Correlation curve between the fluorescence intensity and the amount of the K^+.

We also conducted the detection limit study in the solid state. Figure 2c shows the fluorescence microscope images of the PDA microarrays after incubation with K^+ solution in various concentrations at room temperature for 30 min. The detection limit for the 30 min of incubation results in the microscope images is 0.5 mM. The correlation curve between the fluorescence intensity and the amount of K^+ is shown in Figure 2.2d, and therefore, a quantitative analysis of an unknown K^+ concentration is also achievable.

2.3 Conclusions

We have developed a highly selective PDA liposome-based sensory system to detect K+ even in the presence of Na^+ The tethered G-rich ssDNAs at the liposome . surface provide selectivity by wrapping around K^+ selectively to form quadruplexes. The bulky quadruplexes repulse each other due to the steric hindrance and induce the ene-yne backbone perturbation of the PDA liposomes. This selective event triggers the color change from the blue phase to the red phase of the PDA liposome and also produces red fluorescence emission. We demonstrated quantitative analysis of the K^+ concentration by using the PDA liposome microarray. The

presented design principle can be readily applicable to many other chemical and biosensor developments and allows highly selective and sensitive quantitative analysis.

2.4 Experimental section

2.4.1 Preparation of the Liposome Microarray

An amine-modified glass substrate was placed in a humidity chamber for 30 min at 30℃. The G-rich ssDNA tethered diacetylene liposome solution was spotted onto the amine-modified glass slide by using a manual microarrayer (VP 475, V&P scientific, INC) and stored for 4 h at 90% humidity. After rinsing with di-water and drying under a stream of nitrogen, the microarrayed glass substrate was exposed to 254 nm UV (1 mW/cm^2) for 2 min.

2.4.2 Potassium Detection of the Liposome Microarray

20 mL of 5 mM NaCl solution and 20 mL of 5 mM KCl solution was added onto the liposome microarray having the G-rich ssDNA, respectively and the microarray was incubated for 30 minutes at room temperature before rinsing. The fluorescence images were obtained by using a fluorescent microscope (Olympus BX51 W/DP71).

2.4.3 Quantitative Data of Fluorescence Intensity with Various Concentrations of Potassium

The liposome microarray was incubated with a solution containing various concentrations (0.5, 2.5, 5.0, 12.5, 25, and 50 mM: 0.01 - 1.0 × 10-3 mol in 20 ml) of potassium for 30 min. The fluorescence images were obtained by using a fluorescent microscope (Olympus BX51 W/DP71) and the quantitative fluorescence intensities from the dots were analyzed by using IPLab 4.04

Software (BD Biosciences, USA). The data were obtained with five independent experiments. The error bar is standard deviation and each point represents the mean value.

2.4.4 Potassium Detection of G-rich ssDNA Modified Liposome Solution

To a solution containing 200 µl of 1mM solution of the G-rich ssDNA tethered liposome was added 1µl of concentrated KCl solution to make the final concentration of 0.05, 0.1, 0.5, 1.0, 2.5, 5.0, and 10.0 mM at room temperature. UV spectrum and PL spectrum were taken after 3 hours incubation at room temperature.

2.4.5 Circular Dichroism

A solution of the G-rich ssDNA tethered liposome in di-water was prepared by above mentioned procedure. To a solution of the 0.25 mM G-rich ssDNA tethered liposome (200µl) were added 10 µl of KCl and NaCl solution to make the final concentration of 3 mM for KCl and 100 mM for NaCl and the resulting liposome solution was incubated for 3 hours at room temperature. The CD spectrum of the liposome solution was measured at 6℃.

2.4.6 Synthesis and characterization

Materials and Method

10,12-pentacosadiynoic acid (PCDA) was purchased from GFS Chemicals. 2,2'-(Ethylenedioxy)bis-(ethylamine) (EDEA), N-hydroxysuccinimide (NHS), and N-(3-Dimethylaminopropyl)-N6-ethylcarbodiimide (EDC), Succinic Anhydride (SA) were purchased from Sigma-Aldrich Chemical Co. Amine modified G-rich ssDNA (5'-GGTTGGTGTGGTTGG-3') Oligonucleotides were purchased from Integrated DNA Technologies, Inc. Dialysis membrane was purchased from pierce (Slide-A-Lyzer Dialysis Cassette, 20,000 MWCO, 0.1-0.5 ml capacity). ^{1}H NMR spectra (500 MHz) were obtained from Varian Inova 500 NMR instrumentation. UV/Vis absorption spectra were taken on a Varian

Cary50 UV/Vis spectrophotometer. Fluorescence spectra were obtained using PTI QuantaMasterTM spectrofluorometers equipped with an integrating sphere. Fluorescence images were taken by Olympus BX51 W/DP71 fluorescent micro scope. Circular dichroism spectra were obtained on an Aviv model 202 Circular Dichroism Spectrometer at 6 ℃.

Synthesis of PCDA Derivatives

The diacetylene monomers investigated in this study were prepared by coupling N-hydroxysuccinic esters of PCDA. A typical procedure for the preparation of PCDA-Linker-NHS is as follows

PCDA-NHS: To a 10 mL of methylene chloride solution containing 2.00 g (5.34 mmol) of 10,12-pentacosadiynoic acid (PCDA) was added 0.76 g (6.94 mmol) of N-hydroxysuccinimide and 0.76 g (8.02 mmol) of 1-ethyl-3-[3-dimethylaminopropyl]carbodiimide hydrochloride at room temperature. The resulting reaction mixture was stirred at room temperature for 2 hs. The solvent was removed in vacuo, and the residue was purified by extraction with ethyl acetate to give 2.16 g (86.2 %) of the desired diacetylene monomer PCDA-NHS as a white solid: ^{1}H NMR (500 MHz, CDCl$_3$): δ 0.86 (t, 3H), 1.21-1.52 (m, 36H), 2.21 (t, 4H), 2.60 (t, 2H), 2.87 (s, 4H).

PCDA-EDEA: To a solution containing 1.055 ml (7.21 mmol) of EDEA in 40 ml of methylene chloride was added 1.00 g (2.12 mmol) of PCDA-NHS at room temperature. The resulting solution was stirred at room temperature for 2 h. The solvent was removed in vacuo, and the residue purified by extraction with ethyl acetate. The solvent was removed in vacuo, and the residue was purified by column chromatography (9:1 chloroform : methanol) to give 490 mg (46%) of the desired diacetylene monomer PCDA-EDEA as a pale blue solid: ^{1}H NMR (300 MHz, CDCl$_3$): δ 0.89 (t, 3H), 1.27-1.64 (m, 35H), 2.21 (m, 6H), 2.92 (t, 2H), 3.45-3.63 (m, 14H),6.21(s, 1H), 7.27 (brs, 1H).

PCDA-EDEA-SA: To a solution containing 198.3 mg (1.98 mmol) of succinic anhydride in 10 ml of N,N-dimethylformamide was added 500 mg (0.99 mmol) of PCDA-EDEA at room temperature. The resulting solution was stirred at room temperature for 2 h. The solvent was removed in vacuo, and the residue was purified by extraction with ethyl acetate to give 540 mg (90 %) of the desired diacetylene monomer PCDA-EDEA-SA as a white solid: ^{1}H NMR (300 MHz, CDCl3): δ 0.89 (t, 3H), 1.27-1.64 (m, 39H), 2.22 (m, 6H), 2.45 (t, 2H), 2.65 (t, 2H), 3.45-3.63 (m, 14H), 5.91 (s, 1H), 6.21 (s, 1H), 7.27 (brs, 1H).

PCDA-Linker-NHS: To a solution containing 400 mg (0.66 mmol) of PCDA-EDEA-SA in 20 ml of methylene chloride was 114.1 mg (0.99 mmol) of N-hydroxysuccinimde and 190.1 mg (0.99 mmol) of EDC at room temperature. The resulting solution was stirred at room temperature for 2h. The solvent was removed in vacuo, and the residue was recrystalized in ethyl acetate to give 250 mg (54%) of the desired diacetylene monomer PCDA-Linker-NHS as a white solid: ^{1}H NMR (300 MHz, CDCl$_3$): δ 0.89 (t, 3H), 1.27-1.64 (m, 39H), 2.18 (m, 6H), 2.62 (t, 2H), 2.85 (s, 4H), 3.00 (t, 2H), 3.45-3.63 (m, 14H), 5.91 (s, 1H), 6.21 (s, 1H), 7.27 (brs, 1H).

2.5 References

[1]   a)R. Langer, D. A. Tirrell, *Nature* **2004**, *428*, 487; b)J. J. Storhoff, C. A. Mirkin, *Chemical Reviews* **1999**, *99*, 1849; c)A. B. Sanghvi, K. P. H. Miller, A. M. Belcher, C. E. Schmidt, *Nat Mater* **2005**, *4*, 496.

[2]   S. Wang, B. S. Gaylord, G. C. Bazan, *Journal of the American Chemical Society* **2004**, *126*, 5446.

[3]   Q.-H. Xu, S. Wang, D. Korystov, A. Mikhailovsky, G. C. Bazan, D. Moses, A. J. Heeger, *Proceedings of the National Academy of Sciences of the United States of America* **2005**, *102*, 530.

[4]   S. Wang, B. S. Gaylord, G. C. Bazan, *Advanced Materials* **2004**, *16*, 2127.

[5]   K. Lee, J.-M. Rouillard, T. Pham, E. Gulari, J. Kim, *Angewandte Chemie International Edition* **2007**, *46*, 4667.

[6]   a)R. W. Carpick, T. M. Mayer, D. Y. Sasaki, A. R. Burns, *Langmuir* **2000**, *16*, 4639; b)R. W. Carpick, D. Y. Sasaki, A. R. Burns, *Langmuir* **2000**, *16*, 1270; c)K. Morigaki, T. Baumgart, U. Jonas, A. Offenhäusser, W. Knoll, *Langmuir* **2002**, *18*, 4082; d)Q. Huo, K. C. Russell, R. M. Leblanc, *Langmuir* **1999**, *15*, 3972.

[7]   H. He, M. A. Mortellaro, M. J. P. Leiner, R. J. Fraatz, J. K. Tusa, *Journal of the American Chemical Society* **2003**, *125*, 1468.

[8]   Y. Lu, Y. Yang, A. Sellinger, M. Lu, J. Huang, H. Fan, R. Haddad, G. Lopez, A. R. Burns, D. Y. Sasaki, J. Shelnutt, C. J. Brinker, *Nature* **2001**, *410*, 913.

[9]   Q. Cheng, R. C. Stevens, *Langmuir* **1998**, *14*, 1974.

[10]   S. Kolusheva, T. Shahal, R. Jelinek, *Journal of the American Chemical Society* **2000**, *122*, 776.

[11]   R. R. Chance, *Macromolecules* **1980**, *13*, 396.

[12]   K. Tashiro, H. Nishimura, M. Kobayashi, *Macromolecules* **1996**, *29*, 8188.

[13]   D. Charych, J. Nagy, W. Spevak, M. Bednarski, *Science* **1993**, *261*, 585.

[14]   a)Y. Lu, H. Fan, A. Stump, T. L. Ward, T. Rieker, C. J. Brinker, *Nature* **1999**, *398*, 223; b)H.-C. Kuo, C.-F. Cheng, R. B. Clark, J. J. C. Lin, J. L. C. Lin, M. Hoshijima, V. T. B. Nguyêñ-Trân, Y. Gu, Y. Ikeda, P.-H. Chu, J. Ross, W. R. Giles, K. R. Chien, *Cell* **2001**, *107*, 801; c)J. Kim, D. T. McQuade, S. K. McHugh, T. M. Swager, *Angewandte Chemie International Edition* **2000**, *39*, 3868.

[15]   H. Mutlu, E. Silit, Z. Pekkafali, C. C. Basekim, E. Kizilkaya, H. Ay, A. F. Karsli, *AJNR Am J Neuroradiol* **2003**, *24*, 1396.

[16]   a)J. A. Walmsley, J. F. Burnett, *Biochemistry* **1999**, *38*, 14063; b)F. He, Y. Tang, S. Wang, Y. Li, D. Zhu, *Journal of the American Chemical Society* **2005**, *127*, 12343.

[17]   a)P. Balagurumoorthy, S. K. Brahmachari, *Journal of Biological Chemistry* **1994**, *269*, 21858; b)H. Ueyama, M. Takagi, S. Takenaka, *Journal of the American Chemical Society* **2002**, *124*, 14286.

CHAPTER 3

Polydiacetylene–Liposome Microarrays for Selective and Sensitive Mercury(II) Detection

3.1 Introduction

Conjugated polymers (CPs) are emerging materials for many useful applications. One of the more attractive applications of CPs is for sensor design, due to the signal amplification property and the versatility in molecular design of CPs.[1] Many interesting conjugated-polymer sensors for the detection of chemical and biological molecules have been developed.[2] Polydiacetylene (PDA) is a unique conjugated polymer showing the well-known pressure-sensitive color change. The color change is believed to appear from the conformational change of the conjugated backbone of PDA induced by external stimuli, such as heat, pH change, and mechanical pressure.[3] Topochemical polymerization through 254nm UV irradiation is the most commonly used method to polymerize well-packed diacetylene monomers with a high degree of spatial order, such as that found in Langmuir– Blodgett monolayers and self-assembled liposome bilayers.[4] The photoinduced topochemical polymerization converts transparent diacetylene monomers into conjugated PDA with a blue color (absorption lmax at 640 nm). Upon external stimuli, the absorption lmax shifts from 640nm (blue phase) to 540nm (red phase). Interestingly, the triggered red phase of PDA is also weakly fluorescent, so PDA can provide dual signaling capability.[5] The pressure-sensitive mechanochromism of

41

PDAs has been used for colorimetric biosensor development to detect influenza virus, E. coli, microorganisms, cholera toxin, glucose, and nucleic acids, because shape changes of biological molecules accompany the recognition event.[6] We previously developed PDA-based self-signaling microarrays capable of highly selective, sensitive, and quantitative potassium detection.[7] We also developed emissive PDA nanoparticles with dual signaling capability for sensitive and selective immunofluorescence labeling.[8] However, the implemented PDA design principle for the PDA-based biosensors is only suitable for a specific single target molecule, because the sensory PDA films and liposomes were prepared from diacetylene monomers with a fixed particular receptor unit. To detect another analyte, a new diacetylene monomer with a new receptor unit has to be synthesized and purified stringently. However, to achieve a PDA microarray with high throughput capacity, various receptors must be present at the microarray surface. This requires efficient tethering of receptors after the liposome immobilization on a glass substrate for both convenience and to allow for user-prepared microarrays, because in many cases researchers will want to put their own receptors, for example, various proteins, on the chip surface. In this regard, the realization of a universal PDA platform will require the development of a novel molecular-design principle that will allow for the incorporation of various receptor units after preparation of sensory PDA films.
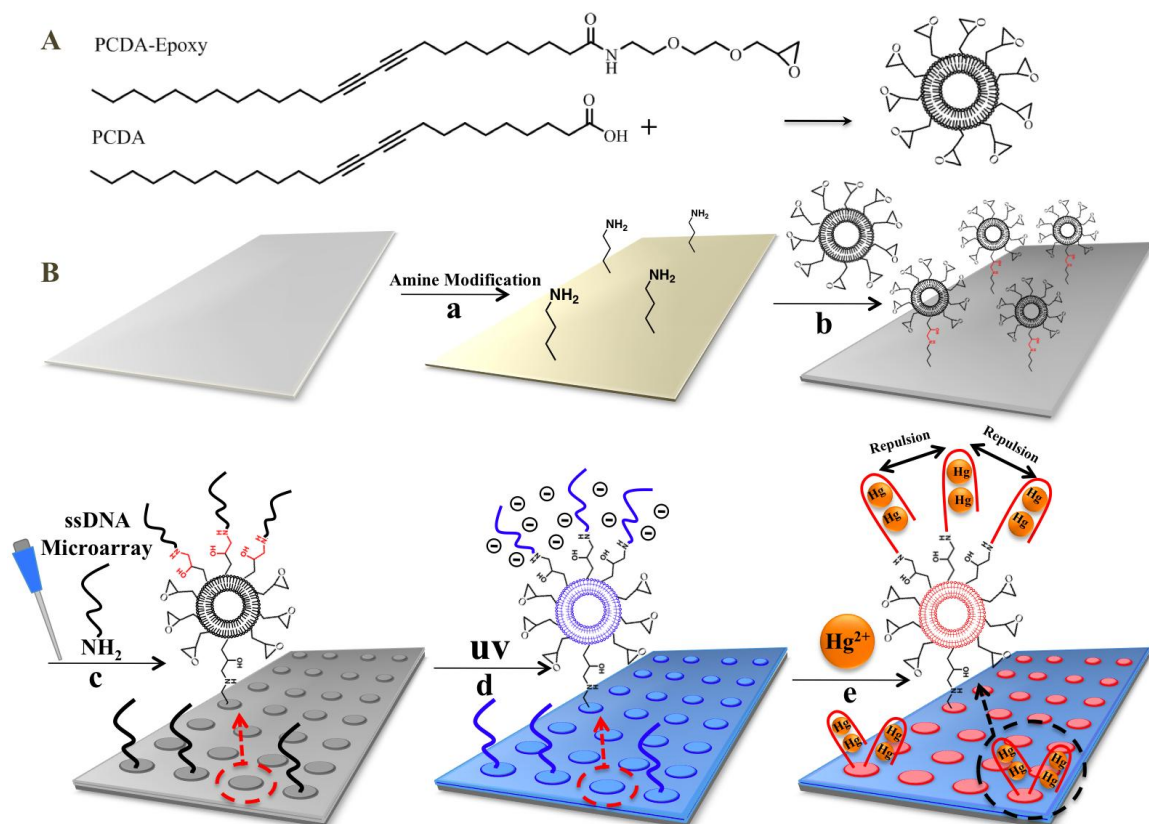
Scheme 3.1. A) Chemical structure of the diacetylene monomers, PCDA and PCDA-Epoxy. B) Schematic illustration of the PDA liposome-based microarray for mercury detection. a) Surface modification of the glass substrate with amine functionality. b) Immobilization of the Epoxy liposomes onto the amine glass slide through epoxy-amine coupling. c) Post-tethering of the ssDNA aptamer by means of a microarrayer. d) Photopolymerization of the PDA liposomes using a 254nm UV lamp. e) Recognition of the target mercury ions results in red fluorescent emission.

3.2 Results and Discussion

Mercury (Hg^{2+}) is a well-known neurotoxin, and its accumulation in the human body induces critical brain damage, resulting in blindness, deafness, memory loss, and death.[9] Therefore, the allowable concentration of mercury in drinking water is strictly regulated to be less than 2 ppb.[10] To detect mercury, various methods have been developed by means of gold nanoparticles, fluorophores, DNAzymes, proteins, and polymers.[11] Our sensory PDA microarrays were developed based on selfassembling diacetylene molecules having an epoxy group to achieve a universal PDA platform for

43

convenient post tethering of receptors. We chose the epoxy group because it can be a versatile functional group for bioconjugation with biological molecules by means of its reaction with ubiquitously present amine groups on biological molecules. Epoxy groups are also stable for storage.[12] N-hydroxysuccinimide (NHS)-activated carboxylic acid is a common choice for immobilization of PDA liposomes on an amine-modified substrate, and an amine is for an aldehydemodified substrate.[7,13] We compared the immobilization efficiency and the stability of the epoxy group with those of NHS-activated carboxylic acid and ethylenediamine.
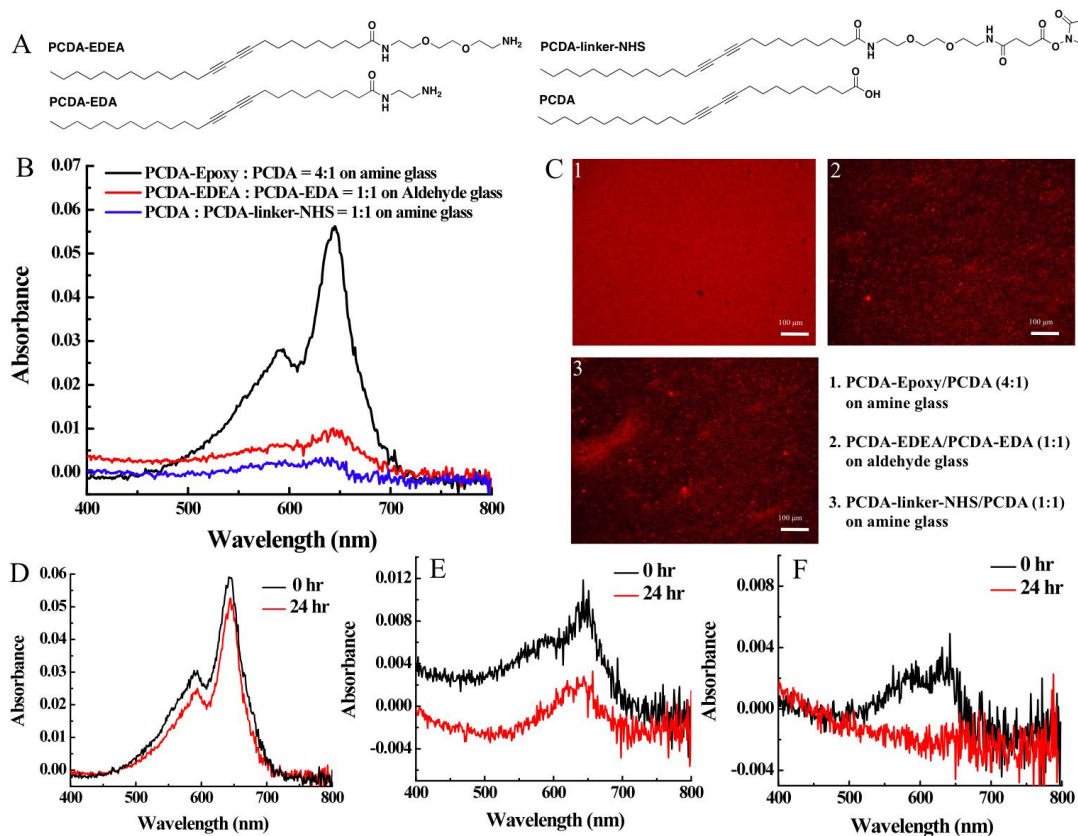
Figure 3.1. A. The chemical structure of diacetylene monomers, PCDA-EDEA, PCDA-EDA, PCDA-linker-NHS, and PCDA. B. UV spectra of the substrates having immobilized PDA liposomes after 20 minutes of incubation. C. Fluorescent microscope images of the immobilized PDA liposomes after 20 minutes of incubation (excitation at 600 nm and a long-pass emission filter with 550 nm cutoff were used) Scale bar is 100 μm. D. UV spectra of immobilized Epoxy liposomes (20 minutes incubation) before and after 24 hours of storage of the liposome solution in room temperature. E. UV spectra of immobilized EDA liposomes (20 minutes incubation) before and after 24 hours of storage of the liposome solution in room temperature. F. UV spectra of immobilized NHS liposomes (20 minutes incubation) before and after 24 hours of storage of the liposome solution in room temperature.

We synthesized PCDA (10,12-pentacosadiynoic acid)-Epoxy according to the procedure described in the experiemntal. The self-assembled diacetylene liposomes (Epoxy liposome) were prepared using a 4:1 mixture of the PCDA-Epoxy and PCDA. The two control liposomes, composed of a 1:1 mixture of PCDA:PCDA-linker-NHS (NHS liposome) and 1:1 mixture of PCDA-EDEA:PCDA-EDA (EDA liposome), were prepared according to the literature procedures.[7,13] We immobilized the Epoxy and NHS liposomes on an amine-modified glass substrate and the EDA liposome on an aldehyde-modified glass substrate respectively, using identical conditions. The results showed that PCDA-Epoxy liposomes have much faster immobilization kinetics, and result in better film quality and better stability than the other two. The chemical structures of PCDA-linker-NHS and PCDA-EDEA are shown in Figure 3.1. We immobilized the Epoxy liposome and the NHS liposome on an amine-modified glass substrate and the EDA liposome on an aldehyde-modified glass substrate, respectively, by using an identical condition. As shown in Figure 3.1B, the PCDA-Epoxy liposome shows much faster immobilization kinetics than the other two liposome systems. After 20 mins of incubation of the liposomes at room temperature the glass slide treated with the Epoxy liposome shows much larger absorption intensity and better film quality than the glass slides treated with the NHS liposome and EDA liposome. To match the same absorption intensity and the quality of the liposome film by using the NHS liposome and EDA liposome it took 6-8 hours of incubation at 37°C.[12] Besides the much faster immobilization the stability of the Epoxy liposome is another advantage. We conducted a time dependent stability test. The freshly prepared liposome solutions (Epoxy liposome, EDA liposome, and NHS liposome) and the same liposome solutions after 24 hours of storage at room temperature were respectively immobilized onto solid substrates. As we can clearly see in Figures 3.1D – F, while the Epoxy liposome shows a slight decrease in the absorption intensity the other two liposome systems show a significant decrease in the absorption intensity. This indicates that the reactivity of the NHS liposome and the EDA

45

liposome decreases significantly after the 24 hours of storage. On the contrary, the activity of the Epoxy liposome was maintained even after a few days of storage demonstrating the superior stability of the Epoxy liposome system.

We developed highly selective and sensitive PDA microarrays for mercury detection based on the Epoxy liposome system developed. Scheme 1 illustrates our design strategy. Note that the same epoxy units were used for liposome tethering onto the substrate and for the post-tethering of the ssDNA aptamer as a selective receptor for mercury detection. Studying the literature, we identified the thymine-rich ssDNA aptamer (5'-TTCTTTCTTCCCCTTGTTTGTT-3') that forms a thymine– HgII–thymine complex (T-Hg-T) by selective binding with Hg^{2+}.[14] As schematically illustrated in Scheme 1, our PDA mercury sensors are designed in such a way that when the ssDNA aptamers recognize and wrap around mercury ions, the resulting bulky T-Hg-T complexes repulse each other. The static repulsion force is then transferred to the PDA liposomes to perturb their conjugated ene-yne backbone, and produces the color change from blue to red and the red fluorescence emission. The PCDA-Epoxy/PCDA (4:1) liposome solution was first immobilized onto an amine glass slide.We then spotted the thymine-rich ssDNA aptamer using a microarrayer onto the liposome layer and incubated the slide at room temp for 3 h under 70% humidity to prevent the aptamer solution from drying out. After rinsing away any unreacted ssDAN aptamers, we photopolymerized the liposome slide using a 254nm UV lamp ($1mW/cm^2$) for 20 s.
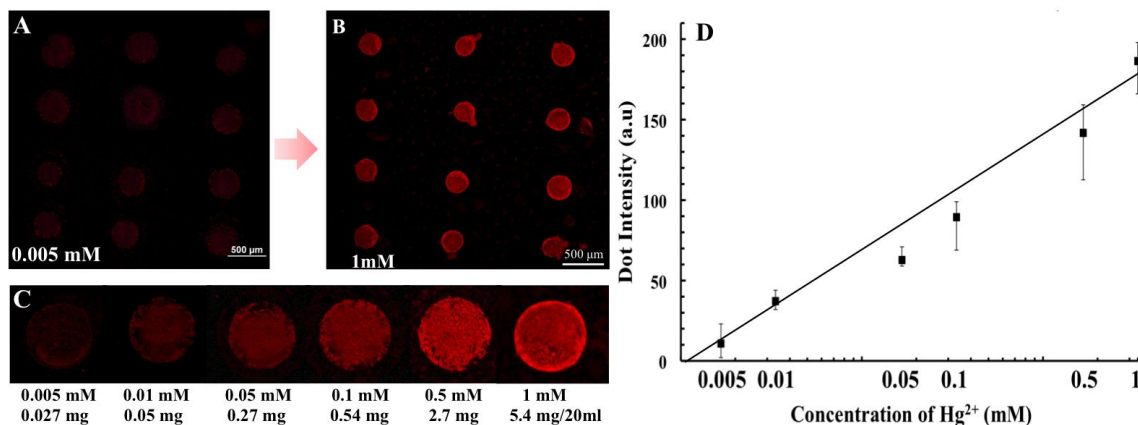
Figure 3.2. Fluorescence microscopy images of the PDA microarray (excitation at 600nm and a long-pass emission filter with 550nm cutoff were used) after 1 h incubation at room temperature with A) 0.005mM of Hg^{2+} and B) 1mM of Hg^{2+} solution. C) Fluorescence microscopy images of the PDA liposome arrays after 1 h incubation at room temperature with Hg^{2+} solutions in various concentrations. Scale bar is 500mm. D) Correlation curve between the fluorescence intensity and the amount of Hg^{2+}.

First, we tested the sensitivity of the PDA microarray. Figure 3.2 shows the fluorescence microscopy images of the PDA microarray after incubation with Hg2þ solution in various concentrations at room temperature for 1 h. The developed red-fluorescence intensity has a close relationship with the concentration of the mercury solution, and the correlation is shown in Figure 3.2D. As the concentration of mercury ions increases, more T-Hg-T complexes will be formed, and induce stronger perturbation of the ene-yne backbone of the PDA liposomes, resulting in the increase in the red fluorescence intensity. Based on the correlation curve, therefore, a quantitative analysis of an unknown mercury concentration is also achievable. The detection limit after 1 h of incubation confirmed by microscopy images was 0.005mM (0.027 mg/20 mL). This detection limit is imposed by our microscope, and could be much better if a more sensitive equipment was used.

We also conducted a detection study with the PDA liposome in solution to better understand the recognition of Hg^{2+} by the ssDNA aptamer. Figure 3.3 shows the UV-vis absorption and PL emission spectra of the PDA-liposome solution upon addition of mercury (Hg^{2+}) ions at room temperature. The absorption peak at 650nm decreased and

the red-phase absorption band appeared upon addition of 0.03mM of Hg^{2+} (Figure 3.3A). The fluorescence intensity of the PDA liposomes also increased upon addition of Hg^{2+} (Figure 3.3B). Interestingly, after 2 h incubation, the UV-vis spectrum showed a bathochromic shift, as shown in Figure 3.3A, and the PDA liposomes formed aggregation. Unlike the PDA liposomes in the solid microarray, the PDA liposomes in solution have freedom of translational movement. Therefore, the thymine-rich ssDNA liposome in solution can form intermolecular as well as intramolecular T-Hg-T complexes, as schematically illustrated in Figure 3.3C. The formation of the intermolecular T-Hg-T complexes is likely the origin of the observed aggregation and the slight bathochromic shift in UV-vis spectrum.
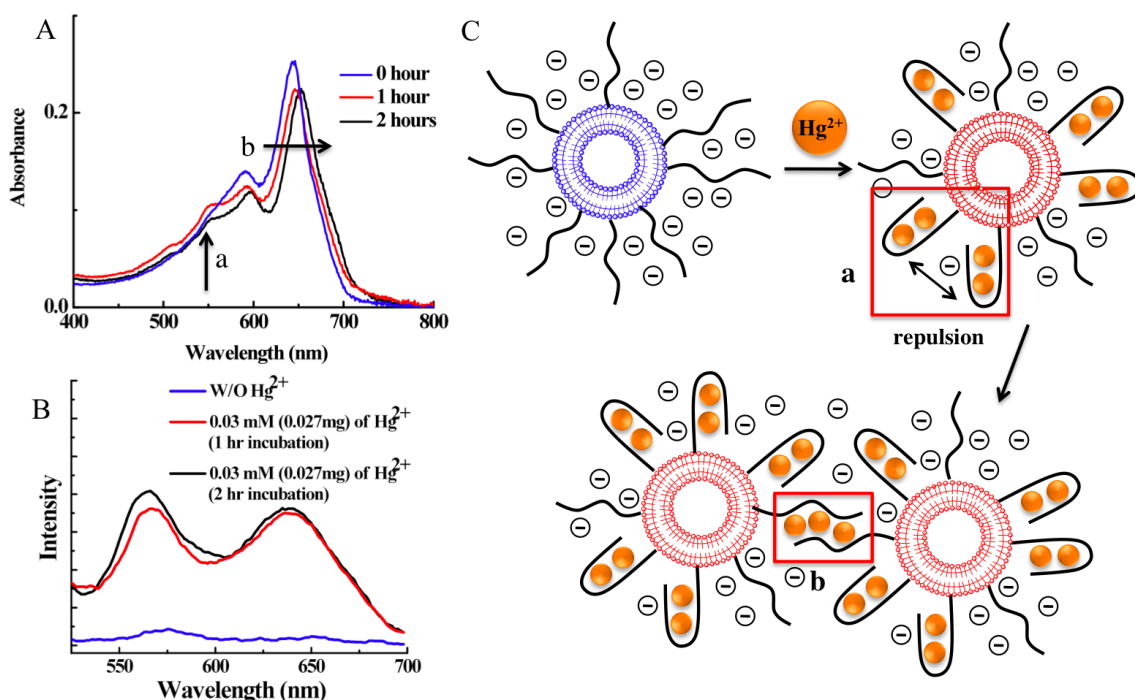
Figure 3.3. A) UV-vis spectra and B) PL spectra of the PDA liposome solution (0.05mM) upon addition of Hg^{2+} (0.03mM) for 1 h (red line) and 2 h (black line) of incubation. C) Schematic illustration of the T-Hg-T conformation in the PDA liposome solution: a) the resulting steric repulsion between the intermolecular T-Hg-T complexes after 1 h incubation at room temperature and b) the formation of the intermolecular T-Hg-T aggregation after 2 h incubation at room temperature.

48
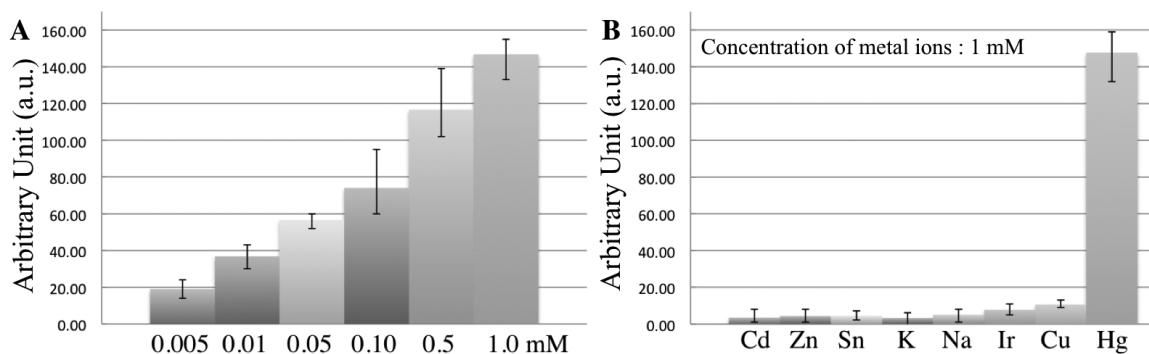
Figure 3.4. A) Fluorescence intensity of the PDA microarray after 1 h incubation with Hg^{2+} (0.005, 0.01, 0.05, 0.10, 0.50, 1.00mM). B) Fluorescence intensity of the PDA microarray after 1 h incubation with each 1.0mM metal ion.

We investigated the selectivity of the PDA microarray by incubating various metal ions, such as Cd^{2+}, K^+, Na^+, Sn^{2+}, Ir^{2+}, Cu^{2+}, and Zn^{2+}, with the PDA microarray. As can be seen in Figure 3.4A and B, the fluorescence-emission intensity induced by other metal ions are orders of magnitude smaller than that induced by the same concentration of mercury ion, demonstrating the excellent selectivity of the PDA-liposome array.

3.3 Conclusions

We have developed PDAliposome- based microarrays for selective and sensitive mercury detection. We investigated and identified the epoxy group as a universal functional group for efficient immobilization of PDA liposome onto a solid substrate, and for the convenient post-tethering of the amine-modified ssDNA aptamer (5'-TTCTTTCTTCCCCTTGTTTGTT-3') on the liposome surface as a selective receptor for the recognition of mercury ion. The PDA mercury sensors are designed in such a way that when the ssDNA aptamers recognize and wrap around mercury ions, the steric repulsion between the resulting bulky T-Hg-T complexes perturbs the conjugated ene-yne backbone of the PDA liposomes, and produces the color change from blue to red and the redfluorescence emission. The detection limit of the PDA microarray is 5 mM. The

49

specificity of the ssDNA aptamer toward Hg^{2+} provides excellent selectivity to the PDA microarray as well. The developed Epoxy-based PDA liposome design is an excellent universal PDA platform that can be readily applicable to other sensor designs, allowing fast formation of the PDA-liposome layer and efficient tethering of receptors after the liposome immobilization on a glass substrate for both convenience and to allow for user-prepared microarrays.

3.4 Experimental section

3.4.1 Preparation of the Liposomes

A mixture of the PCDA-Epoxy and PCDA (4:1 mole ratio) was dissolved in 0.2mL of tetrahydrofuran. The solvent mixture was injected into 5mM 4-(2-hydroxyethyl)-1-piperazineethanesulfonic acid (HEPES) buffer at pH 8.0 (30 mL) and bath-sonicated for 5 min to produce the final concentration of the lipid vesicle of 0.5mM. After the sonication, the solution was filtered through 0.8mm cellulose syringe filter three times to remove liposomes of undesired size, and stored at 5 ^{o}C for 2 h.

3.4.2 Preparation of the Diacetylene Liposome having the Thymine-rich ssDNA Aptamer Immobilization of the Liposomes

To the 200 µl of 0.5 mM of PCDA-Epoxy/PCDA(4:1) liposome solution was added 100 µl (70 nmol) of the amine-modified thymine-rich ssDNA at 10℃. The reaction mixture was stirred and stored in an incubator at 37℃ for 4 hours. The resulting reaction mixture was sonicated for 10 min and cooled at 5℃ for 4 hours. The unbound ssDNA was removed through dialysis (Slide-A-Lyzer Dialysis Cassette, 20,000 MWCO, 0.1-0.5 ml capacity) in deionized water.

3.4.3 Immobilization of the Liposomes

An amine-modified glass slide was incubated in the PCDA-Epoxy/PCDA(4:1) liposome solution for 20 min at room temperature. The PDA-liposome-immobilized glass slide was vigorously rinsed using 10mM HEPES buffer pH 8.0 for 3 min. The glass was dried and stored under nitrogen at 5 ^{o}C. The immobilization of the PCDA-EDEA/PCDA-EDA(1:1) was carried out as described in ref. [12, and the PCDA-linker-NHS/PCDA(1:1) liposome was immobilized according to the procedures in ref. [7].

3.4.4 Fabrication of the PDA Microarray

A solution of 100 mM of ssDNA in 5mM HEPES buffer pH 9.5/3 SSC Buffer (1:1) was prepared. The ssDNA probe solution was then heated at 90 8C for 3 min. Thymine-rich ssDNA was spotted onto the glass slide coated with the PDA liposomes using a manual microarrayer (VP 475,V&P scientific, INC) at 70% humidity. The glass slide with the spotted ssDNA was incubated for 6 h at 75% humidity. After rinsing with 1% SDS buffer pH 8.0 for 3 min and deionized water, the slide was dried under a stream of nitrogen followed by the photopolymerization with 254nm UV light (1mW/cm^2) for 20 s.

3.4.5 Fluorescent Microscope Images

The liposome microarray was incubated with a solution containing various concentrations (0.005, 0.01, 0.050, 0.10, 0.50, and 1 mM: 1 – 130 ppm) of Hg2+for 1 hour. The fluorescence images were obtained by using a fluorescent microscope (Olympus BX51 W/DP71). The excitation wavelength was 600 nm. The data were obtained with five independent experiments. The error bar is standard deviation and each point represents the mean value. Other metal ions concentration and incubation time were the same as the Hg^{2+} incubation protocol.

3.4.6 Mercury Detection with the PDA Liposome in Solution

To a solution containing 100 µl of 0.05 mM solution of the PDA liposome having the thymine-rich ssDNA was added 50µl of concentrated Hg^{2+} solution to make the final concentration of 0.03 mM at room temperature. UV-vis and PL spectra were taken after 1 and 2 hours incubation at room temperature.

3.4.7 Synthesis and characterization

Materials and Method

All solvents were purchased from Sigma-Aldrich Chemicals. 10,12-pentacosadiynoic acid (PCDA) was purchased from GFS Chemicals. 2-(2-Aminoethoxy)ethanol, Nhydroxysuccinimide (NHS), 1-ethyl-3-[3-dimethylaminopropyl]carbodiimide hydrochloride (EDC), and succinic anhydride (SA), metal ions ($CdCl_2$, KCl, NaCl, $IrCl_2$, $SnCl_2$, $CuCl_2$, $ZnCl_2$, $HgCl_2$) were purchased from Sigma-Aldrich Chemical Co. The amine-modified thymine-rich ssDNA (5'-TTCTTTCTTCCCCTTGTTTGTT-3') oligonucleotides was purchased from Integrated DNA Technologies, Inc. Dialysis membranes were purchased from pierce (Slide-A-Lyzer Dialysis Cassette, 20,000 MWCO, 0.1-0.5 ml capacity). The gene frame for the liposome immobilization was purchased from Fisher Scientific. 1HNMR spectra (500 MHz) were obtained from Varian Inova 500 NMR instrumentation. UV/Vis absorption spectra were taken on a Varian Cary50 UV/Vis spectrophotometer. Fluorescence spectra were obtained using PTI QuantaMasterTM spectrofluorometers equipped with an integrating sphere. Fluorescence images were taken by Olympus BX51 W/DP71 fluorescent microscope.

Glass slides were cleaned with chloroform, acetone, and 2-propanol for 5 mins each. The precleaned glass slides were sonicated in sulfuric acid containing no-chromix. After thorough rinse with deionized water and dry, the glass slides were treated with 2

wt% 3-aminopropyltriethoxysilane in toluene solution for 1 hour and baked at 130 °C for 30 min. The glass slides were sonicated in toluene, toluene: methanol (1:1) and methanol for 3 mins each to remove any unbound silane monomer. The synthesis and characterization of the chemicals used in this study are in the supporting materials.Sodium hydroxide, potassium carbonate and all solvents were purchased from Fisher Scientific except ethyl alcohol (Decon Labs, Inc.). 4-Cyanophenol and 1-bromoalkaes were purchased from Acros Organics. All reagents were used as received.

Synthesis of PCDA Derivatives

The diacetylene monomer PCDA-Epoxy investigated in this work was synthesized through the following reaction scheme (Scheme S1).

PCDA-NHS: To a 10 mL of methylene chloride solution containing 2.00 g (5.34 mmol) of 10,12-pentacosadiynoic acid (PCDA) was added 0.76 g (6.94 mmol) of N-hydroxysuccinimide and 0.76 g (8.02 mmol) of 1-ethyl-3-[3-dimethylaminopropyl]carbodiimide hydrochloride at room temperature. The resulting reaction mixture was stirred at room temperature for 2 hs. The solvent was removed in vacuo, and the residue was purified by extraction with ethyl acetate to give 2.16 g (86.2 %) of the desired diacetylene monomer PCDA-NHS as a white solid: 1H NMR (500 MHz, CDCl3): δ 0.86 (t, 3H), 1.21-1.52 (m, 36H), 2.21 (t, 4H), 2.60 (t, 2H), 2.87 (s, 4H).

PCDA-Ethoxy-ethanol: To a 100 mL of methylene chloride solution containing 1.60 g (15.26 mmol) of 2-(2-aminoethoxy)ethanol was added dropwise 2.40 g (5.08 mmol) of PCDA-NHS in 50 mL of methylene chloride. The resulting reaction mixture was stirred for 3hs at room temperature and filtered. The solvent was removed from the filtrate was by applying vacuum. The residue was extracted with methylene chloride and washed with brine 3 times. The residue was further purified by recrystallization in methylene chloride to give 0.55 g (77.6 %) of the desired diacetylene monomer PCDA-Ethoxy-

ethanol as a white solid: 1H NMR (500 MHz, CDCl3): δ 0.85 (t, 3H), 1.22-1.52 (m, 36H), 2.22 (m 6H), 3.44 (q, 2H), 3.55 (q, 4H), 3.72 (q, 2H), 5.81 (s, 1H).

PCDA-Epoxy: 0.10 g (4.24 mmol) of sodiumhydride was suspended in 10 ml tetrahydrofuran at 5 ℃. To the suspension was added dropwise 1.00 g (2.16 mmol) of PCDA-Ethoxy-ethanol in 20 mL anhydrous tetrahydofuran for 15 mins and the reaction mixture was stirred for 4 hs at room temperature. To the mixture solution was added 0.50 g (3.69 mmol) of epibromohydrin and the reaction mixture was stirred at room temperature for overnight. The resulting reaction mixture was filtered and concentrated in vacuo, and the residue was purified by column chromatography (95:5 chloroform: methanol) to give 0.65 g of the desired diacetylene monomer PCDA-Epoxy (46.7 %) as a white solid: 1H NMR (500 MHz, CDCl3): δ 0.85 (t, 3H), 1.21-1.58 (m, 37H), 2.16 (t, 6H), 2.57 (q, 1H), 2.77 (t, 1H), 3.14 (m, 1H), 3.43 (m, 3H), 3.52 (t, 2H), 3.59-3.65 (m, 4H), 3.79 (q, 1H), 5.89(s, 1H).

3.5 References

[1]   a) T. M. Swager, *Acc. Chem. Res.* **1998**, *31*, 201. b) M. Lerclerc, *Adv. Mater.* **1999**, *11*, 1491. c) D. T. McQuade, A. E. Pullen, T. M. Swager, *Chem. Rev.* **2000**, *100*, 2537 d) S. W. Thomas III, G. G. Joly, T. M. Swager, *Chem. Rev.* **2007**, *107*, 1339.

[2]   a) J.-S Yang, T. M. Swager, *J. Am. Chem. Soc.* **1998**, *120*, 5321. b) J. Kim, D. T. McQuade, S. K. Mchugh, T. M. Swager, *Angew. Chem. Int. Ed.* **2000**, *39*, 3868. c) R. Sakai, I. Otsuka, T. Satoh, R. Kakuchi, H. Kaga, T. Kauchi, *Macromol.* **2006**, *39*, 4032.   d) B. Liu, G. C. Bazan, *Chem. Mater.* **2004**, *16*, 4467. e) H. A. Ho, M. Biissinot, M. G. Bergeron, G. Corbeil, K. Dore, D. Boudreau, M. Leclerc, *Angew. Chem. Int. Ed.* **2002**, *41*, 1548. f) C.-C. Pun, K. Lee, H. J. Kim, J. Kim, *Macromol.* **2006**, *39*, 7461. g) K. Lee, L. K. Povlich, J. Kim, *Adv. Func. Mat.*

2007, *17*, 2580. h) K. Lee, K. Maisel, J.-M. Rouillard, E. Gulari, J. Kim, *Chem. Mat.* **2008**, *20,* 2848. i) K. Lee, J.-M. Rouillard, T. Pham, E. Gulari, J. Kim, *Angew. Chem. Int. Ed*. **2007**, *46*, 4667. j) Y. Liu, K. S. Schanze, *Anal. Chem.* **2008**, *80*, 8605. k) I. B. Kim, U. H. F. Bunz, *J. Am. Chem. Soc.* **2006**, *128*, 2818.

[3]   a) J. B. Pang, L. Yang, B. McCaughey, H. S. Peng, H.S. Ashbaugh, C. J. Brinker,Y. F. Lu, *J.   Phys. Chem.* B **2006**, *110*, 7221. b) R. W. Carpick, T. M. Mayer, D. Y. Sasaki, A. R. Burns, *Langmuir* **2000**, *16*, 4639. c) K. Morigaki,T. Baumgart, U. Jonas, A. Offenhausser, W. Knoll, *Langmuir* **2002**, *18*, 4082. d) Q. Cheng, R. C. Stevens, *Langmiur* **1998**, *14*, 1974. e) R. W. Carpick, D. Y. Sasaki, A.R. Burns, *Langmiur* **2000**, *16*, 1270. e) G. Leiser, B. Tieke, G. Wegner, *Thin Solid Films* **1980**, *68*, 77.

[4]   a) G. Wegner, *Naturforsch. Teil B,* **1969**, *24*, 824. b) D. H. Charych, J. O. Nagy, W. Spevak, M. D. Bednarski, *Science* **1993**, *261*, 585. c) Y. Okawa ,M. Aono, *Nature* **2001**, *409*, 683. d) A. Miura, S. D. Feyter, M. M. S. Abdel-Mottaleb, A. Gesquière, P. C. M. Grim, G. Moessner, M. Sieffert, M. Klapper,. Klaus Müllen, F. C. De Schryver, *Langmiur*, **2003**, *19*, 6474.

[5]   a) R. R. Chance, *Macromol.* **1980**, *13*, 396. b) J.-M. Kim, J.-S. Lee, H. Choi, D. Sohn, D. J. Ahn, *Macromol.* **2005**, *38*, 9366.

[6]   a) A. Reichert, J. O. Nagy, W. Spevak, D. Charych, *J. Am. Chem. Soc.*, **1995**, *117*. 829. b) J. Song, Q. Cheng, R. C. Stevens, *Chemistry and Physics of Lipids*, **2002,** *114*, 203. c) Q. Cheng, R. C. Stevens, *Adv. Mater.* **1997**, *9*, 481. d) J.-M. Kim, J.-S. Lee, J.-S. Lee, S. Woo, D. J. Ahn, *Macromol. Chem. Phys*. **2005**, *206*, 2299 e) Y. K. Jung, T. W. Kim, C. Jung, D. Cho, H. G. Park, *Small.* **2008,** *4*, 1778 f) M. A. Reppy, B. A. Pindzola, *Chem. Commun.* **2007**, 4317 g) D. J. Ahn, J.-M. Kim, *Acc. Chem. Res.* **2008**, *41*, 805.

[7]   J. Lee, H. Kim, J. Kim, *J. Am. Chem. Soc.* **2008**, *130*, 5010.

[8]   H. Kim, J. Lee, T. Kim, T. S. Lee, J. Kim, *Adv. Mater*. **2008**, *20*, 1117.

[9]   a) W. Zheng, M. Aschner, J.-F. Ghersi-Egea, *Toxicol. Appl. Pharmacol.* **2003**, *192*, 1. (b) D. P. Wojcik, M. E. Godfrey, D. Christie, B. E. Haley, *Neuroendocrinol. Lett.* **2006**, *27*, 415. (c) J. Mutter, J. Naumann, R. Schneider, H. Walach, B. Haley, *Neuroendocrinol. Lett.* **2005**, *26*, 439.

[10]   Environmental Standards for Mercury, *United State Environmental Protection Agency (EPA).*

[11]   a) J.-S. Lee, M. S. Han, C. A. Mirkin, *Angew. Chem. Int.* **2007**, *46*, 4093. b) C.-C Huang, C.-K. Ching, Z.-H. Lin, K.-H. Lee, H.-T. Chang, *Anal. Chem.* **2008**, *80*, 1497. c) T. Li, S. Dong, E. Wang, *Anal. Chem.* **2009**, *81*, 2144. d) P. Chen, C. He, *J. Am. Chem. Soc.* **2004**, *126*, 728. e) Y. Zhao, Z. Zhong, *J. Am. Chem. Soc.* **2006**, *128*, 9988.

[12]   C. Mateo1, V. Grazu, J. M. Palomo, F. Lopez-Gallego, R. Fernandez-Lafuente, J. M. Guisan. *Nature Protocols* **2007**, *2*, 1022.

[13]   a) J.-M. Kim, Y. B. Lee, D. H. Yang, J.-S. Lee, G. S. Lee, D. J. Ahn, *J. Am. Chem. Soc.* **2005**, *127*, 17580. b) J.-M. Kim, E.-K. Ji, S.-M. Woo, H. Lee, D. J. Ahn, *Adv. Mater.* **2003**, *15*, 1118.

[14]   a) X. Liu, Y. Tang, L. Wang, J. Zhang, S. Song, C. Fan, S. Wang, *Adv. Mater.* **2007**, *19*, 1471. b) A. Ono, H. Togashi, *Angew. Chem. Int. Ed.* **2004**, *43*, 4300. c) X.-J Zhu, S.-T Fu, W.-K. Wong, J.-P. Guo, W.-Y. Wong, *Angew. Chem. Int. Ed.* **2006**, *45*, 3150.

CHAPTER 4

Selective and sensitive detection of melamine by intra/inter liposomal

interaction of polydiacetylene liposomes

4.1 Introduction

Melamine is an organic compound that is often combined with formaldehyde to make a synthetic polymer having both excellent thermal resistance and heat tolerance. The melamine resin is a versatile material having a highly stable structure and is considered as non-toxic plastic. However, above the safety regulation level (2.5 ppm in USA and EU and 1 ppm in China) melamine monomers can cause acute kidney failure, serious renal problems and even death.[1] Unreacted melamine monomers may possibly leach out from the polymer at high temperatures. However, the misuse of melamine is a much more important issue. Melamine has high nitrogen content and this fact was abused to misleadingly fortify protein content by adding melamine to wheat gluten and infant formula. It has been reported that hundreds of pets died of renal failure in 2007 and there were an estimated 300,000 victims and 50,000 babies that were hospitalized from the infant formula containing melamine in 2008.[2] The conventional analytical method for the detection of melamine is a mass spectrometry. However, conventional lab-scale equipment is expensive and requires specific skills for operation. Therefore, there has been much effort to devise an effective and simple detection system for melamine.

Recently, various methods including electrochemical,[3] gas chromatography (GC),[4] liquid chromatography (LC),[5] capillary electrophoresis,[6] ELISA,[7] and colorimetric sensors[8] have been investigated to detect melamine. In this contribution, we report a practical and convenient colorimetric detection system based on polydiacetylene (PDA) liposome having a dual signaling capability for rapid, selective and sensitive detection of melamine. PDA sensory systems are unique in that they have the sensitive colorimetric/fluorescence dual detection capability and are prepared through a simple molecular self-assembly followed by photo-polymerization.[9–11] The photo-induced topochemical polymerization converts well-assembled diacetylene monomers into conjugated PDA with a blue color (absorption lmax at 640 nm). Upon exposure to external stimuli, the absorption lmax of PDA shifts from 640 nm (blue phase) to 540 nm (red phase). Interestingly, the triggered red phase of PDA is also weakly fluorescent, so PDA can provide dual signaling capability.[12,13] The colorimetric change is believed to appear from the conformational change of conjugated backbone of PDA induced by external stimuli including pH, temperature,[14,15] ions,[16,17] and mechanical pressure.[18,19]

4.2 Results and Discussion

The interaction between melamine and cyanuric acid (CA) is well known in the fact that they form a stable melamine–cyanurate complex through hydrogen bonding between imide and amino-pyridine moieties at a neutral pH.[20–22] We rationally encoded the melamine/CA interaction mechanism in our CA-carrying PDA design in such a way that melamine molecules form multiple hydrogen bondings with the CA at the surface of PDA liposomes. As we presented in our previous works,[16,17,23] the steric repulsion resulting from the complex formation between the probe and the target at the liposome surface induces the rearrangement of yne–ene conjugated backbone of PDA and produces the color change to red and fluorescence development. The same phenomenon is
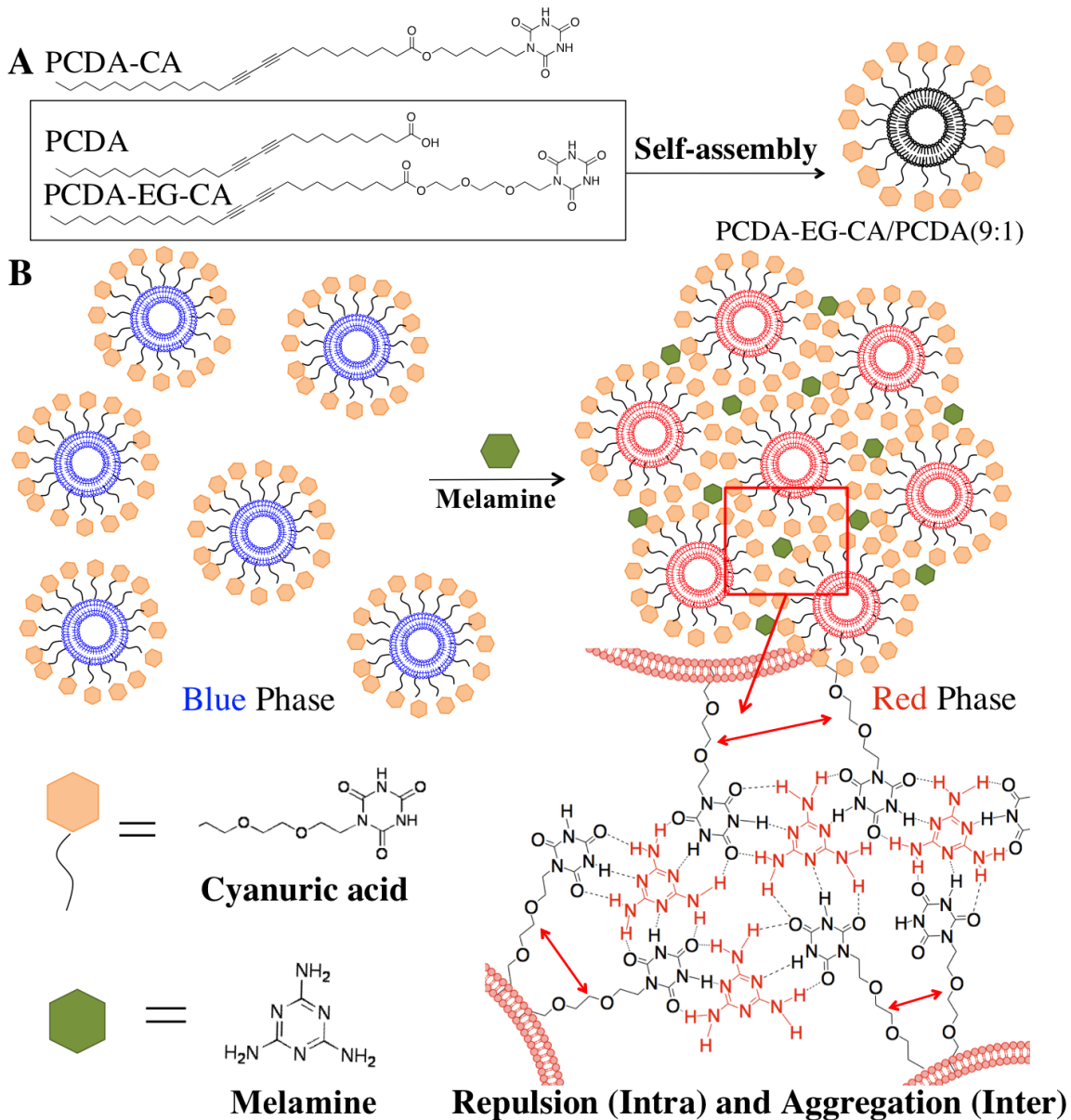
Scheme 4.1. (A) Chemical structure of the investigated diacetylene monomers, PCDA, PCDA-CA and PCDA-EG-CA. (B) Schematic illustration of melamine and CA derived PDA liposome by intra/inter molecular hydrogen bond and resulting steric aggregation and repulsion.

expected to occur in the colorimetric/fluorescent PDA liposome system for melamine detection. The degree of induced color change by melamine should depend on how target melamine molecules form hydrogen bonds with CA at the PDA liposome surface. When densely packed CA probes on the liposome surface recognize melamine by forming hydrogen bonding, two types of CA–melamine–CA hydrogen bonding can be defined.

First, a melamine molecule can form hydrogen bonding with CA molecules of the same PDA liposome. That can be called an intra-liposomal CA–melamine–CA hydrogen bonding. Alternatively, a melamine molecule can form inter-liposomal CA–melamine– CA hydrogen bonding with CA molecules from difference PDA liposomes. The melamine/ CA hydrogen bonding will induce both intra-liposomal repulsion and inter-liposomal aggregation strain to the PDA liposomes resulting in the conformational change of conjugated PDA backbone as schematically illustrated in Scheme 4.1B. The resulting perturbation of the yne–ene backbone of PDA will produce rapid, selective and sensitive colorimetric/fluorescent dual signal in the presence of melamine.
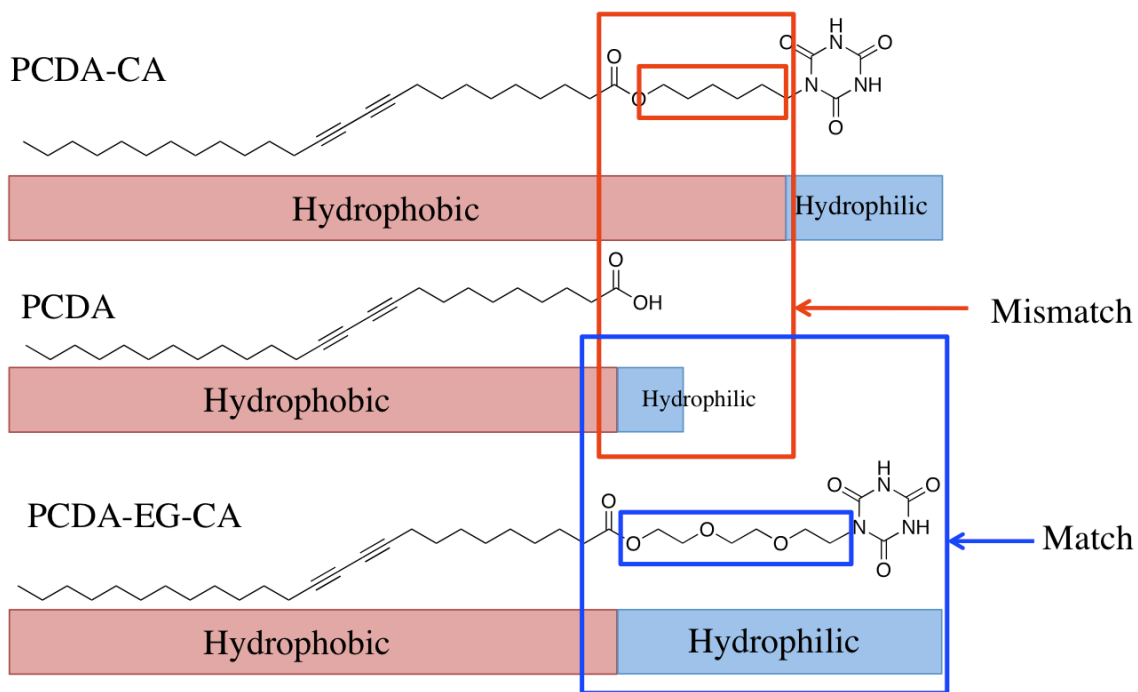
Scheme 4.2. Schematic illustration of amphiphilic matching of PCDA, PCDA-CA and PCDA-EG-CA molecules.

We synthesized two types of CA-carrying PDA monomers (PCDA-CA and PCDA-EG-CA) and examined the sensitivity for melamine detection (Scheme 1A). The PDA liposome solutions were prepared through sonication of the CA-carrying PCDA (PCDA-CA or PCDA-EG-CA) and PCDA (10,12- pentacosadiynoic acid) mixture having

60

various mole ratios (final concentration: 0.2 mM) in 5 mM HEPES buffer, pH 7.0, at 80 1C, followed by cooling for 6 hours and irradiation of 254 nm UV light for 30 s. We first conducted melamine detection tests with PCDA-CA/PCDA liposomes. We could confirm that the PCDA-CA/PCDA liposome (4/1 mole ratio) was able to detect melamine. However, the liposome solution produced a rather weak blue color after the photopolymerization and the detectable range of the optical color change by naked eye was 10 ppm level as shown in Figure 4.1. The rather weak blue color means that the quality of the PDA liposome formation is not good. We reasoned that we could improve the quality of the PDA liposome formation and the ensuing sensitivity of the system by improving the ordered structure of the self-assembled mixed PDA liposomes.
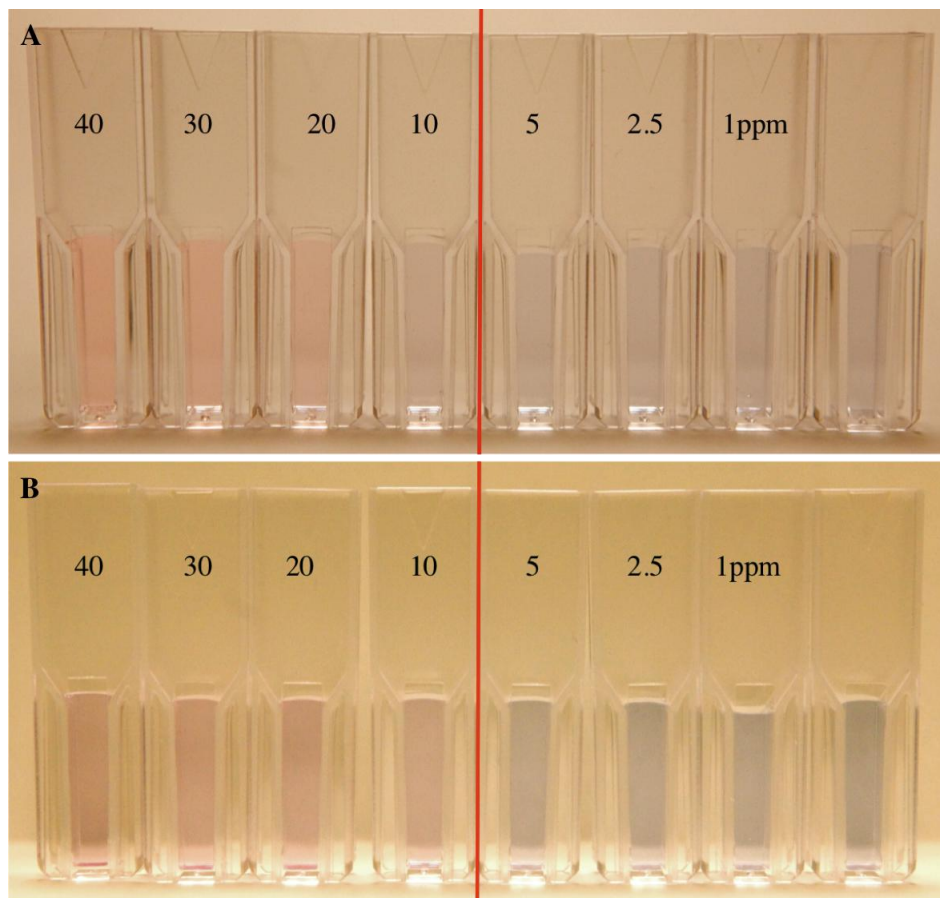
Figure 4.1. Colorimetric change of PCDA-CA/PCDA (4/1 mole ratio) in 5 mM (A) and 50 mM HEPES buffer pH 7.0 (B) upon the various concentration of melamine. Buffer concentration study was conducted to optimize the highest polymerization rate of PDA liposomes. 50 mM of HEPES buffer pH 7.0 showed the highest polymerization rate by blue color intensity.

As one can see in Scheme 4.2, there is spatial mismatch between the hydrophilic and hydrophobic parts of PCDA-CA and PCDA. The weak blue color after the polymerization can be explained by the amphiphilic mismatch and imbalance. Accordingly, we designed PCDA-EG-CA having hydrophilic and flexible linker to achieve improved ordering of the self-assembled liposome. PCDA-EG-CA has the ethylene glycol linker to match the length of its hydrophobic part with that of PCDA and also has a more balanced amphiphilic structure. As expected, PCDA-EG-CA/PCDA liposomes produced intense blue color upon polymerization and as shown in Figure 4.2, 100% of PCDA-EG-CA liposome showed 5 ppm level of detection limit by the naked eye. In the case of 100% of PCDA-CA liposome solution, on the contrary, the blue color intensity was very weak and the colorimetric change was not noticeable by the naked eye upon addition of the same amount of melamine.
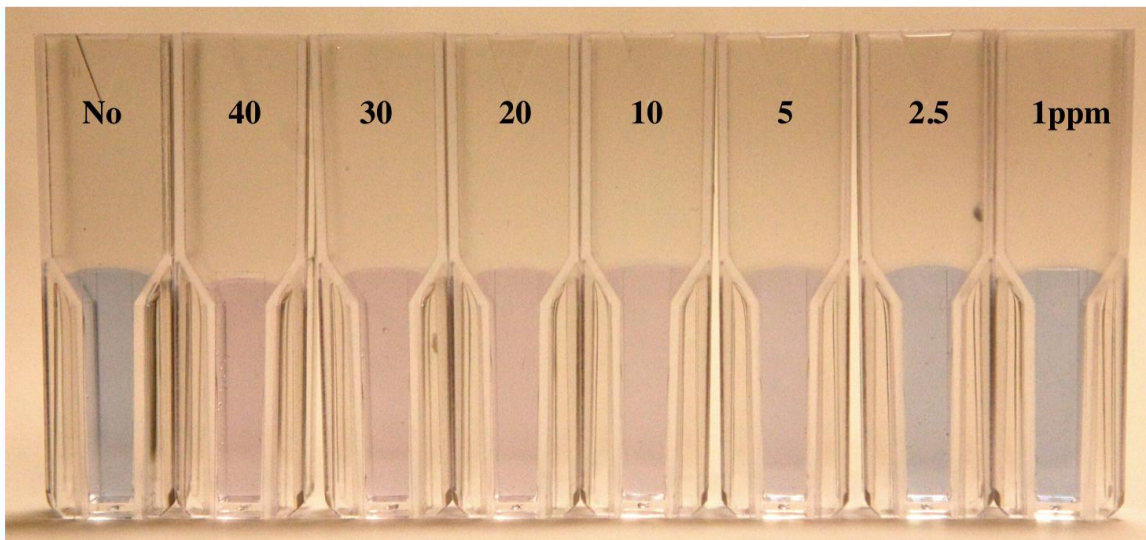
Figure 4.2. Colour change of 100 % PCDA-EG-CA liposome solution in 50 mM HEPES buffer pH 7.0 upon the various concentration of melamine.

We further optimized the PDA sensory system to achieve better detection limit and sensitivity by investigating various mixing ratios between PCDA and PCDA-EG-CA at 1 : 9, 1 : 6, 1 : 3, 1 : 1, 3 : 1, 6 : 1 and 9 : 1 (Figure 4.3). As the amount of PCEA-EG-CA increases the sensitivity also increases. Figure 4.4C shows the color change of the

best performing PCDA-EG-CA/PCDA (9/1 mole ratio) liposome solutions upon addition of various concentrations of melamine from 1 ppm to 40 ppm. 1 ppm level of melamine triggered the color change of the PDA liposome solution and this detection limit is suitable to detect melamine at the world regulation level. Even though it takes 5 min until the liposome solution shows a saturated color change from blue to red, we could observe a noticeable color change within 30 s after the addition of melamine. Prolonged incubation caused aggregation and precipitation of the liposome as shown in Figure. 4.3B.
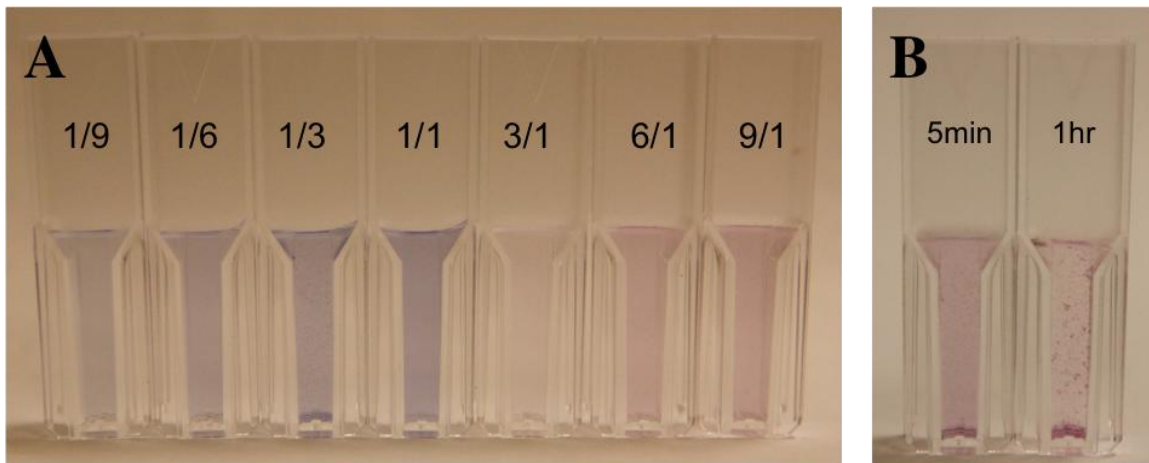
Figure 4.3. (A) Colorimetric response image of PCDA-EG-CA/PCDA (1/9, 1/6, 1/3, 1/1, 3/1, 6/1, 9/1) liposome upon 10 ppm of melamine. (B) Optical image of aggregated PCDA-EG-CA/PCDA (9/1) liposome upon addition of melamine after 5 min (a) and 1 hr (b).

We also confirmed the detection of melamine by the PDA liposome solution by means of UV-vis absorption and PL emission spectra. The absorption peak at 650 nm (blue phase) decreased and the 550 nm (red phase) absorption peak appeared and grew upon the addition of various concentrations of melamine (Figure 4.4A). The fluorescence intensity of the PCDA-EG-CA/PCDA liposome also increased upon the addition of melamine (Figu4.4B). We also conducted selectivity tests by adding uracil, cytosine and thymine. These molecules have similar chemical structures with melamine but do not form proper hydrogen bonds with CA to trigger the color change. Because those molecules can form hydrogen bonds with single CA, the necessary intra-liposomal
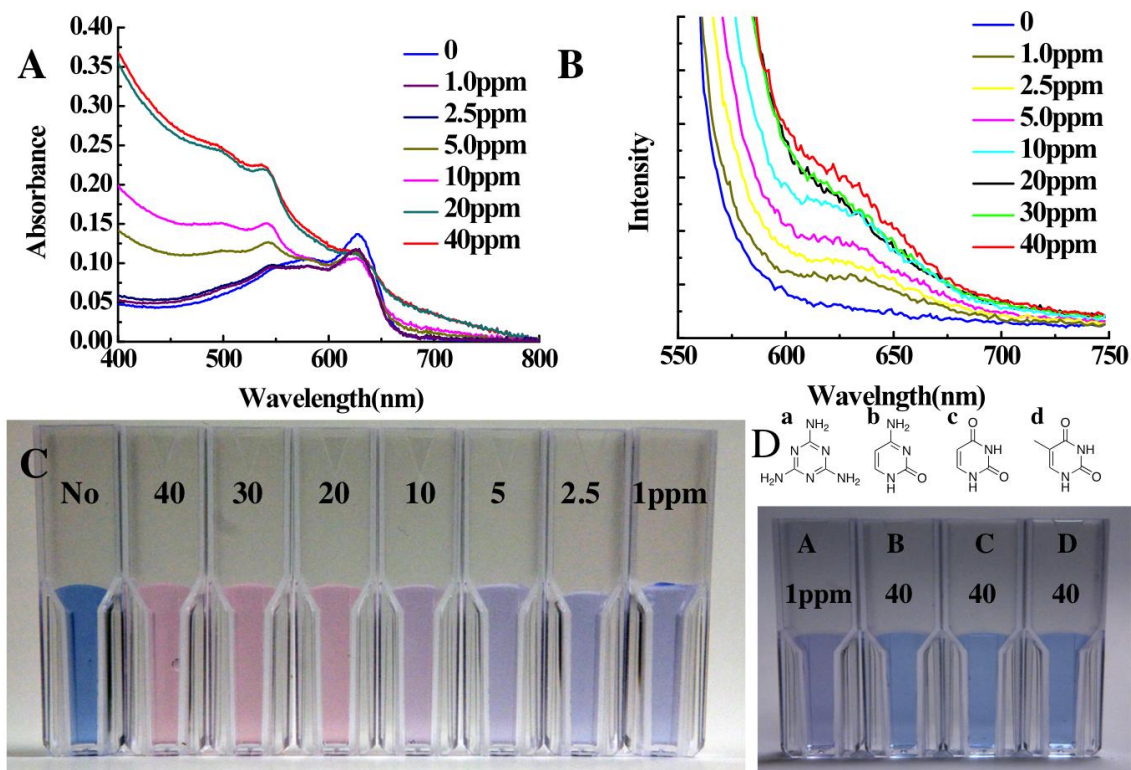
Figure. 4.4. (A) UV-vis spectra and (B) PL spectra of the PCDA-EG-CA/PCDA (9/1) liposome solution (final concentration: 0.2 mM) upon the addition of various concentrations of melamine after 5 min incubation. (C) Optical colorimetric change of polydiacetylene liposome upon addition of melamine (40 ppm–1 ppm). (D) Colour change of PCDA-EG-CA/PCDA (9/1) liposome solution in 50 mM HEPES buffer, pH 7.0, upon the addition of 1 ppm of melamine (a), 40 ppm of thymine (b), cytosine (c) and uracil (d).

repulsion and inter-liposomal aggregation for the colorimetric/fluorescence change are not likely formed. As one can clearly see in Figure 4.4D, we did not observe any detectable colorimetric change nor fluorescent development after adding even 40 ppm of cytosine, thymine and uracil.

We further developed analogous solid-state sensors and investigated the detection limit using the microarray technique. Figure 4.5. shows the fluorescence microscopy images of the PDA liposome microarray and the correlation between the fluorescence intensity and the concentration of melamine. We microarrayed the PCDA-EG-CA/PCA liposome solution to an amine modified glass substrate and the physically attached PDA liposome layer was photopolymerized for 30 seconds. Various concentrations of

melamine were added to the PDA liposome layer. Figure 4.5B shows the red fluorescence development upon the addition of various concentrations of melamine. As the concentration of melamine increases, more CA/melamine complex will be formed, and this induces stronger perturbation to the conjugated PDA backbone, resulting in a more intense red fluorescence. Based on the correlation curve, a quantitative analysis of an unknown melamine concentration is also achievable. The observed detection limit was 0.5 ppm lower than that of the colorimetric detection by the solution system. This detection limit was obtained by our fluorescence microscope, and could be much better if more sensitive equipment is used.
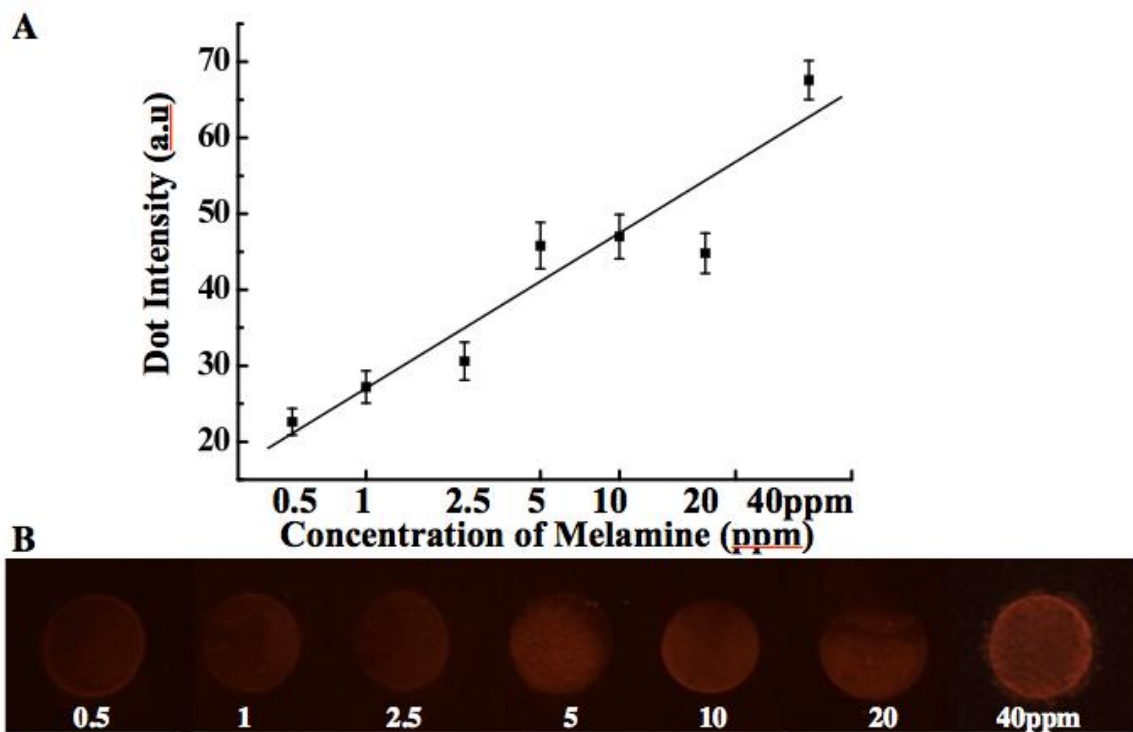
Figure. 4.5. (A) Correlation curve between the fluorescence intensity and the amount of melamine (the error bar is a standard deviation and each point represents the mean value). (B) Fluorescence microscope image of the PDA microarray upon exposure to the various concentrations of melamine from 0.5 to 40 ppm after 30 min incubation at room temperature (excitation at 550 nm and a long-pass emission filter with 600 nm cutoff were used).

4.3 Conclusions

we represented a rapid, sensitive, and selective PDA sensory system for melamine detection based on the multiple hydrogen bondings between cyanuric acid and melamine. The intra/inter liposomal hydrogen bonding between the target melamine and cyanuric acid receptor at the PDA liposome surface induces perturbation of the conjugated PDA backbone and results in rapid and sensitive colorimetric/fluorescence change of the PDA liposome. Detection limit of the developed PDA system is 1.0 ppm and 0.5 ppm for colorimetric PDA liposome solution and fluorescent PDA liposome microarray, respectively. The PDA liposomebased sensor assay can be conveniently prepared by simple self-assembly of rationally designed diacetylene molecules. The presented design principle of the sensing mechanism by intra/inter liposomal interaction of PDA liposome and target molecules can be readily applicable to the development of other PDA-based colorimetric/fluorescent sensory systems to detect various biomolecules and chemicals selectively and sensitively.

4.4 Experimental section

4.4.1 Materials and Method

Materials and Method. All solvents were purchased from Sigma-Aldrich Chemicals. 10,12-pentacosadiynoic acid (PCDA) was purchased from GFS Chemicals. Dicyclohexylcarbodiimide, 4-dimethylaminopyridine, cyanuric acid, 1,8-diazabicycloundec-7-ene, carbon tetrabromide, triphenylphosphine, 6-bromohexan-1-ol, tri(ethylene glycol) were purchased from SigmaAldrich Chemical Co. UV/Vis absorption spectra were taken on a Varian Cary50 UV/Vis spectrophotometer. Fluorescence spectra were obtained using PTI QuantaMasterTM spectrofluorometers equipped with an integrating sphere. Fluorescence images were taken by Olympus BX51 W/DP71 fluorescent microscope. Amine modified glass slides were prepared according

66

to the reference 15. Briefly, glass slides were cleaned with chloroform, acetone, and 2-propanol for 5 min each. The precleaned glass slides were sonicated in sulfuric acid containing no-chromix. After thorough rinse with deionized water and dry, the glass slides were treated with 2 wt% solution of 3-aminopropyltriethoxysilane in toluene for 1 hour and baked at 130 ℃ for 30 min. The glass slides were sonicated in toluene, toluene: methanol (1:1) and methanol for 3 min each to remove any unbound silane monomer

4.4.2 Melamine Detection with the PDA Liposome in Solution

To a solution containing 1 ml of 0.2 mM solution of the PCDA-EG-CA/PCDA (9/1) liposome was added melamine solution to make the each desired concentration from 1 to 40 ppm at room temperature. UV-vis and PL spectra were taken after 5 min incubation at room temperature. Microarray of PDA Liposome: the resulting PDA liposome was spotted onto amine modified glass slide with a manual microarray (V&P Scientitic, VP475A) and stored in a humidity chamber (humidity ~ 70%) for 6 h. Amine modified glass slide was prepared according to the reference.[12] After carefully rinse with 50mM of HEPES buffer pH 7.0, and dried under a stream of nitrogen.

4.4.3 Fluorescent Microscope Images

The liposome microarray was incubated with a solution containing various concentrations (0.5, 1, 2.5, 5, 10, 20, 40 ppm) of melamine for 30 min. The fluorescence images were obtained by using a fluorescent microscope (Olympus BX51 W/DP71). The excitation wavelength was 600 nm. The data were obtained with five independent experiments.

4.4.4 Preparation of the Diacetylene Liposome

Preparation of the Diacetylene Liposome: 100 µl of PCDA-EG-CA/PCDA (9:1 mole ratio) monomer mixture solution was injected rapidly to 20 ml of 50 mM HEPES buffer pH 7.0. The suspended solution was sonicated for 20 min by probe disembrator and filtered with 0.8 µm cellulose acetate syringe filter. The dispersed PDA liposome solution was cooled at 5 ℃ for 6 hours. The final concentration is 0.2 mM.

4.4.5 Immobilization of the Liposomes

An amine-modified glass slide was incubated in the PCDA-Epoxy/PCDA(4:1) liposome solution for 20 min at room temperature. The PDA-liposome-immobilized glass slide was vigorously rinsed using 10mM HEPES buffer pH 8.0 for 3 min. The glass was dried and stored under nitrogen at 5 ^{o}C. The immobilization of the PCDA-EDEA/PCDA-EDA(1:1) was carried out as described in ref. [12, and the PCDA-linker-NHS/PCDA(1:1) liposome was immobilized according to the procedures in ref. [7].

4.4.6 Synthesis of PCDA Derivatives

The diacetylene monomer PCDA-CA and PCDA-EG-CA investigated in this work were synthesized through the following reaction scheme (Scheme S1).

Synthesis of PCDA-CA

6-Bromohexyl pentacosa-10,12-diynoate: To a solution of 10,12-pentacosadiynoic acid (2 g, 5.34 mmol)) in dichloromethane (30 mL) at 0 ^{o}C was added 6-bromohexan-1-ol (1.06 g, 5.88 mmol), dicyclohexylcarbodiimide (1.32 g, 6.41 mmol) and 4-dimethylaminopyridine (0.012 g, 0.10 mmol). After the reaction mixture was vigorously stirred for 2 hours, 20 mL of hexane was poured into the mixture and the white urea solid was filtered off. The filtrate solution was concentrated in vacuo. The residue was purified by silica gel column chromatography (hexane/diethyl ether =10/1) to give 2.24 g (78 %)

of desired diacetylene monomer   6-bromohexyl pentacosa-10,12-diynoate as a colorless oil. ^{1}H NMR (300 MHz, CDCl3): δ 1.23 (t, J = 6.8 Hz, 3H), 1.26-1.62 (m, 38H), 1.85-1.87 (m, 2H), 2.22-2.32 (m, 6H), 3.41 (t, J = 6.6 Hz, 2H), 4.07 (t, J = 6.6 Hz, 2H). ^{13}C NMR (100 MHz, CDCl3): δ 13.98, 19.08, 22.60, 24.88, 25.04, 27.69, 28.24, 28.78, 28.99, 29.52, 31.80, 32.52, 33.52, 34.23, 64.00, 65.21, 173.85, MS (ES): Calcd, 536.3; found (M+Na)$^{+}$, 559.4.

PCDA-CA: To a solution of   6-bromohexyl pentacosa-10,12-diynoate (1.7 g, 3.16 mmol) in dimethylformamide (50 mL) was added cyanuric acid (4.08 g, 31.60 mmol) and 1,8-diazabicycloundec-7-ene (0.47 mL, 3.16 mmol). The reaction mixture was heated under 60 ^{o}C for 8 hours, poured into the water and extracted with chloroform. The organic layer was washed 3 times with water to eliminate the excess cyanuric acid, dried with MgSO4 and filtered. Most of solvent was removed under vacuo. The residue was recrystallized in ethyl acetate to give 1.5 g (81 %) of the desired diacetylene monomer PCDA-CA as a white solid. mp 127 ^{o}C. ^{1}H NMR (400 MHz, CDCl$_3$): δ 0.87 (t, J = 6.8 Hz, 3H), 1.25-1.64 (m, 40H), 2.21-2.26 (m, 4H), 2.28 (t, J = 7.2 Hz, 2H), 3.85 (t, J = 6.8 Hz, 2H), 4.05 (t, J = 6.6 Hz, 2H), 9.10 (brs, 2H) . ^{13}C NMR (100 MHz, CDCl$_3$): 14.07, 19.15, 22.63, 24.88, 25.46, 26.14, 27.58, 28.26, 28.30, 28.42, 28.72, 28.81, 28.86, 29.05, 29.29, 29.42, 29.55, 29.57, 29.59, 31.86, 34.28, 41.85, 64.09, 65.16, 65.24, 77.39, 77.57, 147.81, 148.97, 173.99. MS (ES): Calcd, 585.4; found (M+Na)$^{+}$, 608.4.

Synthesis of PCDA-EG-CA

2-(2-(2-Bromoethoxy)ethoxy)ethanol: To a solution of tri(ethylene glycol) (4.08 g, 27.14 mmol) in dichloromethane (50 mL) at 0 ^{o}C was added carbon tetrabromide (3.00 g, 9.05 mmol) and triphenylphosphine (2.61 g, 9.95 mmol). The reaction mixture was stirred at room temperature for 2 hours, and the solvent was removed in vacuo. The residue was purified by silica gel column chromatography (hexane/ethyl acetate=1/2) to

give 1.61 g (83 %) of desired monomer 2-(2-(2-bromoethoxy)ethoxy)ethanol as yellowish oil (1.61 g). ^{1}H NMR (400 MHz, CDCl$_3$): δ 2.18 (brs, 1H), 3.44 (t, J = 6.4 Hz, 2H), 3.58 (m, 2H), 3.64 (s, 4H), 3.70 (m, 2H), 3.78 (t, J = 6.2 Hz, 2H).

2-(2-(2-Bromoethoxy)ethoxy)ethyl pentacosa-10,12-diynoate: To a solution of 10,12-pentacosadiynoic acid (2 g, 5.34 mmol)) in dichloromethane (30 mL) at 0 ^{o}C was added 2-(2-(2-bromoethoxy)ethoxy)ethanol (1.32 g, 5.34 mmol), dicyclohexylcarbodiimide (1.32 g, 6.41 mmol) and 4-dimethylaminopyridine (0.012g, 0.10 mmol). After the reaction mixture was vigorously stirred for 2 hours, 20 mL of hexane was poured into the mixture and the white urea solid was filtered off. The solvent was removed in vacuo. The residue was purified by silica gel column chromatography (hexane/ethyl acetate =10/1) to give 2.7 g (89 %) of desired diacetylene monomer 2-(2-(2-bromoethoxy)ethoxy)ethyl pentacosa-10,12-diynoate as a colorless oil. ^{1}H NMR (400 MHz, CDCl3): δ 0.84 (t, J = 6.8 Hz, 3H), 1.21-1.32 (m, 26H), 1.43-1.59 (m, 6H), 2.20 (t, J = 6.8 Hz, 4H), 2.29 (t, J = 7.6 Hz, 2H), 3.43 (t, J = 6.2 Hz, 2H), 3.62-3.68 (m, 6H),3.77 (t, J = 6.2 Hz, 2H), 4.19 (t, J = 4.8 Hz, 2H). ^{13}C NMR (100 MHz, CDCl$_3$): δ 13.99, 19.04, 22.55, 24.72, 28.23, 28.61, 28.77, 28.96, 29.21, 29.34, 29.52, 30.11, 31.78, 34.00, 63.14, 65.17, 69.13, 70.41, 71.12, 77.34, 173.48. MS (ES): Calcd, 568.3; found (M+Na)$^+$, 591.3

PCDA-EG-CA: To a solution of 2-(2-(2-Bromoethoxy)ethoxy)ethyl pentacosa-10,12-diynoate (1.9 g, 3.33 mmol) in dimethylformamide (50 mL) was added cyanuric acid (4.30 g, 33.33 mmol) and 1,8-diazabicycloundec-7-ene (0.50 mL, 3.33 mmol). The reaction mixture was heated under 60 ^{o}C for 8 hours, poured into the water and extracted with ethyl acetate. The organic layer was washed 3 times with water to eliminate the excess cyanuric acid, dried with MgSO4 and filtered. Most of solvent was removed under vacuo. The resulting solution was recrystallized from methyl alcohol and ethyl acetate to give 1.56 g (76 %) of desired diacetylene monomer PCDA-EG-CA as a white solid. mp

80 °C. ^{1}H NMR (400 MHz, CDCl$_3$): δ 0.875 (t, *J* = 7.0 Hz, 3H), 1.25-1.47 (m, 26H), 1.49-1.57 (m, 4H), 1.60 (t, *J* = 7.0 Hz, 2H), 2.22-2.25 (m, 4H), 2.32 (t, *J* = 7.6 Hz, 2H), 3.65-3.69 (m, 6H), 3.76 (t, *J* = 5.2 Hz, 2H), 4.07 (t, *J* = 5.2 Hz, 2H), 4.22 (t, *J* = 4.8 Hz, 2H), 9.49 (brs, 2H) . ^{13}C NMR (100 MHz, CDCl$_3$): δ 14.07, 19.15, 22.63, 24.78, 28.27, 28.30, 28.73, 28.81, 28.86, 29.05, 29.29, 29.42, 29.59, 31.86, 34.12, 40.46, 63.27, 65.17, 65.24, 67.32, 69.00, 69.80, 70.42, 77.38, 77.55, 148.24, 149.22, 173.97. MS (ES): Calcd, 617.4; found (M+Na)$^+$, 640.4.

4.5 References

[1]   L. Zhu, G. Gamez, H. Chen, K. Chingin and R. Zenobi, *Chem. Commun.*, **2009**, 559-561.

[2]   http://en.wikipedia.org/wiki/2008_Chinese_milk_scandal.

[3]   H. Zhu, S. Zhang, M. Li, Y. Shao and Z. Zhu, *Chem. Commun.*, *46*, 2259-2261.

[4]   J. P. Toth and P. C. Bardalaye, *J. Chromatogr. A*, **1987**, *408*, 335-340.

[5]   M. S. Filigenzi, E. R. Tor, R. H. Poppenga, L. A. Aston and B. Puschner, *Rapid. Commun. Mass SP.*, **2007**, *21*, 4027-4032.

[6]   H. A. Cook, C. W. Klampfl and W. Buchberger, *Electrophoresis*, **2005**, *26*, 1576-1583.

[7]   E. A. E. Garber, *J. Food. Protect.*, **2008**, *71*, 509.

[8]   K. Ai, Y. Liu and L. Lu, *J. Am. Chem. Soc.*, **2009**, *131*, 9496-9497.

[9]   D. J. Ahn, S. Lee and J.-M. Kim, *Adv. Func. Mater.*, **2009**, *19*, 1483-1496.

[10]   D. J. Ahn and J.-M. Kim, *Accounts Chem. Res.*, **2008**, *41*, 805-816.

[11]   K. Lee, L. K. Povlich and J. Kim, *Analyst*, **2010**, DOI: 10.1039/c0an00239a.

[12]   R. R. Chance, *Macromolecules*, **1980**, *13*, 396-398.

[13]   J.-M. Kim, J.-S. Lee, H. Choi, D. Sohn and D. J. Ahn, *Macromolecules*, **2005**, *38*, 9366-9376.

[14] S. Lee and J.-M. Kim, *Macromolecules*, **2007**, *40*, 9201-9204.

[15] J. Pang, L. Yang, B. F. McCaughey, H. Peng, H. S. Ashbaugh, C. J. Brinker and Y. Lu, *J. Phys. Chem. B*, **2006**, *110*, 7221-7225.

[16] J. Lee, H. Jun and J. Kim, *Adv. Mater.*, **2009**, *21*, 3674-3677.

[17] J. Lee, H.-J. Kim and J. Kim, *J. Am. Chem. Soc.*, **2008**, *130*, 5010-5011.

[18] K. Tashiro, H. Nishimura and M. Kobayashi, *Macromolecules*, **1996**, *29*, 8188-8196.

[19] R. W. Carpick, D. Y. Sasaki and A. R. Burns, *Langmuir*, **2000**, *16*, 1270-1278.

[20] J. M. Lehn, M. Mascal, A. Decian and J. Fischer, *J. Chem. Soc., Chem. Commun.*, **1990**, 479-481.

[21]   F. J. Hoeben, J. Zhang, C. C. Lee, M. J. Pouderoijen, M. Wolffs, F. Würthner, A. P. Schenning, E. Meijer and S. De Feyter, *Chem–Eur. J.*, **2008**, *14*, 8579-8589.

[22]   S. Yagai, S. Hamamura, H. Wang, V. Stepanenko, T. Seki, K. Unoike, Y. Kikkawa, T. Karatsu, A. Kitamura and F. Wurthner, *Org. Biomol. Chem.*, **2009**, *7*, 3926-3929.

[23] D. Seo and J. Kim, *Adv. Funct. Mater.*, **2010**, *20*, 1397-1403.

CHAPTER 5

Colorimetric Detection of Warfare Gases by Polydiacetylenes toward Equipment-free detection

Manuscript in preparation

5.1 Introduction

Nerve agents are one of the lethal weapons of mass destruction (WMD) containing organophosphates (OP) that disrupt the nerve transfer mechanism. When nerve agents were inhaled into a human body, they make strong covalent bonds with acetylcholinesterase (neurotransmitter enzyme) and inhibit the enzyme from degrading acetylcholine.[1] As a result acetylcholine continues to transmit nerve impulses and muscle contractions do not stop. Consequently whole nerve system begins to operate abnormally causing vomiting, muscle twitching and convulsion. Nerve agents are known as G-agents (Tarbun, Soman, Cyclosarin, Sarin) and VX. For example, Sarin, a G-agent, was released by the terrorist at a Tokyo subway station in 1995 Japan, resulting in more than 5000 human casualties. The VX is ten-fold more toxic than G-agents and considered as the most toxic chemical ever synthesized. Unfortunately these nerve agents are highly adhesive and volatile but colorless, odorless, and tasteless making detection of these chemicals very difficult. Therefore, developing a reliable nerve agent detection system is highly demanding but critically desirable in this worrisome terror-threatening era.

Conventional analytical methods such as gas chromatography[2] and mass spectroscopy[3] are still considered as the most assuring techniques even though recently various sensors based on fluorescence[4], carbon nano-tube[5], microcantilever[6], liquid

crystal[7] have been investigated to detect nerve agents. The conventional analytical detection systems, however, require expensive equipment that are commonly not portable due to heaviness and bulkiness and only operable by well-trained personnel. Therefore, a simple and fast yet reliable detection system is highly desirable. Particularly, equipment-free detection such as colorimetric detection by naked eyes would be the most advantageous and practically useful method.

In this contribution, we present our recent development of a rapid, highly selective and sensitive, and convenient colorimetric nerve agent detecting system based on rationally designed polydiacetylene (PDA) liposomes both in solutions and in solid films. PDA-based sensory systems are unique in that they have a colorimetric/fluorescence dual detection capability and self-signaling property[8]. Furthermore, the preparation protocol is very simple through convenient molecular self-assembly followed by fast photo-polymerization. The photo-induced topochemical polymerization converts diacetylene monomers into conjugated PDA having a blue color (absorption λ_{max} at 640 nm) via 1,4 addition polymerization. Interestingly, the absorption λ_{max} shifts from 640 nm (blue phase) to 540 nm (red phase) when an external stimulus is applied to PDA and the red phase also generates red fluorescence providing a dual signaling capability.[9] The colorimetric transition is believed to appear from the conformational change of the conjugated backbone of PDA induced by external stimuli including bacteria[10], pH[11], temperature[12], ions[13], and mechanical stress[14].

5.2 Results and Discussion

In this chapter we designed diacetylene molecules having an oxime (OX) functional group to utilize the attractive dual signaling capability of PDA liposome for the development of nerve agents detection system. OX has been used to make an antidote such as 2-pralidoxime (2-PAM) to detoxify organo-phosphorous nerve agents. Typically

2-PAM is a chloride salt having an oxime (OX) functional group and reversibly binds to OP-inactivated acetylcholinesterase first then attaches to the OP efficiently reducing the irreversible binding of organophosphates to acetylcholinesterase. Because the reversible binding of 2-PAM does not inactivate the enzyme function, 2-PAM is an effective antidote.[15] We applied the reactivity between 2-PAM and OP to the PDA based sensor system. We designed the oxime-modified polydiacetylene (OX-PDA) derivatives shown in **Scheme 1A**. We previously demonstrated that steric repulsion of probe/target complex at a liposome surface induces rearrangement of conjugated backbone of PDA and produces color transition from blue to red and also fluorescence development[13, 16]. We also found that inter-liposomal interactions played an critical role in sensitive optical signal generation.[16b] The similar steric perturbation and inter-liposomal interaction are expected to occur in our PDA-based nerve agent detection system as schematically described in Scheme 1C. The OX at the surface of PDA liposomes will rapidly react with OP molecules, and the resulting OX/OP complexes produce repulsive strain to the conjugated backbone of the self-assembled PDA liposomes. In addition, the liposome surface will become more hydrophobic by the OX/OP complex formation likely causing massive aggregation of liposomes in aqueous environment. The two factors of repulsion and aggregation will impose large stress on the conjugated backbone of PDA inducing the conformational change of PDA backbone as illustrated in **Scheme 1C**. The conformational change will appear as a rapid and sensitive colorimetric transition of PDA liposomes.
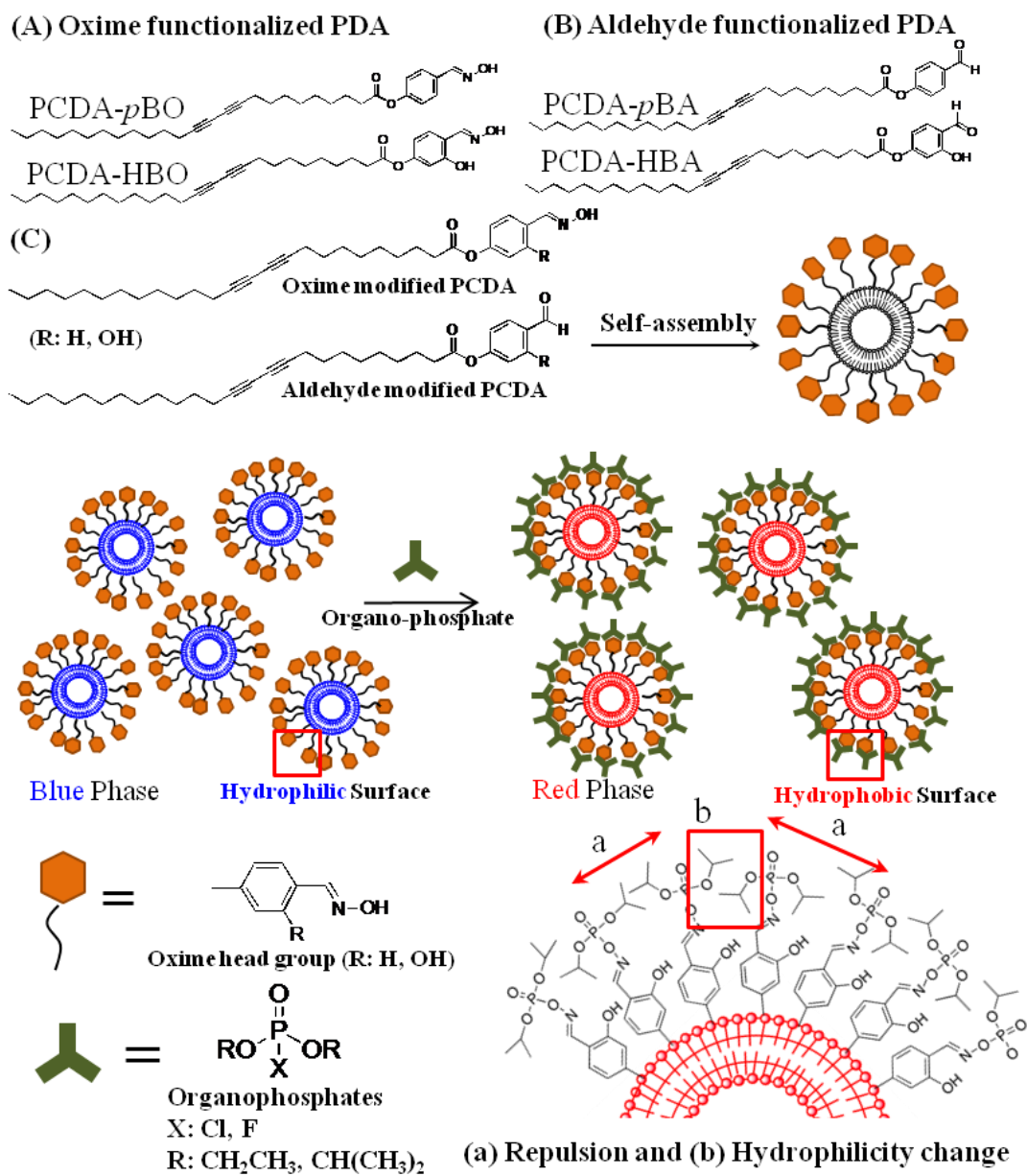
Scheme 5.1. Investigated (A) oxime functionalized and (B) aldehyde functionalized PDA monomers. (C) Schematic illustration of organophosphate detection using PDA liposome by (a) repulsion and (b) surface property change from hydrophilic to hydrophobic.

Scheme 5.1 shows the chemical structure of the investigated PDA monomers having oxime (OX-PDAs) and aldehyde functionality. The reactivity of OX toward OP molecules is significantly enhanced by the α-effect of the hydroxyl group[4b]. OX is known to be 100-fold more reactive with organo-phosphorous electrophiles than phenols having a similar pKa[17]. We synthesized PCDA-*p*BO and PCDA-HBO having an ester

linkage. The stability of PDA liposomes is closely related to the sensitivity of the PDA sensory system and can be tuned by adjusting the intermolecular self-assembling force between the diacetylene molecules. for example adding and removing hydrogen bonds[12b].
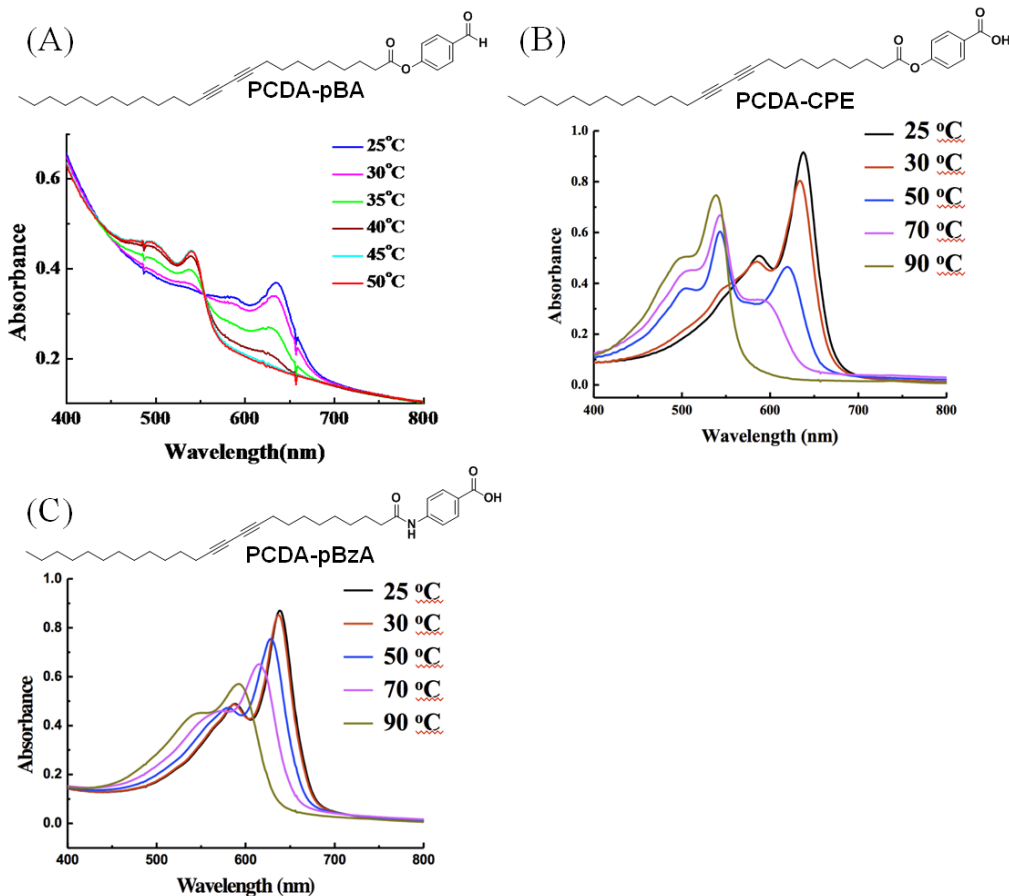
Figure 5.1. Chemical structure and UV-vis spectra change of the PCDA- *p*BA (A), PCDA-CPE (B) and PCDA-*p*BzA liposome solution (final concentration: 0.5 mM) upon heating.

As can be seen in Figure 5.1, PDA liposomes solution having an ester linkage (PCDA-CPE) showed less stability and changed color at lower temperature ($70^{o}C$) than PDA liposomes ($>>90^{o}C$) having an amide linkage (PCDA-*p*BzA) due to the lack of hydrogen bonding. However, the PCDA-*p*BO and PCDA-HBO liposomes solution hardly changed their color to red after incubation with 100mM of DCP and DFP. We hypothesized that the strong intermolecular hydrogen bonding between OXs of PCDA-*p*BO generated strong aromatic stacking resulting in lower sensitivity, and also the self-

assembled structure of PCDA-pBO by intermolecular hydrogen bonding was failed to induce the proper distance for polymerization resulting weak blue intensity.(Figure 5.2) In case of PCDA-HBO, the strong intramolecular hydrogen bonding between OX and β-hydroxy generated a planar structure of PCDA-HBOs and resulted in stronger aromatic stacking between self-assembled PCDA-HBOs and also the self-assembly was proper for the polymerization resulting in solid blue color intensity but the increased stability induced less sensitivity[18]. (Figure 5.2).

We believe that above inter/intra hydrogen bonds of PCDA-*p*BO and PCDA-HBO molecules are too strong reducing their sensitivity. Therefore, we designed analogous diacetylene molecules (PCDA-*p*BA and PCDA-HBA) having an aldehyde instead of OX to remove possible strong aromatic stacking of PCDA-HBO and hydrogen bonding between PCDA-*p*BOs. Figure 5.1 shows sensitive color change of PCDA-*p*BA at the lowest temperature (30-35°C) compared to acid modified PCDA-CPE (70-80°C) having strong head group hydrogen bond. When the aldehyde-modified PDAs are co-assembled with their oxime-modified equivalent into a liposome we anticipate that they break intermolecular hydrogen bond and aromatic stacking between the oximes provide better mobility between OX-PCDA molecules as well as the most sensitivity.
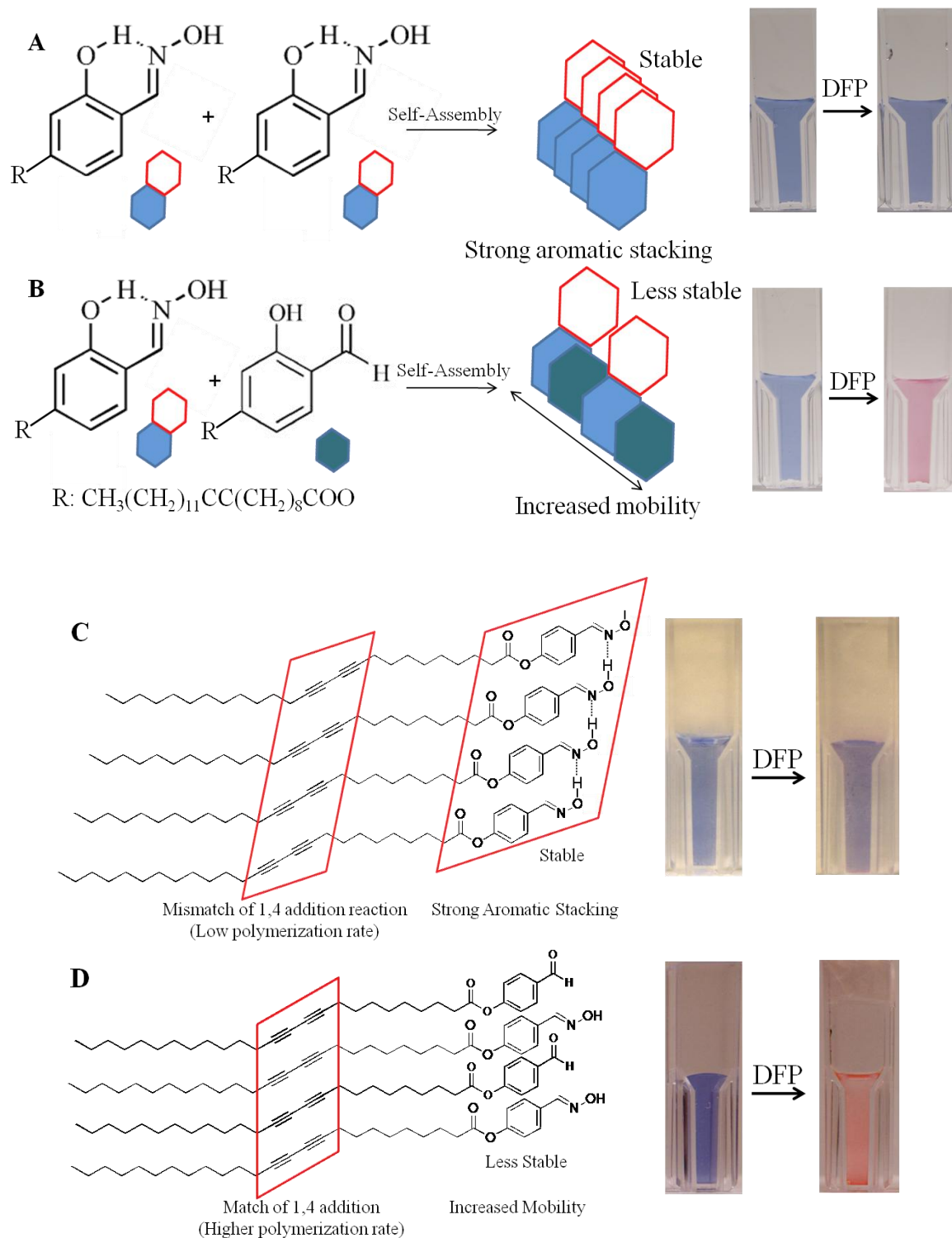
Figure 5.2. Crystal structure and color transition image of a) PCDA-HBO, b) PCDA-HBO/PCDA-HBA, c) PCDA-*p*BO and d) PCDA-*p*BO/PCDA-*p*BA(1/1). (DFP concentration: 100mM)
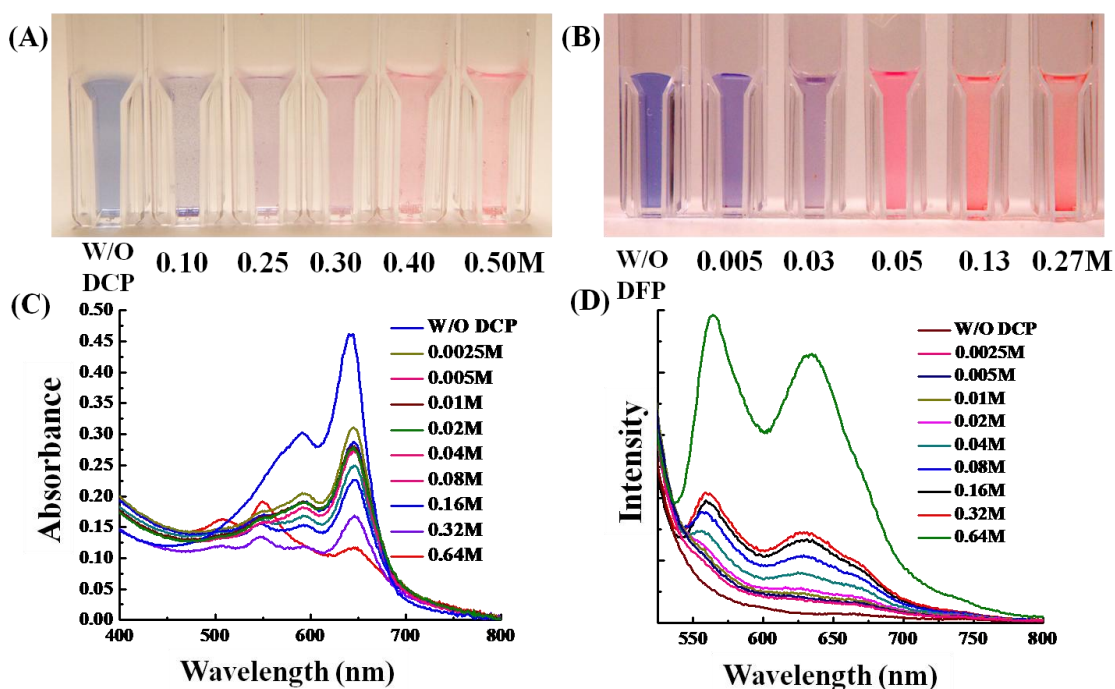
Figure 5.3. Colorimetric transition of PCDA-*p*BO/PCDA-*p*BA liposomes solution upon addition of various concentrations of (A) DCP and (B) DFP. (C) UV-vis and (D) PL spectra of PCDA-*p*BO/PCDA-*p*BA liposome solution toward DCP.

We studied the color/fluorescent transition of OX-PDA liposomes upon exposure to diethylchlorophosphate (DCP) and diisopropylfluorophosphate (DFP), nerve gas simulants, in three different conditions: aqueous phase, semi-wet phase (agarose gel), and solid phase. We initially conducted selectivity tests with PCDA-*p*BO/PCDA-*p*BA (1/1 mole ratio) liposomes in an aqueous solution. We confirmed that PCDA-*p*BO/PCDA-*p*BA liposomes solution selectively and rapidly detected DCP and DFP as shown in Figure 5.3. The absorption peak at 650nm (blue phase) decreased and 550nm (red phase) absorption peak appeared upon addition of various concentrations of DCP (Figure 5.3C). The fluorescence intensity of the PCDA-*p*BO/PCDA-*p*BA liposome also increased upon the addition of DCP (Figure 5.3D). Moreover, we did not observe any color transition upon addition of HCl, HF, HNO$_3$, and H$_3$PO$_4$ implying a good selectivity (Figure 5.4).
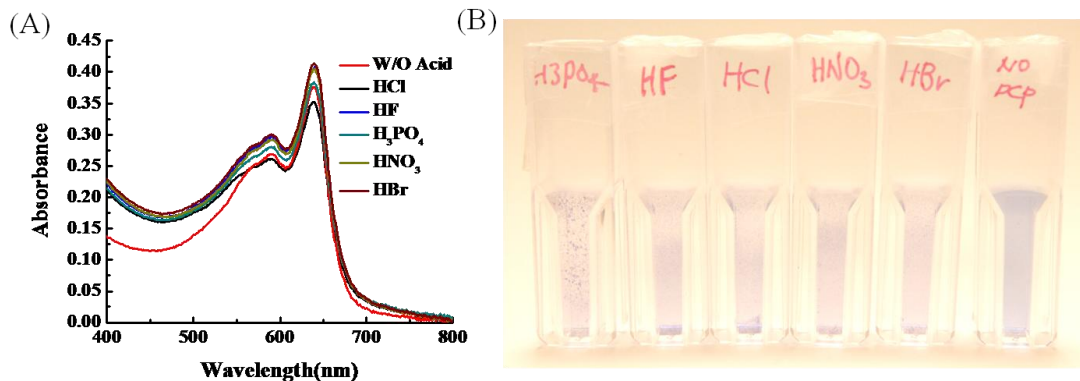
Figure 5.4. (A) UV-vis spectra and (B) color change of the PCDA-pBO/PCDA-pBA(2/1) liposome solution (final concentration: 0.2 M) upon the addition of HCl, HF, H_3PO_4, HNO_3, HBr (500mM) after 10s incubation.

The colorimetric transition was almost spontaneous and saturated within 10 seconds. Although PCDA-*p*BO/PCDA-*p*BA liposome solution showed rapid and selective detection, a portable solid-state detection device will be more useful for real application. In this regard, we further investigated solid phase detection systems.
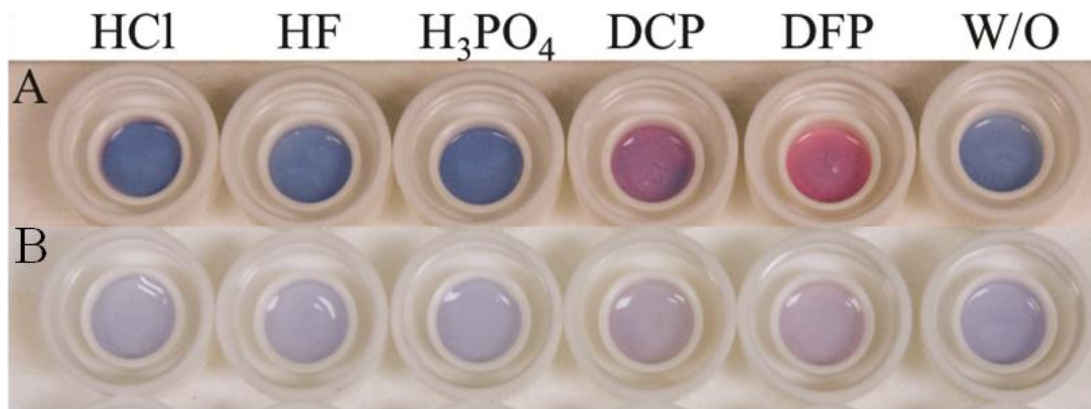
Figure 5.5. Color transition image of (A) PCDA-HBO/PCDA-HBA (1/1), and (B) PCDA-pBO/PCDA-pBA(1/1) liposome embedded agarose gels upon addition of 2.5M HCl, HF, H_3PO_4 and 100mM DCP and DFP.

We prepared a gel phase sensory system with agarose. The OX-PDAs liposomes were simply embedded into agarose gel and exposed to DCP and DFP. Figure 5.5 shows the color transition of investigated OX-PDAs/Aldehyde-PDAs liposome-embedded agarose gels upon direct exposure to a solution of HCl, HF, H_3PO_4, DCP and DFP. As we expected the designed PCDA-pBO/PCDA-pBA, PCDA-HBO/PCDA-HBA liposomes-embedded gels showed highly selective color transition toward only DCP and DFP even at 25 times lower concentration (0.1M) than 2.5M of HCl, HF and H_3PO_4. As shown in Figure 5.5, the PCDA-HBO/PCDA-HBA liposomes-embedded agarose gel showed solid blue color and most notable color transition only upon exposure to DCP and DFP. As we hypothesized, the hydroxyl group at β-position induced the better self-assembly of diacetylene molecules and resulted in better polymerization rate, and therefore, showed solid blue colored liposomes solution. These results provide a possibility to develop a convenient and portable sensory system for nerve gas detection. However, the investigated gel phase PDA sensor system did not show sensitive color change upon the vapor of DCP and DFP. To realize a practically useful system we aimed to improve the sensitivity further. We believed that the aqueous phase of the agarose gel may not be an optimum environment for the reaction between OX and OP because DFP and DCP are not very soluble in water before hydrolysis. Therefore, we investigated a solid sensory system without aqueous phase. We embedded OX-PDAs/Aldehyde-PDAs liposomes into a cellulose acetate membrane filter. PDA liposomes were stably deposited into the filter paper because the cellulose acetate filter is a highly porous hydrophilic membrane. We prepared PCDA-HBO/PCDA-HBA liposomes in 5mM HEPES pH 9.5 buffer to enhance the reaction rate of OX to OP by generating a oximate anion under high pH.[19] Cellulose acetate membrane filters having a 0.65μm pore size was soaked with the liposome solution and completely dried under nitrogen flow. PCDA-HBO/PCDA-HBA liposomes were used because of their strong blue color after photo-polymerization and high color transition contrast observed in the previous agarose gel test (Figure 5.5). We conducted

detection tests by using vapor of HCl, HF, H₃PO₄, DCP and DFP. As can be seen in Figure 5.6(A), PCDA-HBO/PCDA-HBA liposome showed rapid color transition only upon exposure to the DCP and DFP vapor in 30 seconds.
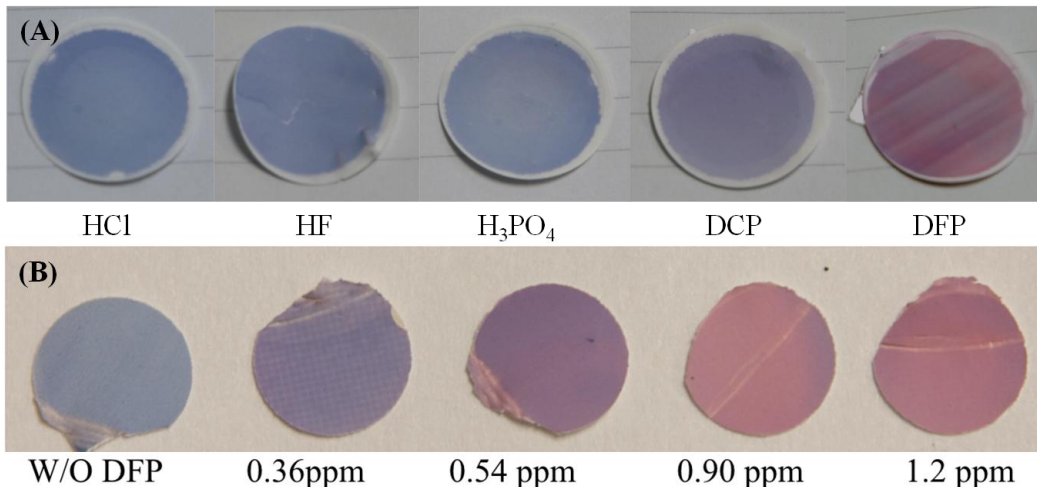
Figure 5.6. Colorimetric transition of (A) PCDA-HBO/PCDA-HBA(1/1) liposomes embedded filter upon the vapor of HCl, HF, H₃PO₄, DCP and DFP and (B) upon exposure to various concentrations of DFP vapor for 30s (color transition was observed almost instantaneously upon the exposure to the vapor) (ppm; mg/m^3)

We further carried out a detection limit study. OX-PDA liposome-embedded cellulose acetate membrane filters showed a noticeable color change by naked eyes upon exposure to 360 ppb DFP vapor in 30 seconds (Figure 5.6). The concentration of DFP vapor in the detection chamber was precisely quantified by Gas Chromatography (GC). Table 1s shows the inhalation lethal toxicity of DFP vapor to several species[20]. We quantified the concentration of DFP vapor after 30 sec incubation and there was no further color transition of PDA sensory filter after several min. Therefore time unit can be added to the detection limit of 360 ppb (0.36 mg*min/m^3). Therefore the sensitivity of investigated OX-PDA sensor system (0.36 mg*min/m^3) is almost 2000 times sensitive than the lethal inhalation dose of monkey (800 mg*min/m^3). Table 5.2 shows the lethal dose of G and V-agents. VX has the most toxic lethal dose by breathing (600-700 mg*min/m^3) compared to other nerve agents. The G agents and VX is usually considered to have much higher reactivity upon oxime than DCP and DFP by their extremely higher

83

toxicity..Therefore, we believe that our OX-PDA based sensory system is anticipated to show much better sensitivity toward G and VX in real applications.

Species	$L(CT)_{50}$ (mg min m^{-3})
Mouse	5900
Rat	2800
Guinea Pig	8000
Rabbit	8000
Dog	5000
Monkey	800

Table 5.1. Inhalation lethal toxicity of DFP vapor to several species.

Agent	Vapor (CT) (mg-min/m^3)	Liquid	
		µg/person	mg/kg
Tabun	20,000–40,000 15,000[a]	1,000–1,500	50–70
Sarin	12,000–15,000 10,000[a]	1,000–1,700	25–50
Soman	10,000 2,500[a]	600 350[a]	5–20
Cyclosarin	15,000 2,500[a]	350	—
VX	600–700 150[a]	3.4–6.0 <5[a]	0.1–0.2

Table 5.2. Lethal dose of G, V-agents.

Another important feature in the investigated OX-PDA liposome sensory system is the detoxification. OX-PDA monomers were designed by mimic the antidote of 2-PAM and as a result nerve agents stimulants (DCP and DFP) were decomposed by OX-

PDAs liposomes solution upon the whole detection process. Thus OX-PDA liposome can be used as a potential detoxifier as well as detector

5.3 Conclusions

In summary, we developed a rapid, convenient, sensitive, and selective nerve agent detection system using oxime-modified PDA liposomes. The rapid reaction between OX and OP induced purturbation of the conjugated PDA backbone by repulsion and hydrophobic aggregation, producing a rapid and sensitive colorimetric change. The developed OX-PDA liposome-based sensor assay can be coveniently prepared by simple self-assembly of rationally designed diacetylene molecules. We further developed a portable solid-state PDA sensory system by using cellulose acetate filter papers. PCDA-HBO/PCDA-HBA(1/1) liposome-embedded filter papers detected as small as 360 ppb (mg/m^3) of DFP vapor. The presented design principle and the sensory device fabrication protocol renders the possibility of readily applicable PDA-based optical sensory systems to detect nerve gases and also to detoxify the OP molecules.

5.4 Experimental section

5.4.1 PDA liposome solution.

A mixture of the OX-PCDA and aldehyde PCDA monomer mixture was dissolved in 100 ul of tetrahydrofuran. The mixture solution was injected rapidly into 20 ml of 5mM HEPES buffer at pH 8.0 (solution and gel phase) and 9.5 (solid phase), and was sonicated for 20 min. The suspension was filtered with 0.8 µm syringe filter and stored for 4 hr at 5°C. The PDA liposome solution was polymerized for 30s under 254nm UV lamp before use.

5.4.2 PDA liposome embedded agarose gel.

1wt% of Agarose was mixed with 0.2mM of PDA liposomes in 5mM HEPES buffer pH 8.0 and the mixture solution was mild heated. The residue solution was stored at 5°C for 30min. PDA liposome embedded gel was photo-polymerized under exposure to 254 nm UV light for 1min.

5.4.3 PDA liposome embedded cellulose membrane filer.

0.2mM of PDA liposome solution was penetrated through 0.65um sized cellulose acetate membrane filter using Millipore Stainless-steel Filter Holder. PDA liposome embedded membrane filter was dried under nitrogen and photo-polymerized under 254 nm UV light for 30s.

5.4.4 Synthesis and characterization.

Materials and Method

All solvents were purchased from Sigma-Aldrich Chemicals. 10,12-pentacosadiynoic acid (PCDA) was purchased from GFS Chemicals. Dicyclohexylcarbodiimide, 4-dimethylaminopyridine, cyanuric acid, 1,8-diazabicycloundec-7-ene, carbon tetrabromide, triphenylphosphine, 6-bromohexan-1-ol, tri(ethylene glycol) were purchased from SigmaAldrich Chemical Co. UV/Vis absorption spectra were taken on a Varian Cary50 UV/Vis spectrophotometer. Fluorescence spectra were obtained using PTI QuantaMasterTM spectrofluorometers equipped with an integrating sphere. Fluorescence images were taken by Olympus BX51 W/DP71 fluorescent microscope.

Synthesis of PCDA Derivatives

PCDA-CPE To a solution containing 1.39 g (3.70 mmol) of 10,12-pentacosadiynoic acid in 20 mL of methylene chloride was added dropwise 0.94 g (7.4 mmol) of oxalyl chloride at room temperature. The resulting solution was stirred at room temperature for 1 h. To the solution was added a catalytic amount (one drop) of DMF and stirred for an additional hour. After concentrating in vacuo, the residue was redissolved in 15 mL of methylene chloride. The resulting solution was added dropwise to the solution containing 0.66 g (4.81 mmol) of 4-hydroxybenzoic acid in 15 mL of THF. The resulting mixture was allowed to stir for overnight at room temperature. The solvent was removed in vacuo, and the residue was purified by silica gel column chromatography (4:1 chloroform: methanol) to give 0.48 g (26%) of the desired diacetylene monomer PCDA-CPE as a white solid. mp 75 ℃. ^{1}H NMR (300 MHz, CDCl$_3$) δ 0.88 (t, 3H), 1.20-1.80 (m, 36H), 2.22 (t, 4H), 2.35 (t, 2H), 7.07-7.55 (m, 5H), 7.18 (brs, 1H).
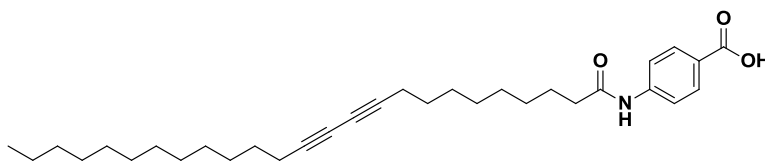
PCDA-*p*BzA To a solution of 10,12-pentacosadiynoic acid (2.00 g, 5.34 mmol) in dichloromethane (20 mL) at room temperature was added dropwise oxalyl chloride (2.03 g, 16.02 mmol). The resulting solution was stirred at room temperature for 30 min. To the solution was added a catalytic amount of dimethylformamide and stirred for an additional hour. After concentrating in vacuo, the residue was redissolved in THF (15 mL). The resulting solution was added dropwise to the solution containing 4-aminobenzoic acid (1.10 g, 8.01 mmol) and TEA (2.16 g, 21.36 mmol) in THF (15 mL). The resulting mixture was allowed to stir for overnight at room temperature, poured into the water and extracted with ethyl acetate. The organic layer was washed 3 times with water to eliminate the excess 4-aminobenzoic acid, dried with MgSO4 and

filtered. The solvent was removed under vacuo. The resulting solution was recrystallized from methyl alcohol and isopropyl alchol to give 2.20 g (83 %) of desired diacetylene monomer PCDA-pBzA as a white solid. mp 190°C ^{1}H NMR (400 MHz, CDCl$_3$): δ 0.85 (t, 3H), 1.23-1.60 (m, 32H), 2.25-2.28 (m, 4H), 2.31-2.35 (m, 2H), 7.69 (d, 2H), 7.86 (d, 2H), 10.15 (s, 1H).
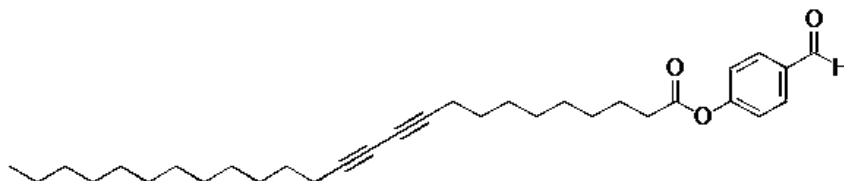
PCDA-*p*BA To a solution of 10,12-pentacosadiynoic acid (1.00 g, 1.33 mmol) in dichloromethane (20 mL) at room temperature was added dropwise oxalyl chloride (1.01 g, 7.98 mmol). The resulting solution was stirred at room temperature for 30 min. To the solution was added a catalytic amount (one drop) of dimethylforamide and stirred for an additional hour. After concentrating in vacuo, the residue was redissolved in tetrahydrofuran (15 mL) and added dropwise to the solution containing 4-hydroxybenzaldehyde (0.65 g, 5.32 mmol) in pyridine (15 mL). The resulting mixture was allowed to stir for overnight at room temperature. The residue was extracted with ethyl acetate and dried with MgSO$_4$ and filtered. The solvent was removed under vacuo. The residue was further purified by silica gel column chromatography (hexane:ethylacetate =6:1) to give 1.00 g (86.2 %) of desired diacetylene monomer **PCDA-*p*BA** as a white solid. mp 80 °C. ^{1}H NMR (400 MHz, DMSO-d_6): δ 0.85 (t, 3H), 1.15-1.64 (m, 32H),
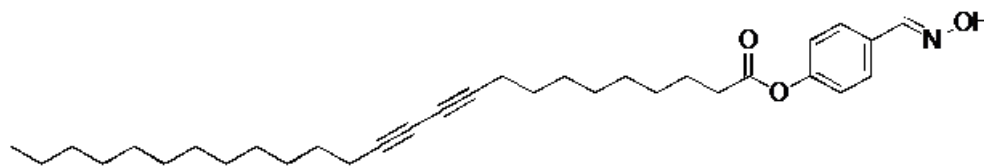
2.26 (t, 4H), 7.35 (d, 2H), 7.98 (d, 2H), 9.90 (s, 1H).

PCDA-*p*BO To a solution of PCDA-*p*BA (1.00 g, 2.09 mmol) in 2-propanol (100 mL) at room temperature was added dropwise hydroxylamine hydrochloride (0.17 g, 2.51 mmol) and sodium carbonate (0.20 g, 2.51 mmol) in 60 ml of 2-propanol/di-water (1/2). The reaction mixture was refluxed at 80 °C for 2 hours. After cooling, the reaction mixture was concentrated

in vacuo and extracted with diethylether. The residue was recrystalized in 2-propanol/di-water

(1/1) and further purified with gel column chromatography (ethylacetate: hexane = 1:5) to give

0.60 g (59 %) of desired diacetylene monomer **PCDA-*p*BO** as a white solid. mp 100 ℃. ^{1}H NMR

(400 MHz, DMSO-d_6): δ 0.84 (t, 3H), 1.15-1.66 (m, 34H), 2.27 (t, 4H), 2.61 (t, 2H), 7.12 (d, 2H),

7.60 (d, 2H), 8.12 (s, 1H). 11.25 (s, 1H).
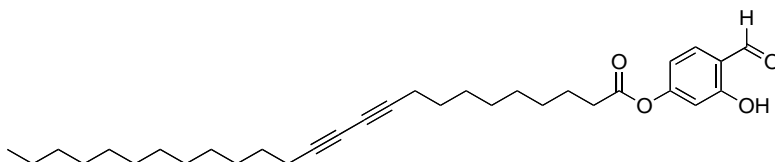
PCDA-HBA To a solution of 10,12-pentacosadiynoic acid (2.00 g, 5.33 mmol) in

dichloromethane (20 mL) at room temperature was added dropwise oxalyl chloride (2.00 g, 15.7

mmol). The resulting solution was stirred at room temperature for 30 min. To the solution was

added a catalytic amount (one drop) of dimethylforamide and stirred for an additional hour. After

concentrating in vacuo, the residue was redissolved in 2-butanone (20 mL). The resulting solution

was added dropwise to the solution containing 2,4-dihydroxybenzaldehyde (0.72 g, 5.27 mmol)

and TEA (0.62 g, 6.17 mmol) in 2-butanone (50 mL). The resulting mixture was allowed to stir

for 6 hours at room temperature. The solvent was removed under vacuo and the residue was

crystallized in methanol for 40 min. The residue was further purified by silica gel column

chromatography (hexane:ethyl acetate =9:1) to give 1.2 g (44 %) of desired diacetylene monomer

PCDA-HBA as a white solid. Mp 90 ℃. ^{1}H NMR (400 MHz, DMSO-d_6): δ 0.78 (t, 3H), 1.17-

1.71 (m, 32H), 2.26 (t, 4H), 2.51 (t, 2H), 6.64-6.68 (m, 2H), 7.64 (s, 1H), 10.18 (s, 1H).
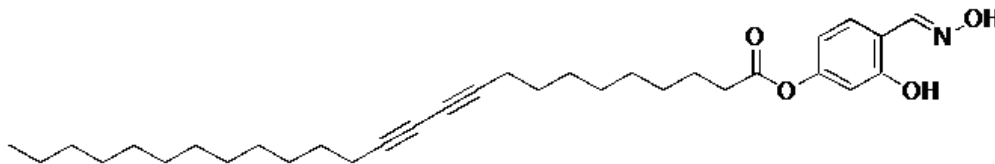
PCDA-HBO To a solution of PCDA-HBA (0.38 g, 0.62 mmol) in ethanol (20 mL) at

room temperature was added hydroxylamine hydrochloride (0.14 g, 2.06 mmol) and sodium carbonate (0.43 g, 4.13 mmol) in 10 ml of ethanol/di-water (1/1). The reaction mixture was refluxed at 44 ℃ for 6 hours. After concentrating in vacuo, the residue was recrystalized in 2-propanol/water (1/1) and dichloromethane. The residue was further purified with gel column chromatography (ethyl acetate: hexane = 1:5) to give 0.30 g (73 %) of desired diacetylene monomer **PCDA-HBO** as a white solid. mp 107 ℃. ^{1}H NMR (400 MHz, DMSO-d_6): δ 0.85 (t, 3H), 1.15-1.63 (m, 32H), 2.27 (t, Hz, 4H), 2.54 (t, 2H), 6.62 (m, 2H), 7.49 (d, 1H), 8.29 (s, 1H), 10.35 (s, 1H), 11.29 (s, 1H).

References

[1]   J. Bajgar, in *Advances in Clinical Chemistry, Vol. Volume 38* (Ed.: S. M. Gregory), Elsevier, **2004**, pp. 151.

[2]   R. Subramaniam, C. Åstot, L. Juhlin, C. Nilsson, A. Östin, *Analytical Chemistry* **2010**, *82*, 7452.

[3]   W. A. Harris, P. T. A. Reilly, W. B. Whitten, *Analytical Chemistry* **2007**, *79*, 2354.

[4]   a)T. J. Dale, J. Rebek, *Journal of the American Chemical Society* **2006**, *128*, 4500; b)T. Dale, J. Rebek, *Angewandte Chemie International Edition* **2009**, *48*, 7850; c)S.-W. Zhang, T. M. Swager, *Journal of the American Chemical Society* **2003**, *125*, 3420.

[5]   K. A. Joshi, M. Prouza, M. Kum, J. Wang, J. Tang, R. Haddon, W. Chen, A. Mulchandani, *Analytical Chemistry* **2005**, *78*, 331.

[6]   Y. Yang, H.-F. Ji, T. Thundat, *Journal of the American Chemical Society* **2003**, *125*, 1124.

[7]   K. D. Cadwell, N. A. Lockwood, B. A. Nellis, M. E. Alf, C. R. Willis, N. L. Abbott, *Sensors and Actuators B: Chemical* **2007**, *128*, 91.

[8]   a)B. Yoon, S. Lee, J.-M. Kim, *Chemical Society Reviews* **2009**, *38*, 1958; b)M. A. Reppy, B. A. Pindzola, *Chemical Communications* **2007**, 4317; c)K. Lee, L. K. Povlich, J. Kim, *Analyst* **2010**, *135*, 2179.

[9]   a)R. R. Chance, *Macromolecules* **1980**, *13*, 396; b)J. Olmsted, M. Strand, *The Journal of Physical Chemistry* **1983**, *87*, 4790.

[10]   a)D. Meir, L. Silbert, R. Volinsky, S. Kolusheva, I. Weiser, R. Jelinek, *Journal of Applied Microbiology* **2008**, *104*, 787; b)S. Kolusheva, T. Shahal, R. Jelinek, *Journal of the American Chemical Society* **2000**, *122*, 776.

[11]   D. J. Ahn, E.-H. Chae, G. S. Lee, H.-Y. Shim, T.-E. Chang, K.-D. Ahn, J.-M. Kim, *Journal of the American Chemical Society* **2003**, *125*, 8976.

[12]   a)S. Lee, J.-M. Kim, *Macromolecules* **2007**, *40*, 9201; b)J.-M. Kim, J.-S. Lee, H. Choi, D. Sohn, D. J. Ahn, *Macromolecules* **2005**, *38*, 9366; c)J. Pang, L. Yang, B. F. McCaughey, H. Peng, H. S. Ashbaugh, C. J. Brinker, Y. Lu, *The Journal of Physical Chemistry B* **2006**, *110*, 7221; d)H. Peng, X. Sun, F. Cai, X. Chen, Y. Zhu, G. Liao, D. Chen, Q. Li, Y. Lu, Y. Zhu, Q. Jia, *Nat Nano* **2009**, *4*, 738.

[13]   a)J. Lee, H. Jun, J. Kim, *Advanced Materials* **2009**, *21*, 3674; b)J. Lee, H.-J. Kim, J. Kim, *Journal of the American Chemical Society* **2008**, *130*, 5010.

[14]   a)K. Tashiro, H. Nishimura, M. Kobayashi, *Macromolecules* **1996**, *29*, 8188; b)R. W. Carpick, D. Y. Sasaki, A. R. Burns, *Langmuir* **2000**, *16*, 1270; c)R. W. Carpick, et al., *Journal of Physics: Condensed Matter* **2004**, *16*, R679.

[15]   D. Milatovic, M. Jokanovic, in *Handbook of Toxicology of Chemical Warfare Agents* (Ed.: C. G. Ramesh), Academic Press, San Diego, **2009**, pp. 985.

[16]   a)D. Seo, J. Kim, *Advanced Functional Materials* **2010**, *20*, 1397; b)J. Lee, E. Jeong Jeong, J. Kim, *Chemical Communications* **2011**.

[17]   F. Terrier, P. Rodriguez-Dafonte, E. Le Guevel, G. Moutiers, *Organic & Biomolecular Chemistry* **2006**, *4*, 4352.

[18] A. G. Smith, P. A. Tasker, D. J. White, *Coordination Chemistry Reviews* **2003**, *241*, 61.

[19] I. Oh, R. I. Masel, *Electrochemical and Solid-State Letters* **2007**, *10*, J19.

[20] J. Brodeur, K. P. DuBois, *Journal of Occupational and Environmental Medicine* **1964**, *6*, 164.

CHAPTER 6

Multiphasic Alginate Particles having Polydiacetylene Liposomes toward Sensitive Dual Detection in Aqueous Solution

Manuscript in preparation

6.1 Introduction

Conjugated polydiacetylenes (PDA) have attracted great attention in the sensor application because PDAs are unique in terms of their colorimetric/fluorescence dual detection capability and the convenient fabrication method of molecular self-assembly of diacetylene monomers followed by simple photopolymerization. PDAs undergo dramatic blue to red chromatic transition and also have red fluorescence emission upon being exposed to external stimuli such as heat[1], pH[2], organic solvent[3] and mechanical stress[4]. It is well-known that the external steric repulsion resulted in the rearrangement of ene-yne conjugated backbone of PDA, and produced the colorimetric/fluorescence dual signals.[5] PDAs have been studied with great effort for the bio and chemo-sensor applications due to the label-free dual signalling capability.[6] Many successful PDA sensor systems have been developed in forms of aqueous suspensions[7] as well as thin-films on the solid substrate[8]. In general the chemically functionalized probing diacetylene (DA) monomers are dispersed in an aqueous solution and form self-assembled liposomes by means of sonication. DA monomers also can be transferred onto a glass substrate through the Langmuir-Blodgett (LB) or the Langmuir-Schaefer (LS)

method to form well-defined self-assembled monolayer or multilayers.[8] These well-ordered DA monomers are then subsequently photopolymerized through UV irradiation.

PDA sensor systems, however, have several fundamental limitations in terms of the sensor signal generation efficiency and the stability of PDA liposomes. The aqueous PDA sensor system loses their blue optical intensity once the probe solution is incubated with the large volume of target solution. PDA liposomes also tend to aggregate or polymerize upon being exposed to an ambient condition for a long time. Moreover, a single PDA aqueous sensory system can recognize only one type of target lacking of a high-throughput multi-targeting capability. In order to overcome above listed limitations, several new approaches have been developed such as encapsulation of the probe PDA liposomes into the host matrices such as poly-vinyl alcohol (PVA)[9], agar scaffold[10], hybrid sol-gel matrices[11], silica nanocomposites[12] and electrospining[13] or PDA liposomes was microarrayed onto the glass substrate for multi-targeting[14]. Indeed these new approaches enhance the stability of PDA liposomes by suppressing aggregation possibility of PDA liposomes and the microarray format provides a possible multi-targeting capability. However, simultaneous detection of multiple targets in homogeneous solution has its own merit and unique applications but has not been developed well yet.

6.2 Results and Discussion

Tremendous research efforts have been devoted to develop efficient sensor systems based on polydiacetylene (PDA) liposomes due to their sensitive mechanochromism that can be efficiently and conveniently applied in self-signalling sensor design.[7b, 11, 14a] In this chapter, we introduce a novel concept and fabrication principle of the biphasic and triphasic Janus particles loaded with PDA liposomes loaded and investigate their sensitive and selective multi-targeting capability. The biphasic

property of alginate particles having PDA liposomes was achieved by the simple centrifugation of PDA liposome/alginate mixture solutions into the $CaCl_2$ solution. The size of particle and the fraction of the each component were independently controlled with the centrifugal force and the type of PDA liposomes as confirmed by fluorescence microscopy and optical microscopy. Efficient fabrication of triphasic microbeads was also demonstrated toward simultaneous detection of multiple analytes in homogeneous aqueous environment.
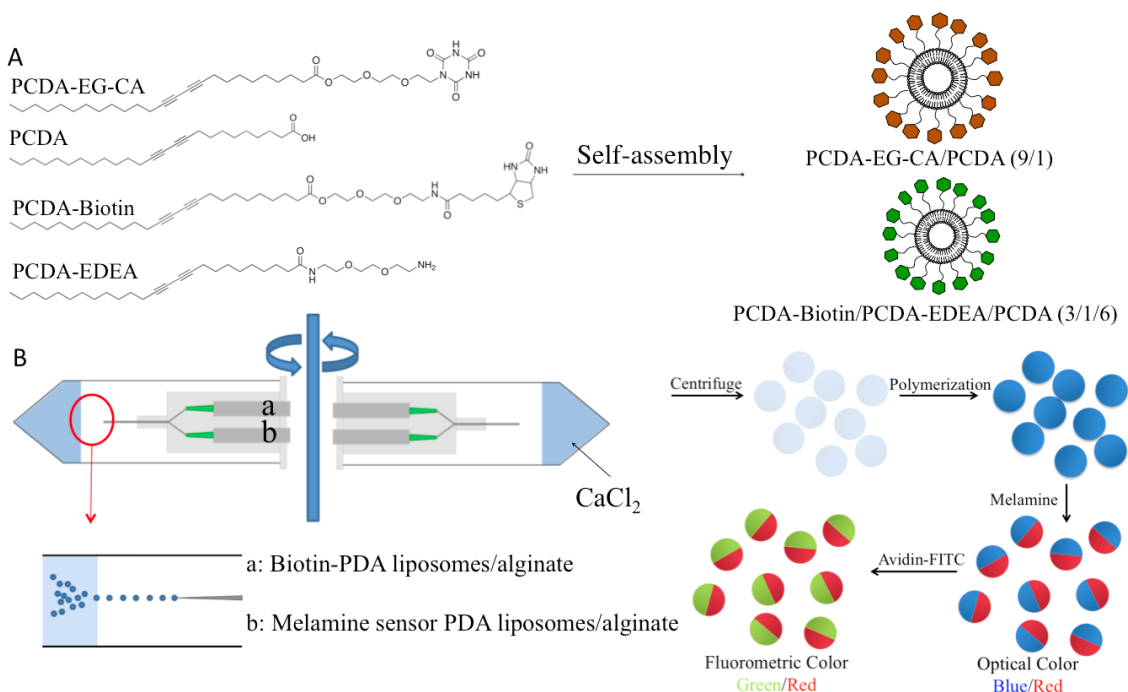
Scheme 6.1. (A) Chemical structures of the investigated PDA molecules and (B) the schematic illustration of biphasic PDA liposomes loaded Janus alginate particle generation: (a) centrifugation of PDA/alginate mixture solution into the $CaCl_2$ soultion, (b) photopolymerization of biphasic PDA liposomes loaded alginate particle, (c) hemispherical red color transition and fluorescence emission upon the addition of melamine (d) hemispherical green fluorescence emission upon the addition of avidin-FITC.

Alginate, also called alginic acid is an anionic polysaccharide constituent of the cell walls of algae. Because of its biocompatibility, porosity, and gelation property with multivalent cations such as Ca^{2+}, it has been widely used for encapsulation of chemicals components and drugs[15]. We applied the gelation and porous nature of a cross-linked

alginate micro particle to encapsulate PDA liposomes into the alginate matrix. A PDA sensory system based on alginate particles loaded with PDA liposomes was rationally designed to maintain the initial blue optical intensity of PDA liposomes by suppressing aggregation that is required for the sensitive colorimetric blue to red transition. We also designed an interesting feature in the Janus alginate particle sensory system with two distinct hemispherical phases providing a multi targeting capability. Biphasic property of polymeric structure is also very important in that they can be applicable to wide range of other applications such as drug delivery, cosmetics, and display. Much efforts have been devoted to develop biphasic polymeric structures including micro-contact printing[16], electrified jetting[17] and microfluidic systems[18]. However, it is difficult to practically use those techniques in that they require serious investigation and experienced skills for the device fabrication to control the size, homogeneity and the biphasic property of the particles. Our designed system described in this chapter provides a convenient fabrication protocol for biphasic particles. We simply applied the centrifugal force to form alginate droplets. First single-phase alginate beads loaded with PDA liposomes were made by centrifugation of a PDA liposomes/alginate mixture solution into a $CaCl_2^+$ solution to optimize the solution concentration and g-force for the beads formation. Biphasic alginate beads loaded with PDA liposomes were then produced by simultaneous parallel injection of two alginate/PDA liposome mixture solutions into a $CaCl_2$ solution as schematically illustrated in Figure 1. The composition of each phase can be independently controlled by choosing differently formulated PDA liposomes allowing various of combination of biphasic and extended multiphasic microbeads for many promising potential applications.
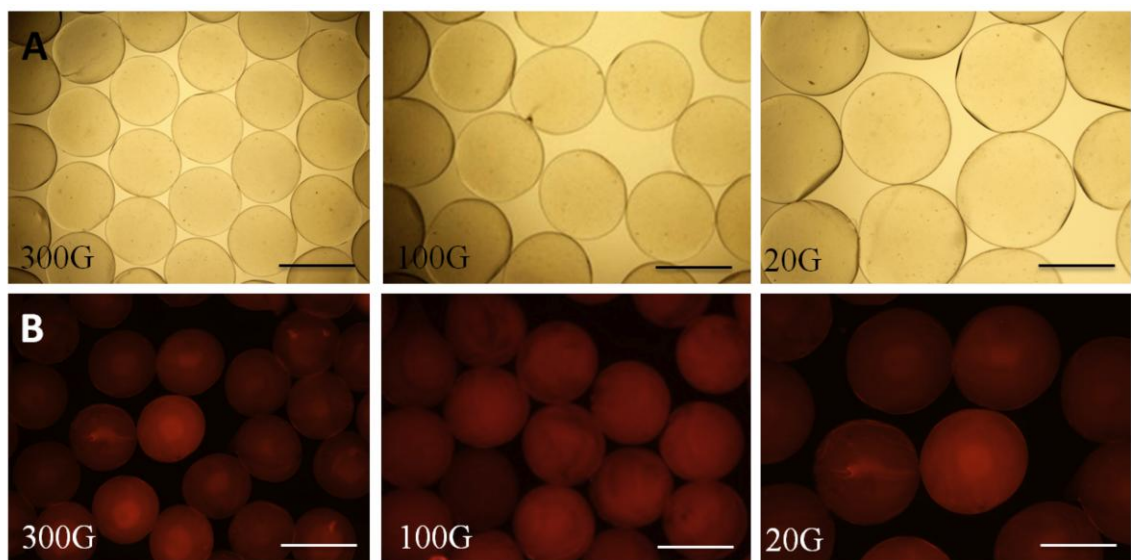
Figure 6.1. (a) Size distribution images of PCDA-EG-CA/PCDA (9/1) liposomes loaded alginate micro particles. (left to right: 300G, 100G, 20G) (Scale bar: 500um). (b) Fluorescence microscope image of the PDA liposomes loaded alginate particles after heating. (Excitation at 550 nm and a long-pass emission filter with 600 nm cut-off were used)

We adapted the single-phase alginate PDA bead system to our recent development of melamine detection to investigate the applicability as a sensitive sensory platform. It is well-known that melamine can induce the kidney disease to human body and the melamine contents have been strictly regulated by the national health organizations. As described in Chapter 4, we previously invented a solution based colorimetric sensory system for melamine detection by devising cyanuric acid tethered PDA liposomes.[7a] We applied the same detection mechanism of the melamine sensor to generate the alginate particle-based sensor system, and further compared the sensitivity of the two systems. We prepared a PCDA-EG-CA/PCDA (9/1) liposomes/alginate mixture solution (2/1(v/v)) and injected the solution dropwise to a $CaCl_2$ solution by means of centrifugation (Scheme 6.1). The PDA liposomes/alginate droplets were physically cross-linked by Ca^{2+} ions in the $CaCl_2$ solution. The size of micro particles was varied approximately from 300um to 1mm depending on the centrifugal force. As the centrifugal force increases, the size of particles decreased and in contrast the larger particles were obtained at a lower centrifugal force. The correlation is plotted in Figure

6.2. Figure 6.1 also shows the size distribution of the alginate microbeads having PCDA-EG-CA/PCDA (9/1) liposome. The alginate microbeads having PCDA-EG-CA/PCDA (9/1) liposomes were subsequently photo-polymerized. Strong blue color from the alginate beads confirms that the PDA liposomes were successfully entrapped in the alginate matrices and effective photo-polymerized (Figure 6.4B). In addition, the blue intensity of the single-phase particles did not change even after storing in a large amount of aqueous solution for a long time demonstrating superior stability of PDA liposomes in the alginate beads to that in solution.
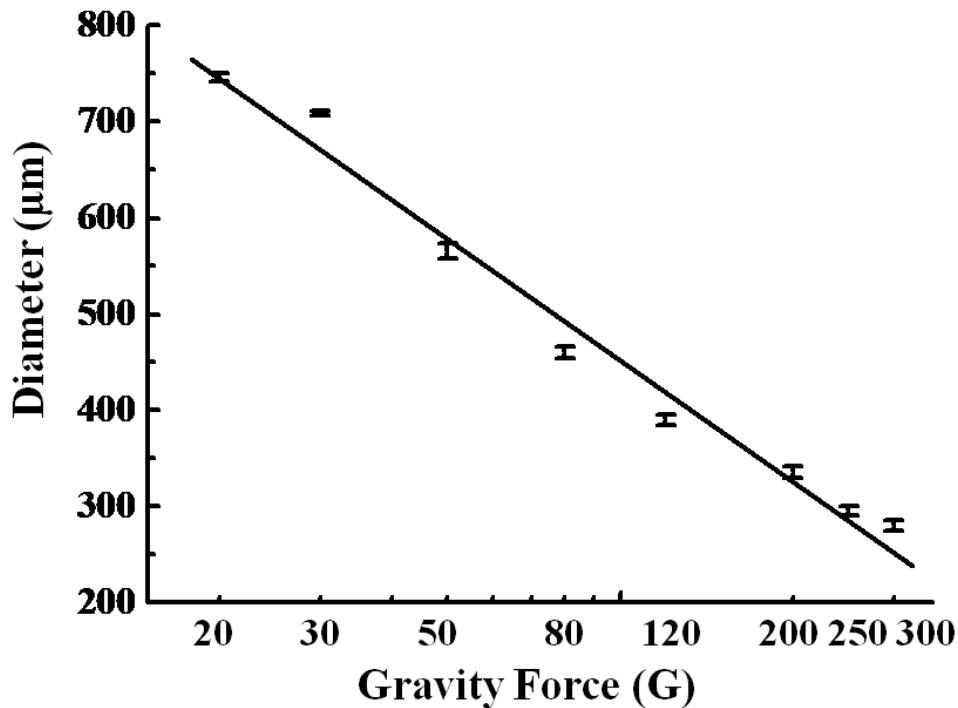
Figure 6.2. (a) Correlation curve between the diameter of PCDA-EG-CA/PCDA(9/1) liposomes loaded alginate particles and G-force.
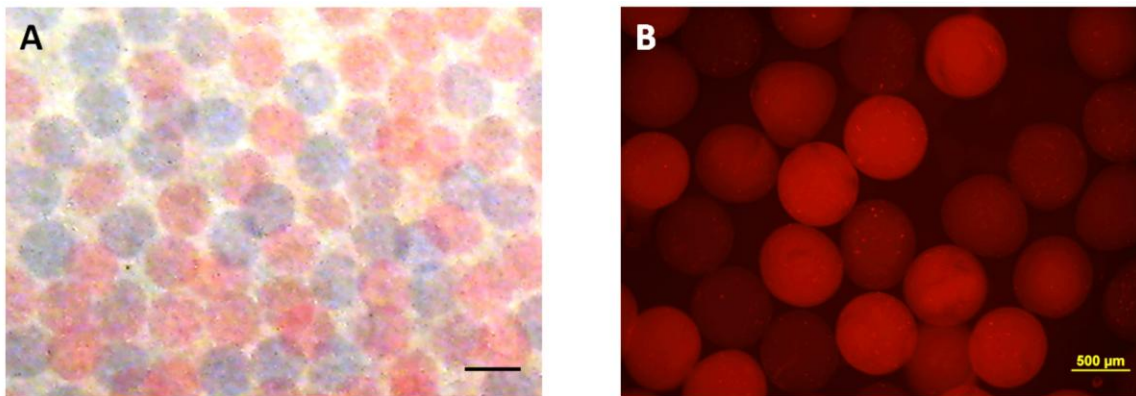
Figure 6.3. (a) Colorimetric transition and (b) red fluorescent emission image of PCDA-EG-CA/PCDA (9/1) liposomes loaded alginate micro particles after incubation in 50 ppm of melamine solution.
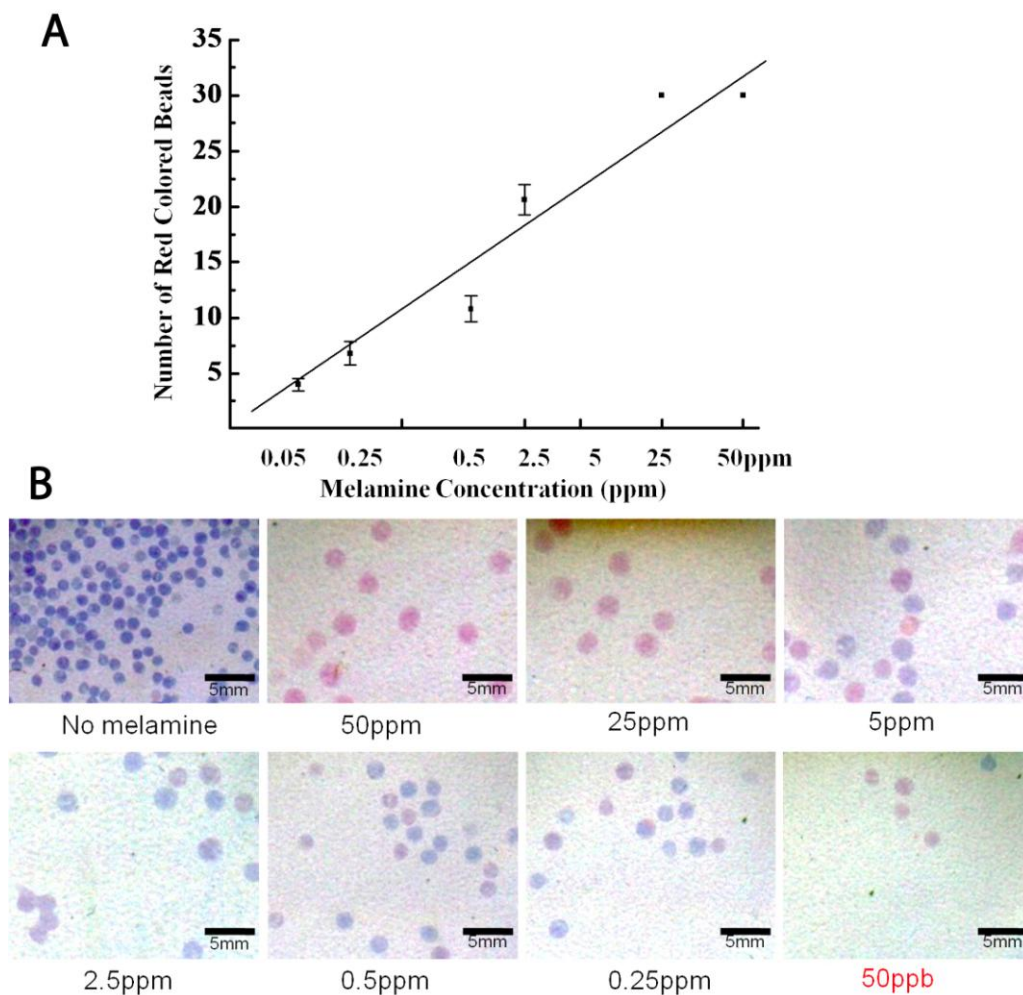
Figure 6.4. (A) Correlation curve between the number of red colored particles and the concentration of melamine. (B) Colorimetric transition of PCDA-EG-CA/PCDA (9/1) liposome embedded alginate micro beads after incubation in various concentration of melamine solution.

99
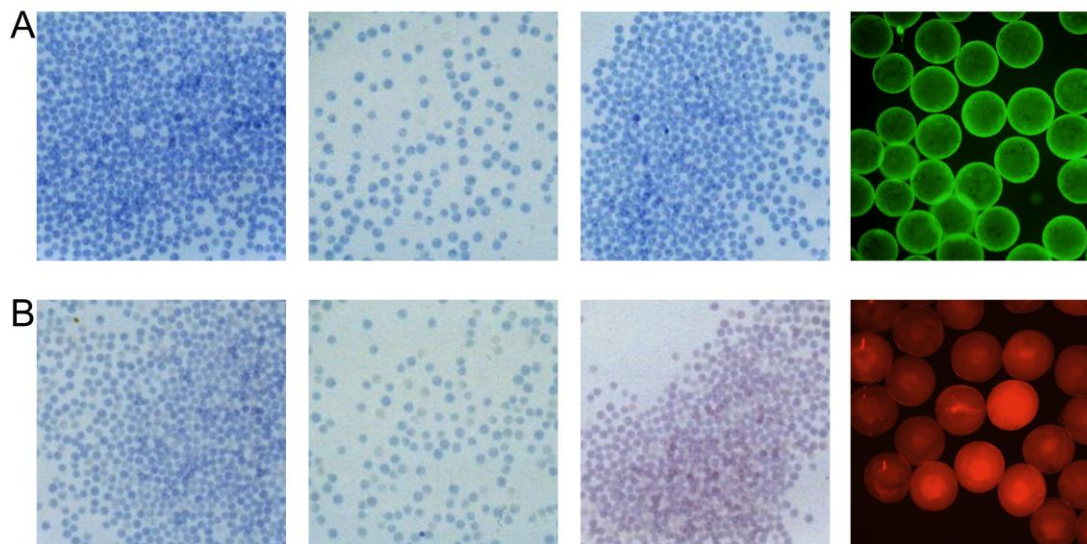
Figure 6.5. Colorimetric transition of biotin-PCDA liposomes loaded alginate particles (A) and PCDA-EG-CA/PCDA (9/1) liposomes loaded alginate particles (B) upon addition of avidin-FITC (middle) and melamine (left).

Since our PDA liposomes loaded particle solved the dilution problem of aqueous sensor system, we conducted sensitivity tests on the alginate beads having the PCDA-EG-CA/PCDA (9/1) liposomes toward melamine. We counted approximately 100 beads using micropipette and incubated the beads in a melamine solution at 50 ppm. The cross-linked alginate micro beads were very stable and the particles could be handled one by one by means of a micropipette or a tweezer. As in Figure 6.3, approximately 70 beads showed the blue to red color transition and red fluorescence emission after 2 hours incubation in the melamine solution demonstrating that the sensory property of the PDA is maintained in the alginate beads. We further conducted a detection limit study with 30 particles with various concentrations of melamine. All beads changed their color from blue to red at 50 ppm and 25 ppm of melamine solution but interestingly no color transition of micro particles was observed from the melamine solution at 5 ppm. The number of red particles decreased from 30 to 4 as the concentration of melamine decreased to 0.05 ppm. The correlation curve between the number of red particles and the amount of melamine is shown in Figure 6.5A demonstrating that a quantitative analysis

of an unknown melamine concentration is also achievable by simply counting the number of red beads. Moreover, the results show that the alginate beads-based sensory provides a much better sensitivity by detecting a lower melamine concentration (50ppb) compared to the solution (1ppm) and microarray-based detection system (0.5ppm).
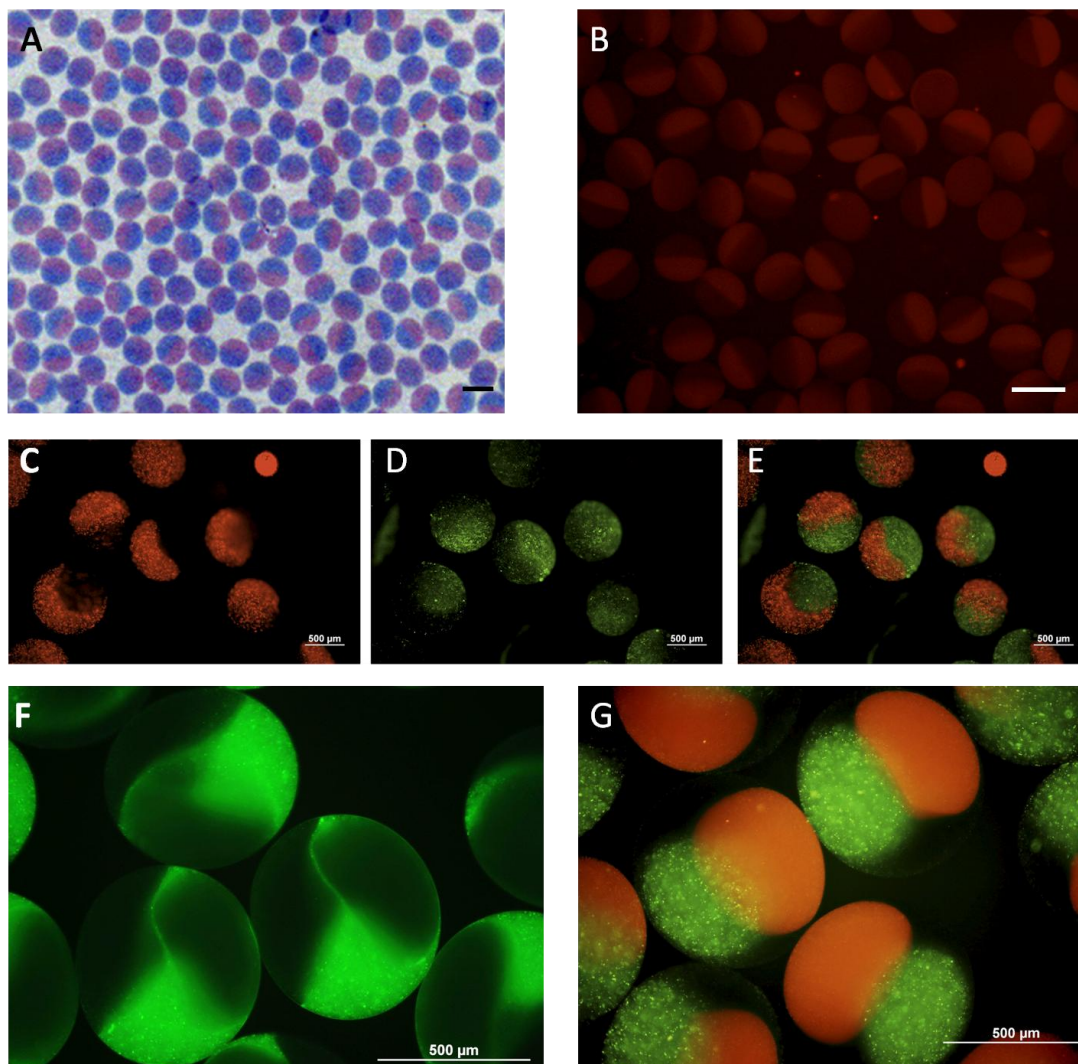
Figure 6.6. (A) Hemispherical colorimetric transition and (B) red fluorescence emission image of none functionalized PCDA liposomes and melamine probe PCDA liposomes loaded Janus alginate particles upon melamine. (C) Red fluorescence emission of biphasic PDA liposome loaded Janus alginate micro particles after incubation in 50 ppm of melamine solution. (D) Green fluorescence emission after incubation in avidin-FITC solution (1mg/1ml in 1XPBS buffer). (E) The overlay of two phase fluorescence image representing the biphasic property of PDA liposomes loaded Janus alginate particles. (scale bar: 500um) (F) Triphasic image of PDA liposomes loaded alginate aprticles after incubation with avidin-FITC (E) Triphasic image of PDA liposomes loaded alginate particles after incubation with avidin-FITC and subsequently with melamine solution.

101

After demonstrating the sensitive detection capability of PDA liposome loaded alginate micro beads, we directed our research toward the development of a multi targeting sensory system. We designed Janus alginate PDA beads having a melamine sensor phase and a negative control phase. For that, we prepared none-functionalized PDA liposomes/alginate mixture solution and the PCDA-EG-CA/PCDA (9/1) liposomes/alginate mixture solution having the same viscosity. The two syringe needles were combined together in such a way that the droplet of each PDA liposome/alginate mixture solution meets together at the end of the two needles and forms the biphasic beads. Microbeads having a 300 μm diameter were obtained after 15 minutes centrifugation at g-force of 250G and the imbedded liposomes were subsequently polymerized under 254 nm UV light. As shown in Figure 6.7a only the half sphere changed color to red and produced red fluorescence emission after incubating with melamine while the other half remained in blue as a negative control. From this we demonstrated that the biphasic alginate beads having a sensory unit and a negative control can be easily fabricated to improve the fidelity of the detection as well as sensitivity.

We further conducted a series of experiments to devise biphasic alginate PD microbeads having multi-targeting capability. First, we synthesized a biotin-functionalized PDA monomer as shown in Scheme 6.1. It is well known that biotin has a strong affinity (K_d of $\sim 10^{-14}$ mol/L) to avidin.[19] We prepared single-phase alginate particles containing the biotin-PCDA liposomes and the PCDA-EG-CA/PCDA (9/1) liposome, respectively. We incubated the alginate beads having biotin-PCDA liposomes with a FITC labelled avidin (1mg/1ml) solution and subsequently with a melamine solution (50 ppm). Green fluorescence caused by the avidin-FITC was found but no red fluorescence was observed after incubation in melamine solution. We also confirmed that the avidin-FITC did not turn on the PCDA-EG-CA/PCDA (9/1) liposomes either (Figure 6.5). Interestingly although the biotin-PCDA liposomes in the alginate particles

successfully interacted with the avidin-FITC, there was no red fluorescence emission from the PDA liposomes after the avidin/biotin interaction. We believe that cross-linked structure of alginate particle decreased the mobility of biotin-PCDA liposomes, and these restriction of mobility induced less corformational change of self-assembled structure of biotin-PDA liposomes. Thus we were able to use the biotin-PCDA liposomes and the PCDA-EG-CA/PCDA (9/1) liposomes to make biphasic Janus alginate beads having hemispherical red/green fluorescence. The biotin-PCDA liposomes/alginate mixture solution and the PCDA-EG-CA/PCDA (9/1) liposomes/alginate mixture solution having the same viscosity were injected together into a $CaCl_2$ solution using the combined needle injection system. To confirm the biphasic property of alginate beads, we incubated the obtained micro beads with the melamine/avidin-FITC mixture solution for 2 hours. We observed the hemispherical red/green fluorescence by the melamine and avidin-FITC interaction respectively (Figure 6.6). We confirmed that each of the biotin-PCDA and PCDA-EG-CA/PCDA (9/1) liposomes selectively interacted with the desired target of avidin-FITC and melamine without interference of each other. Exact half-half hemispherical red/green fluorescent particle could be reproducibly produced by closely matching the viscosity of each PDA/alginate mixture solution to prevent convective mixing of two solutions. This result is very attractive in that the process is very simple and convenient requiring no complicated device but just centrifuge and the simple combined needle injection system.

We further enhanced the PDA/alginate particle having multi phase properties. The three syringe needles were combined together in the same way with the biphasic particle generation protocol and the droplet of each PDA liposome/alginate mixture solution (PCDA, biotin-PCDA, PCDA-EG-CA/PCDA(9/1) liposomes) injected to the 1 wt% of $CaCl_2$ solution. The viscosity of each PDA liposomes/alginate mixture solution was precisely matched for good triphasic property. As shown in Figure 6.6f, we observed that 1/3 of single particle showed green fluorescence after incubation of PDA liposomes

loaded alginate particles in avidin-FITC. After subsequently incubation in melamine solution, the red/green fluorescence by the melamine and avidin-FITC interaction was observed and also the other half remained in dark as a negative control. We demonstrated that the triphasic alginate beads having a sensory unit, indicator unit and also a negative control can be easily fabricated to improve the capability of the detection. This protocol can be utilized to screen the unknown target molecules as in the figure 6.7.
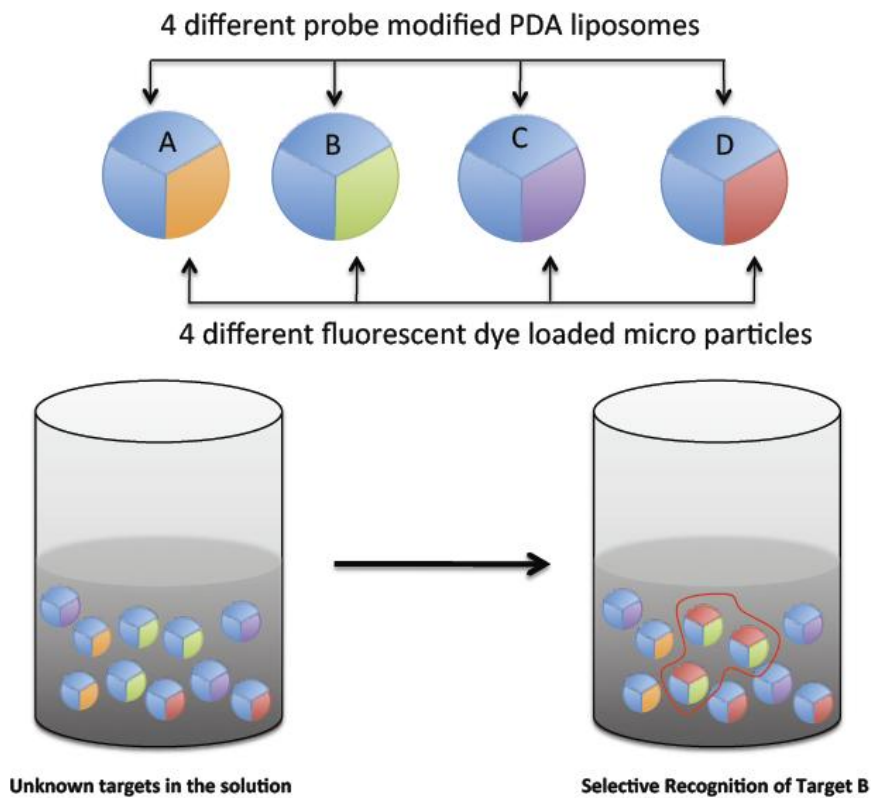
Figure 6.7. Illustration of unknown target screening using triphasic microbeads.

Another important feature of microbeads based PDA sensor system is the stability of sensor analytes. The aqueous based PDA liposomes has fundamental limits such as undesired aggregation after a long time storage in the ambient conditions. Our novel microbeads based PDA sensor system solved the disadvantage of PDA liposomes system using solid matrices supported system. After a month storage we did not observe any

aggregation and the microbeads showed exactly same optical properties of blue/red phase with the initial status. This resulted provided the possibility as a conventional and commercially available sensor generation requiring no additional cautious handling.

6.3 Conclusions

We developed a convenient and efficient fabrication method of Janus alginate microbeads having sensory PDA liposomes. The obtained microbeads showed selective and sensitive melamine detection down to 50 ppb level in a homogeneous aqueous solution that is a much better detection limit compared to the 1 ppm level of the solution phase detection system. We also demonstrated the dual signalling capability on multiple targets by using the biphasic Janus alginate PDA beads and further provided the possibility for target screening system using multi-phase microbeads.. These results may open up a new approach of the PDA sensor fabrication toward ultra sensitive detection of multi-targets. The developed convenient and simple protocol of Janus particles generation may further find wide range of applications from a multi component loaded drug delivery system to smart immunofluorescence labelling.

6.4 Experimental section

6.4.1 PDA liposomes formation.

A mixture of the PCDA-EG-CA and PCDA (9:1 mole ratio) monomer mixture was dissolved in 100 ul of tetrahydrofuran. The PDA mixture solution was injected rapidly into 20 ml of 50mM HEPES buffer pH 7.0 and was sonicated for 20 min. The suspension was filtered with 0.8 μm syringe filter and stored for 4 hr at 5oC (Final concentration of liposomes: 1mM). Biotin functionalized PDA liposomes were

generated in the di-water using PCDA-biotin, PCDA-EDEA and PCDA (3:1:6 mole ratio) monomer with the same protocol.

6.4.2 Monophase PDA liposomes loaded alginate micro particles.

1 mM of PCDA-EG-CA/PCDA (9/1) liposomes solution in 50mM of HEPES buffer pH 7.0 was added to the 4 wt% of alginic acid solution by 2:1 ratio. The PDA liposomes/alginate mixture solution was injected into the 2.5wt% $CaCl_2$ solution by centrifugation. (Needle size: 25G, centrifuge force: 21G) The PDA liposomes loaded alginate micro particles were stayed in the $CaCl_2$ solution for additional 30 minutes. Biotin functionalized PDA liposomes loaded alginate particles were generated with the same protocol. The red fluorescence image was taken using a fluorescence microscope (Olympus BX51) after 2 hours incubation in the desired concentration of melamine or avidin-FITC solution at room temperature.

6.4.3 Biphasic and triphasic phase PDA liposomes loaded alginate micro particles.

The experimental setup for Janus particle was similar to that of mono phase particle. Briefly, PCDA-EG-CA/PCDA (9/1) liposomes and PCDA-biotin/PCAD-EDEA/PCDA (3/1/6) liposomes solution was separately added to the 4wt% alginic acid solution by 2:1 ratio. The each mixture solution was injected together into the 2.5wt% $CaCl_2$ solution through the combined needle by the centrifugation for 1hour. The PDA liposomes loaded alginate micro particles were stayed in the $CaCl_2$ solution for additional 30 mins. The red/green biphasic fluorescence image was taken after 2 hours incubation in the melamine (50 ppm) /avidin-FITC (1mg/1ml) mixture solution using a fluorescence microscope (Olympus BX51). Triphasic phase PDA liposomes loaded particles were generated with the same protocol by attaching additional syringe containing PCDA liposomes/alginate mixture solution.

6.4.4 Synthesis and characterization

Materials and Method

All solvents were purchased from Sigma-Aldrich Chemicals. 10,12-pentacosadiynoic acid (PCDA) was purchased from GFS Chemicals. Dicyclohexylcarbodiimide, 4-dimethylaminopyridine, cyanuric acid, 1,8-diazabicycloundec-7-ene, carbon tetrabromide, triphenylphosphine, 6-bromohexan-1-ol, tri(ethylene glycol) were purchased from Sigma-Aldrich Chemical Co. UV/Vis absorption spectra were taken on a Varian Cary50 UV/Vis spectrophotometer. Fluorescence spectra were obtained using PTI QuantaMasterTM spectrofluorometers equipped with an integrating sphere. Fluorescence images were taken by Olympus BX51 W/DP71 fluorescent microscope.

Synthesis of PCDA Derivatives

Synthesis of PCDA-EG-CA
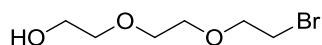
2-(2-(2-Bromoethoxy)ethoxy)ethanol

2-(2-(2-Bromoethoxy)ethoxy)ethanol To a solution of tri(ethylene glycol) (4.08 g, 27.14 mmol) in dichloromethane (50 mL) at 0°C was added carbon tetrabromide (3.00 g, 9.05 mmol) and triphenylphosphine (2.61 g, 9.95 mmol). The reaction mixture was stirred at room temperature for 2 hours, and the solvent was removed in vacuo. The residue was purified by silica gel column chromatography(Hexane/ethyl acetate=1/2) to give 1.61g (83%) of desired monomer **2-(2-(2-Bromoethoxy)ethoxy)ethanol** as yellowish oil (1.61 g). ^{1}H NMR (400 MHz, CDCl$_3$): δ   2.18 (brs, 1H), 3.44 (t, $J = 6.4$ Hz, 2H), 3.58 (m, 2H), 3.64 (s, 4H), 3.70 (m, 2H), 3.78 (t, $J = 6.2$ Hz, 2H).

2-(2-(2-Bromoethoxy)ethoxy)ethyl pentacosa-10,12-diynoate

2-(2-(2-Bromoethoxy)ethoxy)ethyl pentacosa-10,12-diynoate To a solution of 10,12-pentacosadiynoic acid (2 g, 5.34 mmol)) in dichloromethane (30 mL) at 0 ^{o}C was added **2-(2-(2-Bromoethoxy)ethoxy)ethanol** (1.32 g, 5.34 mmol), dicyclohexylcarbodiimide (1.32 g, 6.41 mmol) and 4-dimethylaminopyridine (0.012g, 0.10 mmol). After the reaction mixture was vigorously stirred for 2 hours, 20mL of hexane was poured into the mixture and the white urea solid was filtered off. The solvent was removed in vacuo. The residue was purified by silica gel column chromatography (Hexane/ethyl acetate =10/1) to give 2.7g (89%) of desired diacetylene monomer **2-(2-(2-Bromoethoxy)ethoxy)ethyl pentacosa-10,12-diynoate** as a colorless oil. ^{1}H NMR (400 MHz, CDCl$_3$): δ   0.84 (t, J = 6.8 Hz, 3H), 1.21-1.32 (m, 26H), 1.43-1.59 (m, 6H), 2.20 (t, J = 6.8 Hz, 4H), 2.29 (t, J = 7.6 Hz, 2H), 3.43 (t, J = 6.2 Hz, 2H), 3.62-3.68 (m, 6H), 3.77 (t, J = 6.2 Hz, 2H), 4.19 (t, J = 4.8 Hz, 2H).

PCDA-EG-CA

PCDA-EG-CA To a solution of **2-(2-(2-Bromoethoxy)ethoxy)ethyl pentacosa-10,12-diynoate** (1.9 g, 3.33 mmol) in dimethylformamide (50 mL) was added cyanuric acid (4.30 g, 33.33 mmol) and 1,8-diazabicycloundec-7-ene (0.50 mL, 3.33 mmol). The reaction mixture was heated under 60 ^{o}C for 8 hours, poured into the water and extracted with ethyl acetate. The organic layer was washed 3 times with water to eliminate the excess cyanuric acid, dried with MgSO$_4$ and filtered. Most of solvent was removed under vacuo. The resulting solution was recrystallized from methyl alcohol and ethyl acetate to

give 1.56g (76%) of desired diacetylene monomer **PCDA-EG-CA** as a white solid. ^{1}H NMR (400 MHz, CDCl$_3$): δ   0.875 (t, J = 7.0 Hz, 3H), 1.25-1.47 (m, 26H), 1.49-1.57 (m, 4H), 1.60 (t, J = 7.0 Hz, 2H), 2.22-2.25 (m, 4H), 2.32 (t, J = 7.6 Hz, 2H), 3.65-3.69 (m, 6H), 3.76 (t, J = 5.2 Hz, 2H), 4.07 (t, J = 5.2 Hz, 2H), 4.22 (t, J = 4.8 Hz, 2H), 9.49 (brs, 2H) . ^{13}C NMR (100 MHz, CDCl$_3$): 14.07, 19.15, 22.63, 24.78, 28.27, 28.30, 28.73, 28.81, 28.86, 29.05, 29.29, 29.42, 29.59, 31.86, 34.12, 40.46, 63.27, 65.17, 65.24, 67.32, 69.00, 69.80, 70.42, 77.38, 77.55, 148.24, 149.22, 173.97. MS (ES): Calcd, 617.4; found (M+Na)$^+$, 640.4.

PCDA-NHS To a solution containing 1.00 g (2.67 mmol) of 10,12-pentacosadiynoic acid in 10 mL   of methylene chloride was added 0.38 g (3.47 mmol) of N-hydroxysuccinimde and 0.38 g (4.01 mmol) of N-(3-Dimethylaminopropyl)-N'-ethylcarbodiimide hydrochloride at room temperature. The resulting solution was stirred at room temperature for 2 h. The solent was removed in vacuo, and the reside purified by extraction with ethyl acetate to give1.08 g (86.2 %) of the desired diacetylene monomer PCDA-NHS as a white solid.: ^{1}H NMR (300 MHz, CDCl3): δ 0.85 (t, 3H), 1.20-1.62 (m, 36H), 2.21 (t, 4H), 2.60 (t, 2H), 2.85 (s, 4H), 7.18 (brs, 1H).

PCDA-EDEA

PCDA-EDEA To a solution containing 1.055 mL (7.21 mmol) of 2,2'-(Ethylenedioxy)bis(ethylamine) in 60 mL of methylene chloride was added dropwise 1.00 g (2.12 mmol) of PCDA-NHS for 3h at room temperature. The resulting mixture was allowed to stir for 2 h at room temperature. The resulting mixture was concentrated in vacuo, and the residue was purified by column chromatography (9:1 chloroform : methanol) to give 0.51 g (46.7 %) as a white solid.: ^{1}H NMR (300 MHz, CDCl3): δ 0.89

(t, 3H), 1.27-1.76 (m, 35H), 2.23 (m, 6H), 2.91 (t, 2H), 3.42-3.63 (m, 12H), 6.21 (t, 1H), 7.27 (brs, 1H).

PCDA-Biotin

PCDA-biotin To a solution containing 0.23 g (0.94 mmol) of biotin in 5 mL of DMF was added   dropwise 0.40 g (0.79 mmol) of PCDA-EDEA in 5 mL methylene chloride. The mixture solution was allowed to stir for overnight at room temperature. The solvent was removed in vacuo, and the residue was purified by column chromatography (9:1 chloroform : methanol) to give 0.18 g (33.9%) of the desired diacetylene monomer PCDA-EDEA-biotin as a white solid.: ^{1}H NMR (300 MHz, CDCl3): δ 0.89 (t, 3H), 1.27-1.76 (m, 41H), 2.23 (m, 8H), 2.74 (d, 1H), 2.94 (m, 1H), 3.17 (m, 1H), 3.42-3.65 (m, 13H), 4.32 (q, 1H), 4.54 (q, 1H), 4.92 (s, 1H), 5.87 (s, 1H), 6.27 (t, 1H), 6.31(t, 1H), 7.27 (brs, 1H).

6.5 References

[1]   J.-M. Kim, J.-S. Lee, H. Choi, D. Sohn, D. J. Ahn, Macromolecules 2005, 38, 9366.

[2]   S. J. Kew, E. A. H. Hall, Analytical Chemistry 2006, 78, 2231.

[3]   A. C. S. Pires, N. d. F. t. F. Soares, L. H. M. da Silva, M. C. H. da Silva, A. B. Mageste, R. m. F. Soares, A. l. V. N. C. Teixeira, N. l. J. Andrade, The Journal of Physical Chemistry B 2010, 114, 13365.

[4]   A. R. Burns, R. W. Carpick, D. Y. Sasaki, J. A. Shelnutt, R. Haddad, Tribology Letters 2001, 10, 89.

[5]   K. Kuriyama, H. Kikuchi, T. Kajiyama, Langmuir 1996, 12, 6468.

[6]   a)Q. Cheng, R. C. Stevens, Langmuir 1998, 14, 1974; b)Q. Cheng, M. Yamamoto, R. C. Stevens, Langmuir 2000, 16, 5333.

[7]   a)J. Lee, E. Jeong Jeong, J. Kim, Chemical Communications 2011; b)S. Kolusheva, L. Boyer, R. Jelinek, Nat Biotech 2000, 18, 225.

[8]   D. Y. Sasaki, R. W. Carpick, A. R. Burns, Journal of Colloid and Interface Science 2000, 229, 490.

[9]   a)J. M. Kim, Y. B. Lee, S. K. Chae, D. J. Ahn, Advanced Functional Materials 2006, 16, 2103; b)J.-M. Kim, S. K. Chae, Y. B. Lee, J.-S. Lee, G. S. Lee, T.-Y. Kim, D. J. Ahn, Chemistry Letters 2006, 35, 560.

[10]   L. Silbert, I. Ben Shlush, E. Israel, A. Porgador, S. Kolusheva, R. Jelinek, Appl. Environ. Microbiol. 2006, 72, 7339.

[11]   I. Gill, A. Ballesteros, Angewandte Chemie International Edition 2003, 42, 3264.

[12]   Y. Lu, Y. Yang, A. Sellinger, M. Lu, J. Huang, H. Fan, R. Haddad, G. Lopez, A. R. Burns, D. Y. Sasaki, J. Shelnutt, C. J. Brinker, Nature 2001, 410, 913.

[13]   S. K. Chae, H. Park, J. Yoon, C. H. Lee, D. J. Ahn, J. M. Kim, Advanced Materials 2007, 19, 521.

[14]   a)J. Lee, H.-J. Kim, J. Kim, Journal of the American Chemical Society 2008, 130, 5010; b)J. Lee, H. Jun, J. Kim, Advanced Materials 2009, 21, 3674.

[15]   Y.-H. Lin, H.-F. Liang, C.-K. Chung, M.-C. Chen, H.-W. Sung, Biomaterials 2005, 26, 2105.

[16]   O. Cayre, V. N. Paunov, O. D. Velev, Journal of Materials Chemistry 2003, 13, 2445.

[17]   K.-H. Roh, D. C. Martin, J. Lahann, Nat Mater 2005, 4, 759.

[18]   T. Nisisako, T. Torii, T. Takahashi, Y. Takizawa, Advanced Materials 2006, 18, 1152.

[19]   N. M. Green, in Advances in Protein Chemistry, Vol. Volume 29 (Eds.: J. J. T. E. C.B. Anfinsen, M. R. Frederic), Academic Press, 1975, pp. 85.

CHAPTER 7

Highly Emissive Self-assembled Organic Nanoparticles having Dual Color Capacity for Targeted Immunofluorescence Labeling

7.1 Introduction

Immunofluorescence labeling is a very important analytical technique for probing the structure of living cells. Such labeling is conventionally carried out by using fluorescent organic dyes. However, some drawbacks including a limited range of light emission and particularly poor photo-stability[1] have limited the usage of organic dyes. After the introduction of semiconducting quantum dots[2,3] many research groups have investigated inorganic quantum dots[4] for immunofluorescence labeling due to their high quantum yield,[5] high molar extinction coefficients, broad absorption with narrow light emission, and good photo physical and chemical stability.[6–9] Despite the promising properties of semiconducting quantum dots for immunofluorescence labeling, cyto-toxicity is a critical problem in any live-cell or animal experiments.[10,11] Alternative choices are dye-loaded latex particles and dye-doped silica colloids having improved photostability compared to conventional dye molecules. However, dye-loaded beads also have a critical limit of brightness due to self-quenching when high density of dyes present at the nanoparticle surface. In this context, developing highly emissive, biocompatible, and chemically readily modifiable luminescent materials is strongly desired. Recently, a few papers have

been published reporting conjugated organic small molecules that showed higher quantum yield in the solid state than in solution.[12–16] In other words, self-quenching does not exist in these unique molecules. It has opened a new possibility to develop non-toxic organic nanoparticles with enhanced emission for various applications including immunofluorescence labeling. The reason for the lower quantum yield in solution of some of these molecules is believed that the conjugated backbone of the molecules is significantly twisted by steric hindrance[13] and the radiative decay pathway of the resulting twisted chromophores[17] is generally suppressive. Therefore, planarization of the twisted conjugated backbone upon aggregation in the solid state accordingly enhances the emissive property of the molecules. On the other hand, another class of molecules that has a larger quantum yield in the solid state has a different reason for the enhanced emissive property. These molecules in solution have a low quantum yield because they dissipate energy for molecular rotation. Therefore, they have even 20% higher quantum yield in the solid state because the molecular rotation is hindered by adjacent molecules in the solid state.[12–17]

7.2 Results and Discussion

We have developed highly emissive organic nanoparticles by using colloidal self-assembly of a hydroxyphenyl-benzoxazole (HBO) derivative and diacetylene monomers. Various heterocyclic molecules including HBO have been investigated by many research groups due to their chemical and thermal stability as well as their high electron mobility. HBO has a high extinction coefficient and excellent stability in the UV range and has shown potential as a UV stabilizer. HBO is also known to undergo excited state intramolecular proton transfer (ESIPT) upon photo-excitation as illustrated in Figure 7.1A.
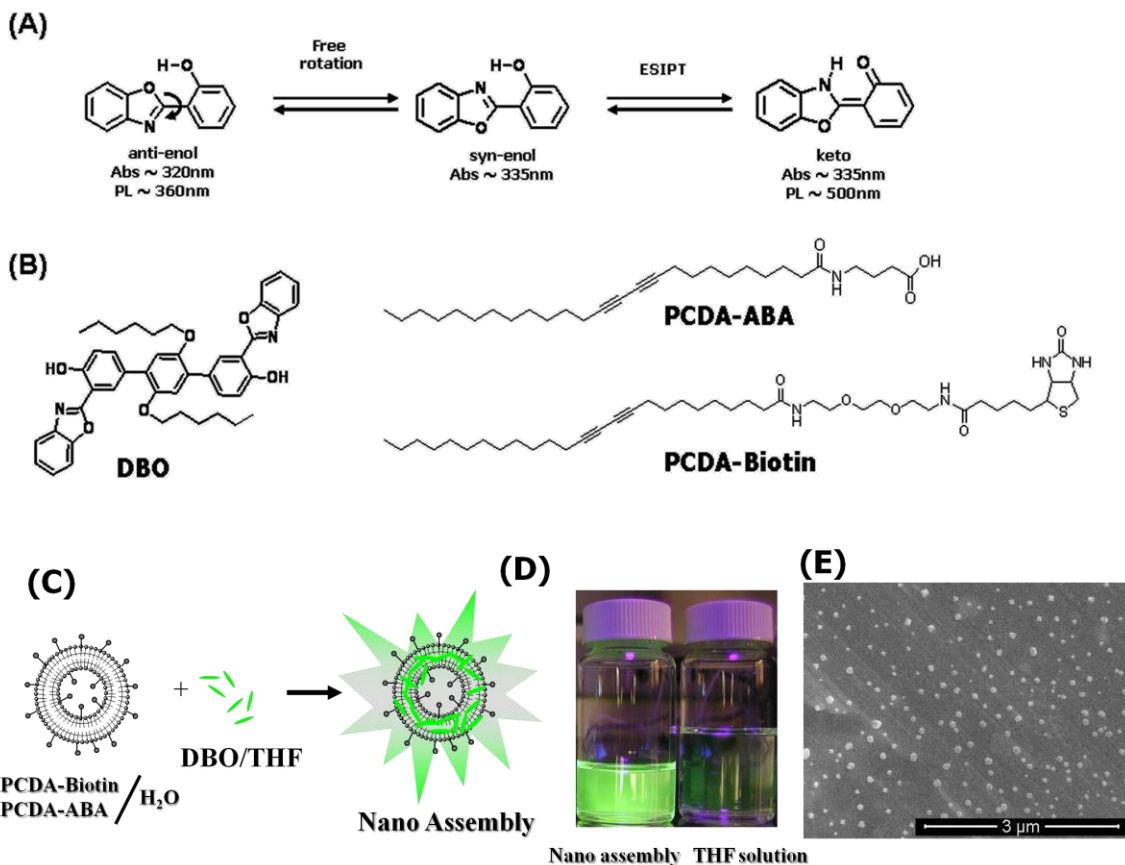
Figure 7.1. A) Rotamer structures (anti-enol and syn-enol) of HBO and its excited state keto formation. The given wavelengths are their absorption and emission lmax. B) Molecular structures of DBO, PCDA-ABA, and PCDA-Biotin. C) Schematic representation of nanoparticle assembly of DBO in a PCDA vesicle. D) A photograph ofDBOin THFsolution and DBO-PCDA nanoparticles under 365nmUV light. E) Scanning electron microscopy image of the DBOPCDA nanoparticle.

We synthesized 1,4-di(3-(benzoxazol-2-yl)-4-hydroxyphenyl)- 2,5-dihexyloxybenzene (DBO) as shown in Figure 7.1B. The absorption and photoluminescence spectra of DBO are shown in Figure 7.2C. Dilute solution of DBO in tetrahydrofuran (THF) has absorption lmax at 335 nm assigned to syn-enol and emits at 518 nm, showing a large Stokes shift due to ESIPT. A nanoparticle dispersion ofDBOwas prepared by adding THF solution of DBO to water to induce aggregate formation. The prepared nanoparticles in the mixed solution of THF:H$_2$O(1:9v/v) showa broad aggregation band above 400nmdue toMie scattering (Figure 7.2C).[18] Interestingly their fluorescence quantum yield (FF) was 10%, which ismore than 3 times larger than the

quantumyield of the THF solution (3%). The enhanced fluorescence emission intensity in the aggregates is believed to originate from a more planar structure induced by J-type aggregation through intermolecular hydrogen bonding evidenced by the absorption red shift by 40 nm from 335 nm (Figure 7.2C).
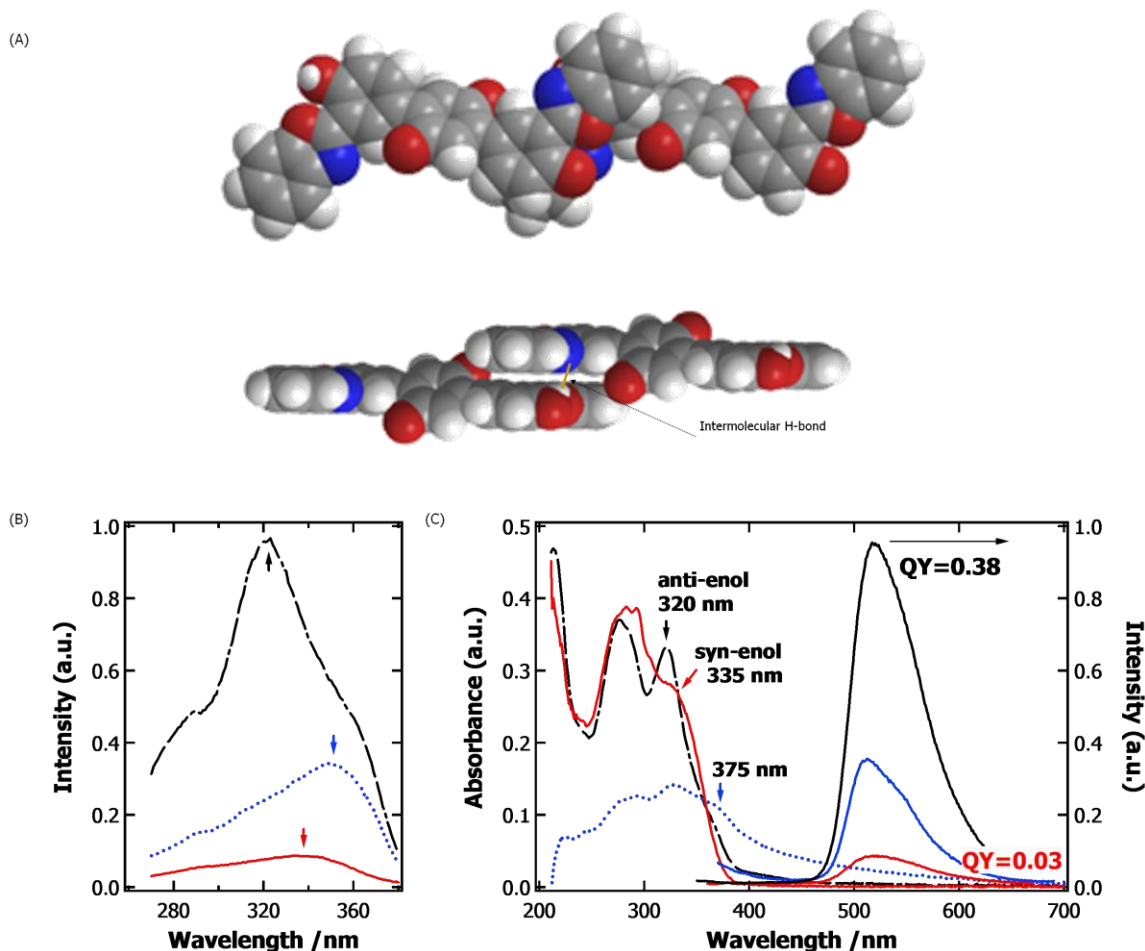
Figure 7.2. A) Geometry optimized molecular structure of DBO produced by using Materials Studio 4.1 with DFT (density functional theory) with BLYP parameter. Two DBOs are organized to show intermolecular hydrogen bonding between benzoxazole units. (B) Excitation spectra of DBO in THF solution (solid line), dispersion in deionized water (dotted line), and dispersion in diacetylene vesicle (broken line) for the 520 nm emission of Figure 2C. C) UV/Vis absorption and photoluminescence spectra ofDBOin THFsolution (solid lines), in THF:H2O(1:9 v/v) (dotted lines), and in the diacetylene vesicle solution (broken lines). The concentration of the DBO solution and dispersions was 10 mM.

To reduce the Mie scattering and prepare DBO nanoparticles having a well-defined size, we investigated amphiphilic surfactant molecules in order to direct the self-assembly of DBO. We anticipated that surfactant molecules would disperse DBO aggregates evenly by passivating the surface of the aggregates. Several amphiphilic molecules such as phospholipids, ionic surfactants, and diacetylenes were used to disperse and assemble DBO or random aggregates of DBO into more defined nanoparticle structures. We found that all the amphiphilic molecules served well as a dispersion agent. In this report, we present the results obtained by using a unique combination of diacetylene molecules as a dispersion agent.[19] 7:3 mole ratio of 10,12-pentacosadiynoic acid-aminobutyric acid (PCDA– ABA) and 10,12-pentacosadiynoic acid–2,20-(ethylenedioxy)- bis(ethylamide)-biotin (PCDA–Biotin) were mixed in HEPES buffer (0.5 mM) and then sonicated to form PCDA vesicles. 0.1 ml of 1mM DBO in THF solution was then added into the 10 ml of PCDA vesicle solution and the mixture solution was sonicated for 10 min to form well-defined (80 ± 10) nm of DBO nanoparticles having PCDA passivation layer as illustrated in Figure 7.1C. The resulting suspension has a 1:50 mole ratio of DBO to PCDA and the SEM image of the self-assembled DBO-PCDA nanoparticles is shown in Figure 7.1E. Note the significantly enhanced fluorescence emission intensity of the self-assembled DBO-PCDA nanoparticles in Figure 7.1D and 7.2C. The quantum yield of the self-assembled DBO-PCDA nanoparticles was 38%, which is almost 13 times larger than that of DBO in THF solution. It is also interesting to note that the DBO-PCDA nanoparticles have strong anti-enol absorption at 320 nm. Considering the fact that only the syn-enol form can undergo ESIPT and the molecular rotation from antienol to syn-enol is suppressed in the solid state, observing the strong emission at 518 nm with ca. 200 nm of Stoke shift was puzzling.[20] We hypothesize that DBO in the DBO-PCDA nanoparticles forms J-type aggregation through intermolecular hydrogen bonding as illustrated in Figure 7.2A. The planarized conjugated backbone of DBO and the restricted molecular rotation in the J-

aggregates are then reasonably believed as the origin of the largely enhanced 38% quantum yield.[13,17] First, as theoretical energy calculation studies and experimental data showed that twisted conjugated organic molecules generally have lower quantum
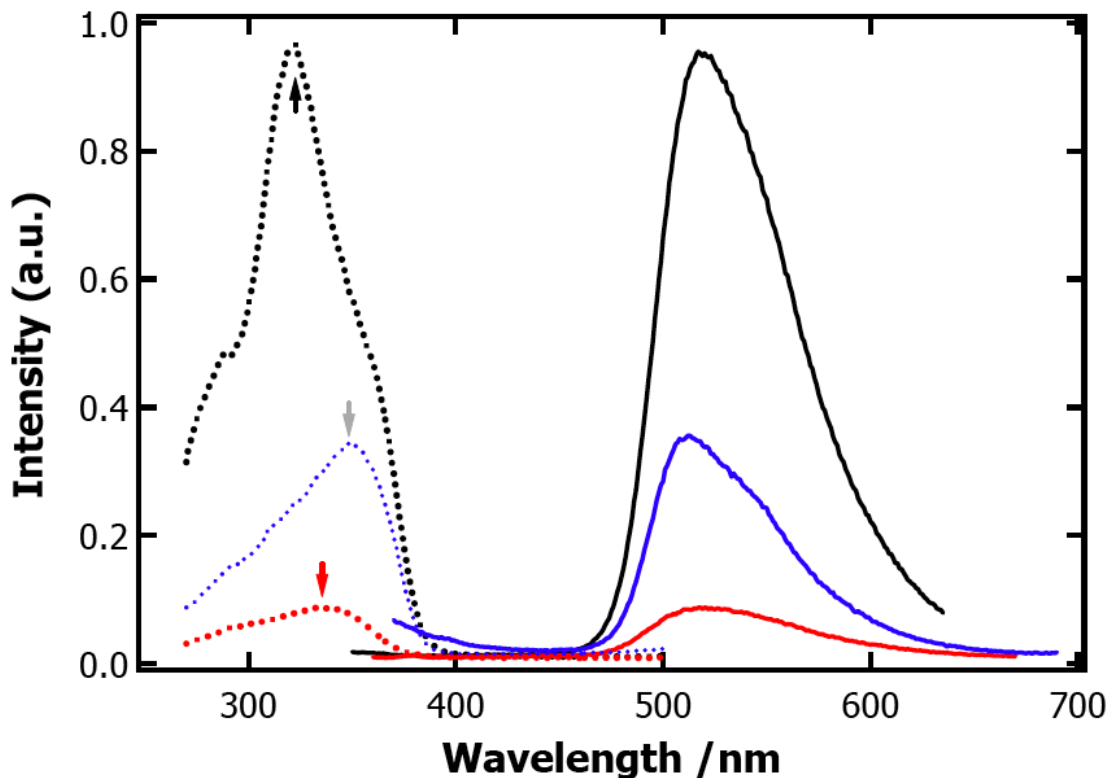
Figure 7.3. Excitation (dotted lines) and emission (solid lines) spectra of DBO in THF solution (red), dispersion in deionized water (blue), and dispersion in diacetylene liposome (black). The concentrations of DBO were 10 μM. There is red shift for the nanoparticles in THF/H2O mixture. The anti-enol species (320 nm) formation is seen for the DBO-PCDA vesicle.

yield,[12–16] it is reasonable that the planarized conjugated backbone of DBO in the self-assembled J-aggregates has a larger quantum yield compared to DBO in solution. Another supporting experimental evidence for our hypothesis is the fact that we obtained much longer life-time from the self-assembled DBO-PCDA nanoparticles than the DBO i n THF solution. The life time of the 518nm emission band when excited at 380 nm was 0.42 and 6.26 ns for the DBO solution in THF and the DBO-PCDA nanoparticles, respectively. The life-time of the 518 nm emission band when the DBO-PCDA nanoparticles were excited at 310 nm (anti-enol) was 6.41 ns which is similar to the 6.26

ns of the syn-enol excitation. Previous experimental studies showed that the lifetime of HBO was increased from ca. 10 ps at room temperature to 5.7 ns at 77 K as the molecular motion was restricted at the 77 K.[21] The authors also reported that the quantum efficiency of HBO increased from 3.5% at room temperature to 37% at 77K. These values of the lifetime and the quantum efficiency are in good agreement with what we
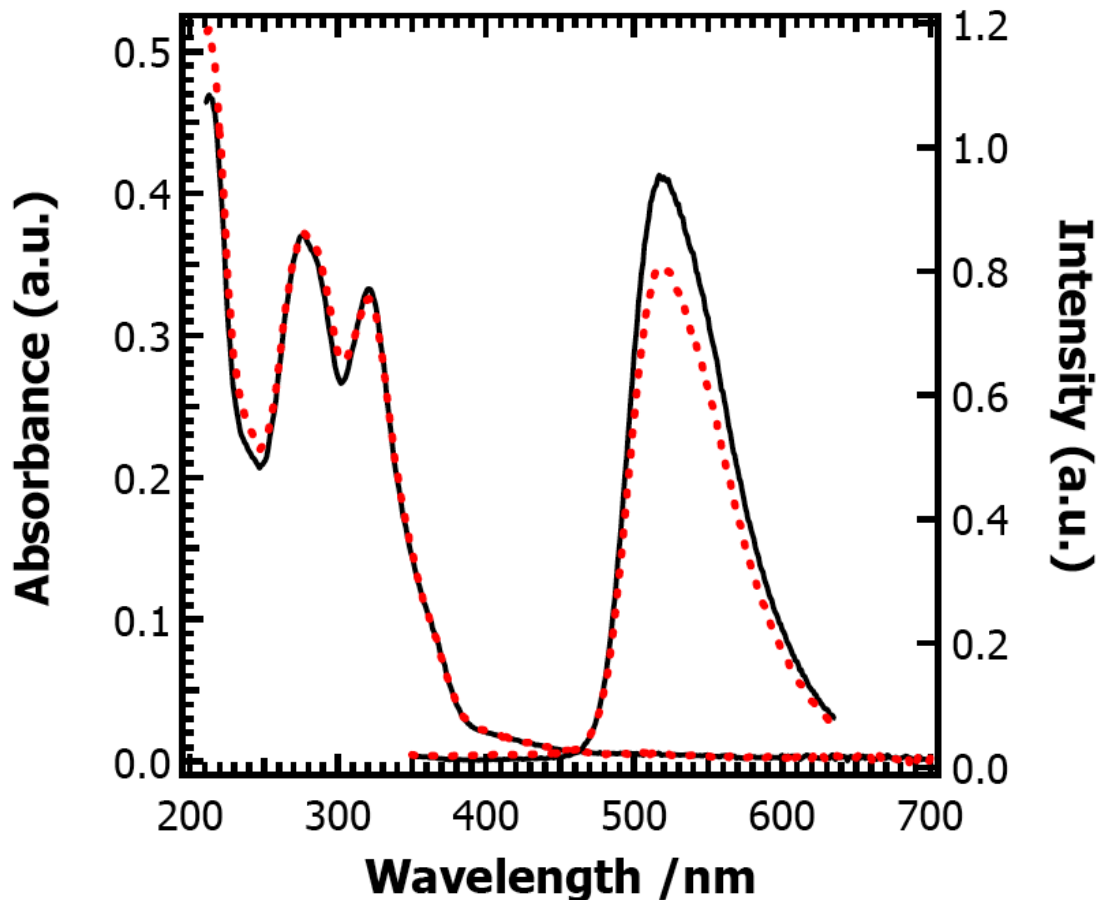
observed from theDBOsolution in THF and DBO-PCDA nanoparticles if we consider the solidstate as a mimic of the frozen solution at 77 K considering the restricted molecular movement in both cases.

Figure 7.4. UV irradiation experiment was done with DBO nanoparticles in THF/H2O mixture. 6W 254nm UV was illuminated 1cm above the suspension. The black line is before UV irradiation and the red lines were obtained after 30min of exposure..

To monitor its photochemical stability, DBO-PCDA nanoparticles were exposed to a 6-W 254-nm handheld UVlight held 1 cm above the sample for 30 min. The fluorescence intensity of DBO-PCDA nanoparticles decreased only by 15% upon the intense UV irradiation while other fluorescent organic dyes[1] (Alexa Fluor 488) and conjugated polymers[22] (poly(p-phenyleneethynylene) and poly(3-hexylthiophene)) experienced 80–90% of quenching under the same condition (data not shown).
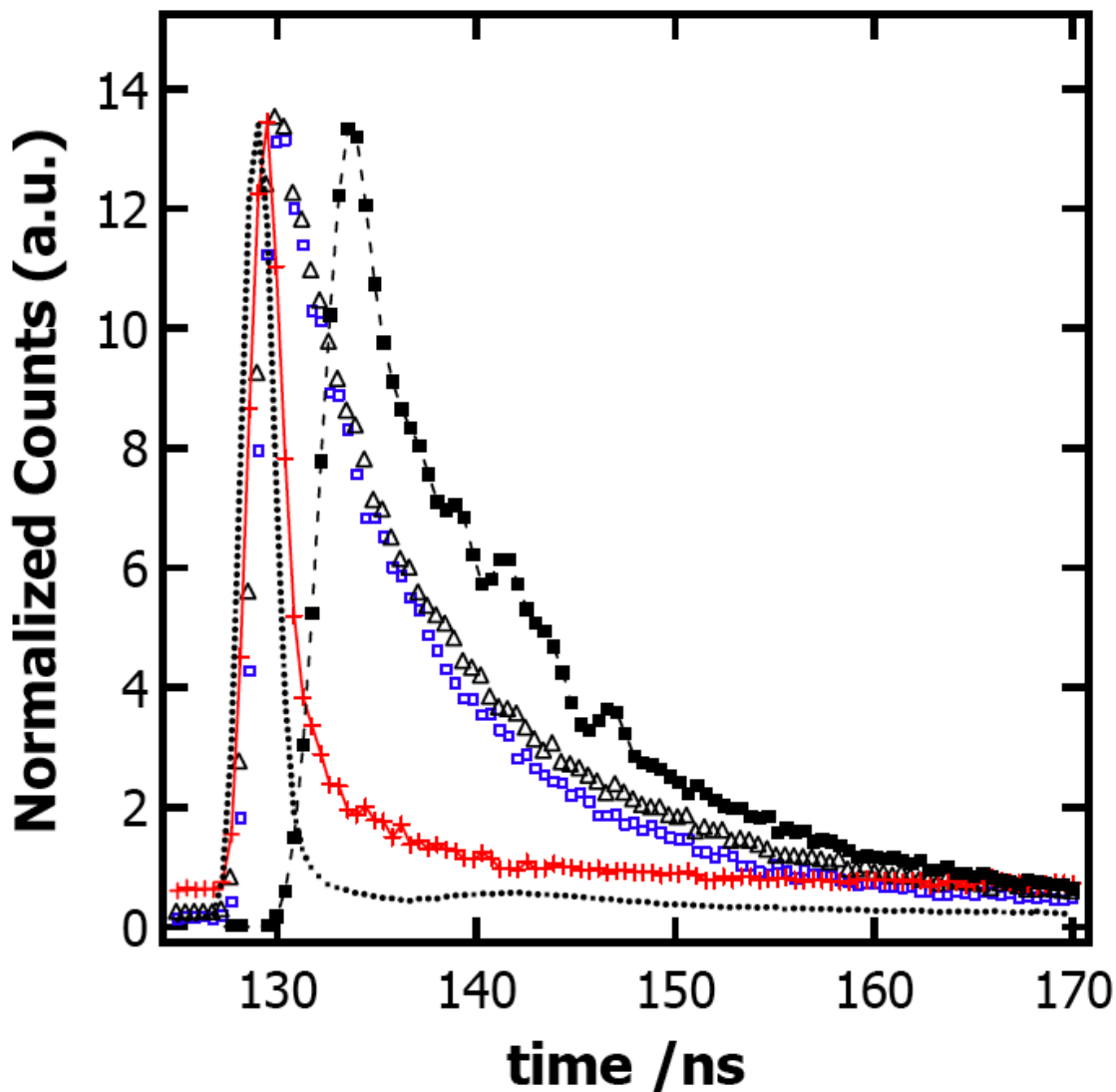
Figure 7.5. Fluorescence lifetime of DBO in THF solution (red), dispersion in THF:H2O 1:9 v/v mixture (blue), and dispersion in diacetylene liposome (black) observed at 380nm excitation wavelength. Lifetime measurement was also done at 310nm excitation for the DBO-PCDA nanoparticles (closed black). Instrument response function is plotted in dotted line.
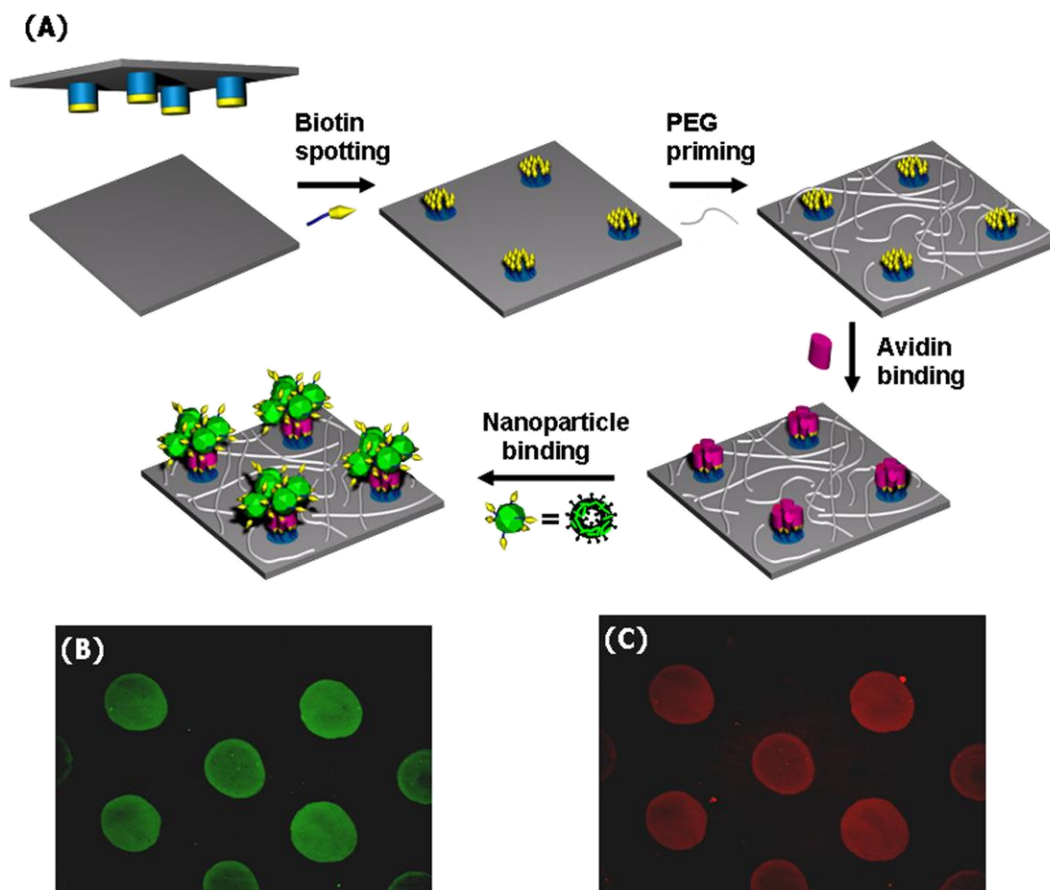
Figure 7.6. A) Schematic illustration of selective fluorescence labeling by means of functionalized DBO-PCDA organic nanoparticles. B) A fluorescence microscopy image obtained by using a 400 nm long-pass emission filter after selective binding of biotinylated DBO-PCDA nanoparticles on the patterned avidin surface. C) A fluorescence microscopy image from a 600 nm long-pass emission filter showing the red fluorescence emission from the red phase of polydiacetylene passivation layer induced by biotin-avidin interaction. The diameter of the dots of the fluorescence microscopy images is 500 mm.

We further investigated the possible application of the highly emissive and biotin-functionalized DBO-PCDA nanoparticles for immunofluorescence labeling. First, sulfo-N-hydrosuccinimide-biotin (1mg/ml^{-1} in phosphate buffered saline (PBS)) was spotted on an amine-functionalized glass surface using a manual micro-arrayer (V&P Scientific, VP478A) (Figure 7.6A). Remaining active amines were blocked with poly(ethylene oxide) and subsequently avidin from egg-white (1 mg/ml^{-1} in PBS) was spread on the biotin-patterned glass slide. After thoroughly washing off unbound avidin, a 0.5 mM solution of the self-assembled DBO-PCDA nanoparticles in HEPES buffer was finally

applied on the avidin-patterned glass slide. After removing non-specifically bound DBO-PCDA nanoparticles by rinsing several times with HEPES buffer, microscopic images were taken as shown in Figure 7.6B. As we can see from the image green fluorescent was observed from only the avidin spots, demonstrating good selectivity and bright emission.

The self-assembled DBO-PCDA also has a dual color capability because the PCDA not only serves as a surfactant and a recognition unit for the target avidin spots but also can generate a sensory signal. We polymerized the PCDA passivation layer after self-assembling the biotinylated DBO-PCDA nanoparticles. The polymerized polydiacetylene (PDA) layer will experience perturbation of the conjugated backbone and undergo mechanochromism from the blue form to the red form during the biotin-avidin recognition/binding. Because the red form is emissive[23] as we anticipated we observed red emission when we used a 600 nm long-pass emission filter with a 550 nm excitation filter as shown in Figure 7.6C.

7.3 Conclusions

We have synthesized DBO and self-assembled DBO with functionalized PCDA molecules to form welldefined DBO-PCDA nanoparticles. The DBO-PCDA nanoparticles showed aggregation-induced fluorescence enhancement having a 38% of quantum yield. Intermolecular hydrogen bonding is believed to form J-aggregates and allows intermolecular excited state proton transfer. Selective targeting and dual color visualization of patterned avidin arrays were achieved by using the highly emissive biotinylatedDBO-PCDA nanoparticles to demonstrate the promising application of the organic nanoparticles for immunofluorescence labeling.

7.4 Experimental section

7.4.1 Immunofluorescence Labeling Fabrication

Glass slides were cleaned in boiling $H_2O:H_2O_2:NH_4OH$ (1:1:4 volume ratio) solution for 30 min, followed by piranha solution ($H_2O_2:H_2SO_4$ 3:7) etching after thorough rinsing with water and drying. The glass slides were further dipped in 2 wt % 3-aminopropyltriethoxysilane in toluene solution for 1 h, and were sonicated in toluene: methanol (1:1) and methanol for 3 min each to remove unbound silanes. The final amine functionalized glass slides were stored in a sealed container at 4 ^{o}C. 1mg of sulfo-NHS-biotin purchased from Aldrich was dissolved in 1 ml of phosphate buffered saline and used right after the preparation before the hydrolysis of sulfo-NHS. 2.2 mg succinimidyl-4-(N-maleimidomethyl) cyclohexane-1-carboxylate (purchased from Pierce, Co.) was dissolved in 200 ml DMSO and further diluted in DMSO:ethanol 2:8 volume ratio mixture. 2.4 mg of mono functional thiolated poly(ethylene oxide) (Mw¼ 2400 g mol/1, purchased from PolymerScience) in 10 ml of PBS. 1mg of Avidin from egg-white purchased from Aldrich was also dissolved in 1ml of PBS buffer with 0.02 wt % Tween20 (PBST). Sulfo-NHS-biotin was spotted on an amine glass with a manual microarray (V&P Scientitic, VP475A) and stored in a humidity chamber (Relative humidity 90%) for 4 h. After rinse with PBS buffer, remaining active amines were reacted with SMCC crosslinker and were blocked further with thiol-poly(ethylene oxide) in PBS and rinsed with water. Avidin solution was spread on the biotin spotted glass for 30 min. After the avidin-biotin binding, the unbound avidin was rinsed off with PBST and stored in PBS until next experiment. The avidin patterned glass slide was immersed in the biotinylated vesicle suspension for 30 min and examined with a fluorescence microscope (Olympus BX51) 3.5 mmol of PCDA-ABA and 1.5 mmol of PCDABiotin were dissolved in chloroform and filtered through a 0.45 mm syringe filter. After the evaporation of chloroform, 10 ml of 1 mM HEPES buffer was added in to give 0.5mMPCDA. The homogeneous PCDA suspension was obtained via sonication for 15 min at the transition temperature of PCDA. Pre-determined amount (0.1 ml) of 1 mM DBO in THF solution was injected after or during the vesicle formation to get 1:50

DBO:PCDA mol ratio. And the final DBOPCDAvesicles were stored at 4 ^{o}C in the dark before use. Nanoparticles in THF:H$_2$O 1:9 mixture were obtained by precipitation of 1 ml of 0.1 mM DBO in THF into 9 ml of deionized water during sonication.

7.4.2 Synthesis and characterization

Synthesis of DBO

2-(benzoxazol-2-yl)-4-bromophenol. 2-Aminophenol (2.51 g, 23.03 mmol) and 5-bromosalicylic acid (5.5 g (23.03 mmol) were added in 30 ml of polyphosphoric acid and the mixture was heated to 130 ℃ and stirred for 4h. After cooling to room temperature, the reaction mixture was precipitated in ice-water, filtered and washed with DI water. The product was recrystallized from acetic acid and dried in vacuo (yield 5.94 g, 88.9%). ^{1}H NMR(300MHz, CDCl$_3$) : δ 11.44 (s, 1H), 8.16-7.04 (m, 7H). tert-butyl-2-(benzoxazol-2-yl)-4-bromophenyl carbonate (1). 2-(benzoxazol-2-yl)-4-bromophenol (0.8 g, 2.76 mmol) was dissolved in dry, distilled tetrahydrofuran (THF) with di-tertbutyldicarbonate and (4-dimethylamine) pyridine (5 mol-%). When the reaction appeared complete by thin-layer chromatography (TLC), the solution was concentrated and precipitated in DI water, 2 washed with ethanol. The product was dried in vacuo (yield 0.77g, 74.5 %). ^{1}H NMR(300MHz, CDCl$_3$) : δ 8.44 (s, 1H), 7.77 (d, 1H), 7.65 (d, 1H), 7.58 (d, 1H), 7.38 (m, 2H), 7.2 (d, 1H), 1.58 (s, 9H).

2,5-dibromo-1,4-dihydroxybenzene. Hydroquinone (50 g, 0.454 mol) was added in acetic acid (240 ml) and stirred vigorously. Bromine (46.6 ml, 0.91 mol) in acetic acid (200 ml) was dropwised to above suspension at 10 ~ 15 ℃. The mixture solution was stirred at room temperature for 12 h and filtered off the pale crystal. The filtrate was reduced to the minimum under vacuum and the white crude product was recrystallized in methanol, filtered and dried in vacuo (yield 29.86 g, 24.55%). ^{1}H NMR(300MHz, CDCl$_3$) : δ 6.98 (s 2H).

2,5-dibromo-1,4-dihexyloxybenzene. A suspension of KOH powder (10.47 g, 186.6 mmol) in dried DMSO (360 ml) was degassed under vigorous stirring for 1h. 2,5-dibromo-1,4-dihydroxybenzene (5 g, 18.66mol) and 1-bromohexane (5.8 ml, 41.06 mmol) were added and stirred for 12 h. The solution was concentrated and precipitated in water, filtered, washed with methanol. The product was recrystallized in ethanol, dried in vacuo (4.518g, 55.5 %). ^{1}H NMR(300MHz, CDCl^3) : δ 7.08 (s, 2H), 3.95 (t, 4H), 1.8 (m, 4H), 1.49 (m, 4H). 1.37 (m, 8H), 0.9 (t, 6H).

2,5-(1,4-dihexyloxyphenyl)diboronic   acid(2).   2,5-dibromo-1,4-dihexyloxybenzene (2 g, 4.58 mmol) was dissolved in ethyl ether (20 ml) and Butyl-Litium (2.5 M in hexane, 5.05 ml) was added and stirred at room temperature for 12 h under argon gas. Triisopropylborate (2.3 ml, 10.05 mmol) was added at -40℃ and stirred over night from -40℃ to room temperature. The reaction was quenched by the addition of HCl 2M solution (50 ml) and the resulting precipitation was collected, washed with water, ethyl ether, and dried under vacuo (yield 0.53 g, 31.61 %). ^{1}H NMR(300MHz, CDCl^3) : δ 7.16 (s, 2H), 3.95 (t, 4H), 1.68 (m, 4H), 1.8 (m, 4H), 1.25 (m, 8H), 0.85 (t, 6H).

t-Boc benzoxazole oligomer. The oligomerization was carried out between 1 and 2. 1 (0.3 g, 0.8 mmol), 2 (0.148 g, 0.4 mmol), palladium catalyst (5 mol %) were placed in a two-necked roundbottom flask charged with 7 ml of THF under argon. 1 M Na2CO3 solution was added and stirred for 48 h at 80 ℃. After cooling, the reaction mixture was poured into methanol. The precipitates were isolated by filtration and washed with DIwater and methanol and dried under vacuo. ^{1}H NMR(300MHz, CDCl$_3$) : δ 8.56 (s, 2H), 7.78 (m, 4H), 7.58 (m, 2H), 7.36 (m, 6H), 7.06 (s, 2H), 3.98 (t, 4H), 1.7 – 01.2 (m, 16H), 0.78(t, 6H).

Benzoxazole oligomer. The t-Boc benzoxazole oligomer was dissolved in chloroform (3 ml) ands trifluoreacetic acid (2 ml) was added. After stirring for 12 h, solvents was removed by evaporation and dried under vacuum oven (yield 0.217 g). ^{1}H

NMR(300MHz, CDCl$_3$) : δ 11.55 (s, 2H), 8.35 (s, 2H), 7.79-7.68 (m, 4H), 7.62 (m, 2H), 7.41 (t. 4H), 7.2 (d, 2H), 7.06 (s, 2H), 3.99 (t, 4H), 1.78 – 1.23 (m, 16H), 0.78 (t, 6H).

Synthesis of PDA molecules

The diacetylene monomers investigated in this study were prepared by coupling Nhydroxysuccininic esters of PCDA. A typical procedure for the preparation of PCDA-ABA and PCDA-biotin is as follows.

PCDA-NHS: To a solution containing 1.00 g (2.67 mmol) of 10,12-pentacosadiynoic acid in 10 mL of methylene chloride was added 0.38 g (3.47 mmol) of N-hydroxysuccinimde and 0.38 g (4.01 mmol) of N-(3-Dimethylaminopropyl)-N´ - ethylcarbodiimide hydrochloride at room temperature. The resulting solution was stirred at room temperature for 2 h. The solent was removed in vacuo, and the reside purified by extraction with ethyl acetate to give1.08 g (86.2 %) of the desired diacetylene monomer PCDA-NHS as a white solid.: ^{1}H NMR (300 MHz, CDCl$_3$): δ 0.85 (t, 3H), 1.20-1.62 (m, 36H), 2.21 (t, 4H), 2.60 (t, 2H), 2.85 (s, 4H), 7.18 (brs, 1H).

PCDA-ABA: To a solution containing 0.56 g (0.50 mmol) of 4-aminobutylic acid in 5 mL of tetrahydrofuran was added 0.25 g (2.55 mmol) of tri-ethylamine, and 1 mL of di-water was added to dissolve completely at room temperature. PCDA-NHS 0.20 g (0.42 mmol) in 5 mL of tetrahydrofuran was added dropwise to a mixture solution. The resulting solution was allowed to stir for overnight at room temperature. The solvent was removed in vacuo, and the residue was purified by extraction with methylene chloride. The organic layer was dehydrated with MgSO4 and recrystallized in methylene chloride to give 0.15 g (77.6 %) of the desired diacetylene monomer PCDA-ABA as a pale blue solid.: ^{1}H NMR (300 MHz, CDCl$_3$): δ 0.85 (t, 3H), 1.20-1.62 (m, 36H), 1.86 (q, 2H), 2.21-2.38 (m, 8H), 3.35 (t, 2H), 7.28 (brs, 1H).

PCDA-EDEA: To a solution containing 1.055 mL (7.21 mmol) of 2,2´ - (Ethylenedioxy)bis(ethylamine) in 60 mL of methylene chloride was added dropwise 1.00 g (2.12 mmol) of PCDA-NHS for 3h at room temperature. The resulting mixture was allowed to stir for 2 h at room temperature. The resulting mixture was concentrated in vacuo, and the residue was purified by column chromatography (9:1 chloroform : methanol) to give 0.51 g (46.7 %) as a white solid.: ^{1}H NMR (300 MHz, CDCl$_3$): δ 0.89 (t, 3H), 1.27-1.76 (m, 35H), 2.23 (m, 6H), 2.91 (t, 2H), 3.42-3.63 (m, 12H), 6.21 (t, 1H), 7.27 (brs, 1H).

PCDA-biotin: To a solution containing 0.23 g (0.94 mmol) of biotin in 5 mL of DMF was added dropwise 0.40 g (0.79 mmol) of PCDA-EDEA in 5 mL methylene chloride. The mixture solution was allowed to stir for overnight at room temperature. The solvent was removed in vacuo, and the residue was purified by column chromatography (9:1 chloroform : methanol) to give 0.18 g (33.9%) of the desired diacetylene monomer PCDA-EDEA-biotin as a white solid.: ^{1}H NMR (300 MHz, CDCl$_3$): δ 0.89 (t, 3H), 1.27-1.76 (m, 41H), 2.23 (m, 8H), 2.74 (d, 1H), 2.94 (m, 1H), 3.17 (m, 1H), 3.42-3.65 (m, 13H), 4.32 (q, 1H), 4.54 (q, 1H), 4.92 (s, 1H), 5.87 (s, 1H), 6.27 (t, 1H), 6.31(t, 1H), 7.27 (brs, 1H).

7.4.3. Characterization

UV/Vis absorption spectra were obtained at Cary50 (Varian) and the photoluminescence spectra and the absolute quantum efficiency were collected with QM4 (PTI, Inc) equipped with an integrating sphere and a Nitrogen dye laser. Fluorescence images were taken with Olympus BX51 fluorescence microscope. The size of the vesicles was measured with the scanning electron microscopy.

7.4.4. Excitation spectrum of DBO nanoparticles

10 μM DBO in THF solution shows its large Stokes' shift at 518nm by maximum excitation of 340 nm. Nanoaggregates in THF: H_2O 1:9 mixture show red shift of the excitation and absorption by 40 nm. While the aggregate dispersed in well defined PCDA vesicle structure shows two distinct absorption and excitation at 320 nm and 370 nm. The latter is from the red shift of the syn-enol species and the former is from the anti-enol species. To check the photo stability, the DBO-PCDA was exposed with 254nm UV for 30min. 6W UV lamp was held 1 cm above the sample. There is 15% decrease in the photoluminescence, but still hold its emissive nature. And the lifetime measurement was done to check the fluorescence decay lifetime of the DBO.

7.5 References

[1]   X. Wu, H. Liu, J. Liu, K. N. Haley, J. A. Treadway, J. P. Larson, N. Ge, F. Peale, M. P. Bruchez, *Nat. Biotechnol*. **2003**, *21*, 41.

[2]   M. Bruchez, Jr, M. Moronne, P.Gin, S.Weiss, A. P. Alivisatos, *Science* **1998**, *281*, 2013.

[3]   W. C. Chan, S. Nile, *Science* **1998**, *281*, 2016.

[4]   X. Michalet, F. F. Pinaud, L. A. Bentolila, J. M. Tsay, S. Doose, J. J. Li, G. Sundaresan, A. M. Wu, S. S. Gambhir, S. Weiss, *Science* **2005**, *307*, 538.

[5]   M. A. Hines, P. Guyot-Sionnest, *J. Phys. Chem*. **1996**, *100*, 468.

[6]   C. J. Murphy, *Anal. Chem*. **2002**, *74*, 520A.

[7]   W. J. Parak, D. Gerion, T. Pellegrino, D. Zanchet, C. Micheel, S. C. Williams, R. Boudreau, M. A. Le Gros, C. A. Larabell, A. P. Alivisatos, *Nanotechnology* **2003**, *14*, R15.

[8]   C. M. Niemeyer, *Angew. Chem. Int. Ed*. **2001**, *40*, 4128.

[9]   P. Alivisatos, *Nat. Biotechnol*. **2004**, *22*, 47.

[10]   A. M. Derfus, W. C. W. Chan, S. N. Bhatia, *Nano Lett*. **2004**, *4*, 11.

[11]   C. Kirchner, T. Liedl, S. Kudera, T. Pellegrino, A. M. Javier, H. E. Gaub, S. St€olzle, N. Fertig, W. J. P. Parak, *Nano Lett*. **2005**, *5*, 331.

[12]   B.-K. An, D.-S. Lee, J.-S. Lee, Y.-S. Park, H.-S. Song, S. Y. Park, *J. Am. Chem. Soc.* **2004**, *126*, 10232.

[13]   S. Kim, Q. Zheng, G. S. He, D. J. Bharali, H. E. Pudavar, A. Baev, P.N. Prasad, *Adv. Funct. Mater*. **2006**, *16*, 2317.

[14]   S. Kim, T. Y. Ohulchanskyy, H. E. Pudavar, R. K. Pandey, P. N. Prasad, *J. Am. Chem. Soc.* **2007**, *129*, 2669.

[15]   Y. Li, F. Li, H. Zhang, Z. Xie, W. Xie, H. Xu, B. Li, F. Shen, L. Ye, M. Hanif, D. Ma, Y. Ma, *Chem. Commun*. **2007**, *231*.

[16]   Z. Li, Y. Dong, B. Mi, Y. Tang, M. H€aussler, H. Tong, Y. Dong, J. W. Y. Lam, Y. Ren, H. H.-Y. Sung, K. S. Wong, P. Gao, I. D. Williams, H. S. Kwok, B. Z. Tang, *J. Phys. Chem. B* **2005**, *109*, 10061.

[17]   G. L. Silva, V. Ediz, D. Yaron, B.A.Armitage, *J. Am. Chem. Soc.* **2007**, *129*, 5710.

[18]   D. Horn, J. Rieger, *Angew. Chem. Int. Ed.* **2001**, *40*, 4330.

[19]   Supporting Information of synthesis of PCDA: J.-M. Kim, J.-S. Lee, H. Choi, D. Sohn, D. J. Ahn, *Macromolecules* **2005**, *38*, 9366.

[20]   O. K. About-Zied, R. Jimenez, E. H. Z. Thompson, D. P. Millar, F. E. Romesberg, *J. Phys. Chem. A* **2002**, *106*, 3665.

[21]   K. Das, N. Sarkar, A. Kumar, G. D. Majumdar, D. N. Nath, K. Bhattacharyya, *J. Phys. Chem.* **1994**, *98*, 9126.

[22]   K. Lee, H.-J. Kim, J. C. Cho, J. Kim, *Macromolecules* **2007**, *40*, 6457.

[23]   J. Olmsted, III, M. Strand, *J. Phys. Chem*. **1983**, *87*, 4790.

CHAPTER 8

Light-driven Color Change of Novel Photo-responsive Polydiacetylene Molecules

Manuscript in preparation

8.1 Introduction

Polydiactylene (PDA) based sensory systems have been extensively investigated since the unique and useful mechanochromism was reported.[1] The sensitive color change from blue to red by external stimuli such as temperature, pH, and ions and mechanical pressure has been utilized in chemical sensor design and recent biosensor applications.[2] Light as an external stimuli has been used for various interesting materials and technologies such as photochromic dyes, photoactuators, photosynthesis, and photolithography just naming a few. However, light has not been explored as an external stimulus to trigger the color change of the PDA. In this chapter, we described a direct light-driven color transition of polydiacetylene (PDA) molecules. We prepared photo-responsive (PR) films by spin casting such PDA molecules on a glass slide or on a filter paper.

8.2 Results and Discussion

Photo-responsive property of 6-nitropiperonyl alcohol (NP) and 4,5-dimethoxy-2-nitrobenzyl alcohol (DN) is well known for their high photo-cleavable property upon 365 nm UV irradiation. This photo-cleavable property has been uniquely utilized in bio-

applications as a moiety for purifying, protecting and identifying target bio-molecules.[3] We utilized the photo-cleavable property of NP and DN in devising photo-responsive PDA molecules. We designed NP and DN modified PR-PDA molecules shown in Scheme 1 (PCDA-DN, PCDA-NP, PCDA-*p*BzA-DN). As we presented in our previous works, the external steric repulsion resulted in the rearrangement of yne-ene conjugated backbone of PDA and produced the colorimetric transition and fluorescence emission[1, 4]. The same mechanism of the color transition is expected to occur in the PR-PDA molecules. Scheme 8.1C and D schematically illustrate the steric disordering and the resulting conformational change of the PR-PDA liposome, which is induced by 365 nm UV irradiation. The initial self-assembled structure of the investigated diacetylene monomers PCDA-NP and PCDA-DN is formed by hydrophobic interactions of the alkyl chains and aromatic interactions but no hydrogen bond is available. As typical the investigated PR-PDA liposomes solutions showed stable blue color after 254 nm UV photo-polymerization. Interestingly, PR-PDA liposome solutions changed their color from blue to red after additional 365 nm UV irradiation for 2 minutes (Figure 8.1). We believe that the cleavage of NP and DN induced disordering of the self-assembled PR-PDA liposome structure resulting in distortion of the conjugated backbone and consequent color transition of the PR-PDA liposome solution. However, the disordered structure was not able to come back to the initial blue phase because there are no hydrogen bondings in the investigated PR-PDA molecules. It was reported that reversible color transition is achievable by enhancing hydrogen bonding strength between PDA molecules.[5] To adapt this strategy into our system to achieve reversible color transition, we synthesized PCDA-*p*BzA-DN. Interestingly, we could observe reversible color transition to initial blue color after cooling the red phase PCDA-*p*BzA-DN liposomes as shown in Figure 1C. As illustrated in scheme 1D the initial self-assembled structure was firstly disordered by the cleavage of DN through 365 nm UV irradiation (Red phase). However, red phase liposomes changed their color back to blue after cooling (Blue

130

phase). We believe that cooling rearranged the disordered PDA structure to the initial self-assembled structure through strong hydrogen bonds between the amide groups which is exactly same with PCDA-pBzA liposomes structure having stable reversibility (figure 8.6). In addition, hydrogen bonds between carboxylic acids and aromatic stacking also aid the reversible formation of the initial structure.
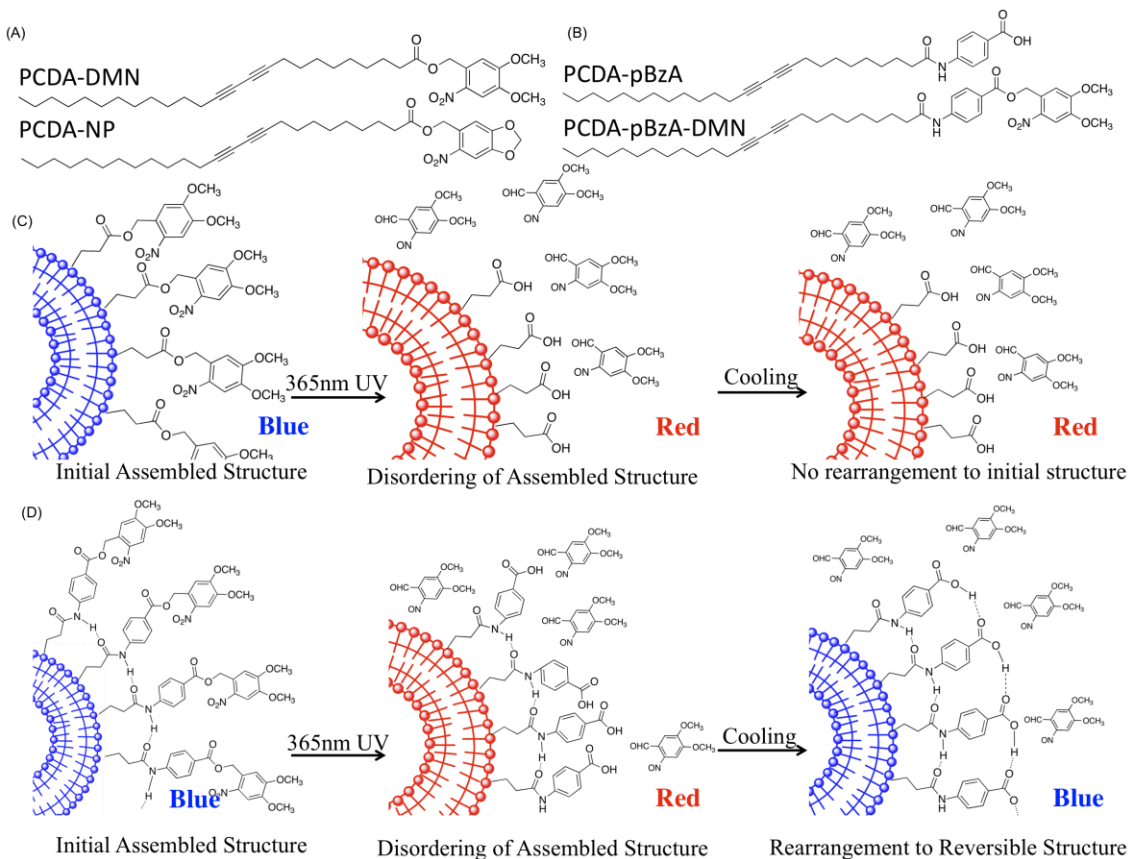
Scheme 8.1. Chemical structure of the diacetylene monomers PCDA-DN and PCDA-NP (A) and PCDA-pBzA/PCDA-pBzA-DN for reversible color transition (B). Schematic illustration of color transition of the PR-PDA liposome for irreversible (C) and reversible (D) upon 365 nm UV light.

We further investigated the photo-responsive property of PCDA-*p*BzA-DN liposome by preparing agarose gel embedded with PCDA-*p*BzA-DN liposome. Figure 8.2 represents the color transition of the agarose gel having PCDA-*p*BzA-DN liposomes. The patterned red image appeared after 365 nm UV light for 2 min and the red patterned image was almost disappeared by subsequent cooling to 15 $^{\circ}$C. As shown in the Figure

8.2, we confirmed that PR-PDA liposome showed reversible color transition providing a possibility of the rewritable device.
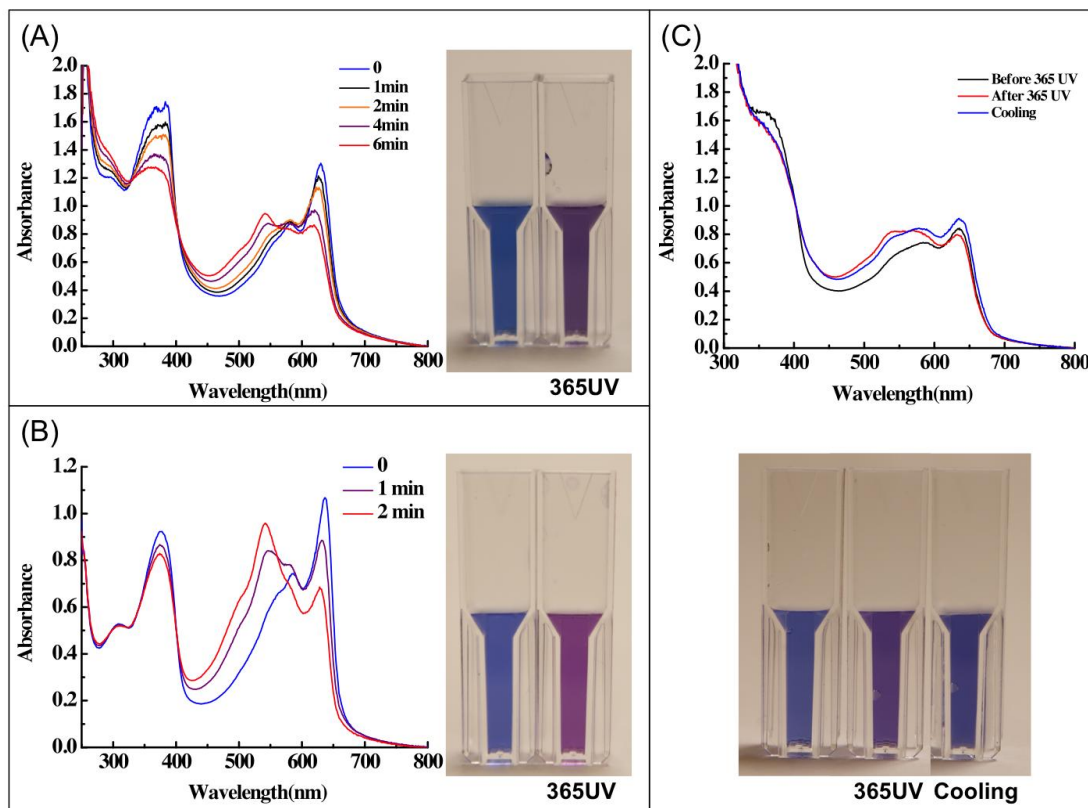
Figure 8.1. UV-vis spectra and color transition image of the PR-PDA liposome solution upon 365 nm UV irradiation: (A) PCDA-NP, (B) PCDA-DN and (C) PCDA-pBzA-DN.

We additionally conducted such a writing and erasing study. We casted the PR-PDA molecules on a bare glass slide. Figure 8.3A shows the color transition and fluorescence emission of the PCDA-NP spin cast film on a glass slide. Among the investigated PR-PDA molecules, PCDA-NP showed the best optical property on substrate compared to other PR-PDA molecules as shown in Figure 8.3. A patterned red colored image appeared rapidly after irradiation with 365 nm UV light for 2 min. The pattern could be erased by subsequent irradiation as can be seen in Figure 8.4A. As discussed above the cleavage of NP from PCDA-NP induced the rearrangement of the self-assembled structure and resulted in the distortion of the conjugated backbone. The color transition and red fluorescence emission of the patterned area was resulted from the

consequent rearrangement of the self-assembled structure. However, we could not generate a reversible color transition using PCDA-*p*BzA-DN molecules in a solid-state because of its poor spin casting property as shown in Figure 8.3. A further study should be carried out to achieve complete rewritable device from PR-PDA molecules. We also prepared PCDA-NP-coated filter papers by soaking the filter papers with a THF (10mg/ml) solution of PCDA-NP. Poly-vinyl alcohol (PVA) films having embedded PCDA-DN liposome were also fabricated. The filter paper wetted with PCDA-NP and the PVA film having PCDA-DN liposome embedded showed the exactly same colorimetric response upon 365 nm UV light as shown in Figure 8.4.
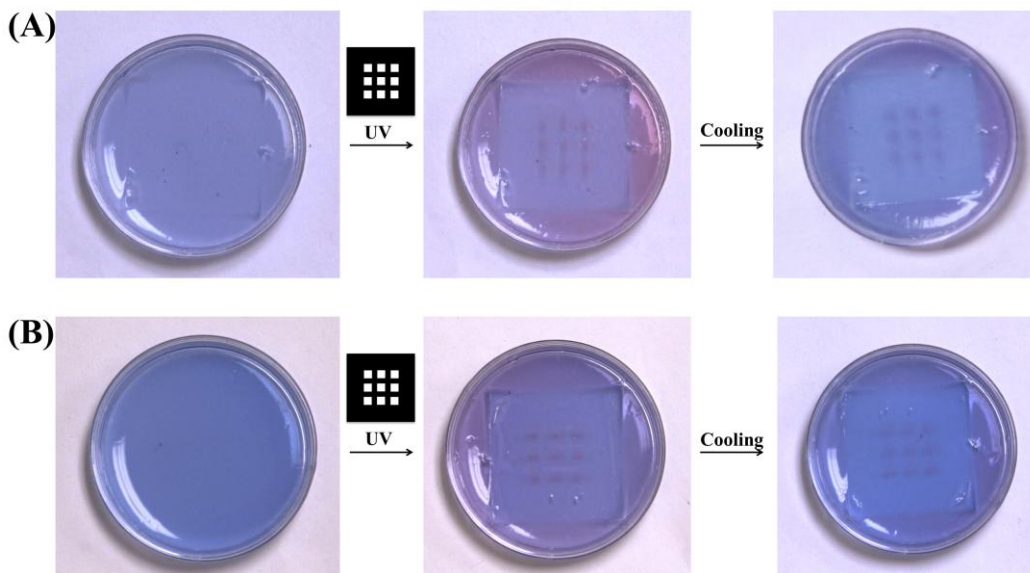
Figure 8.2. Reversible color transition of PCDA-*p*BzA-DN/PCDA-*p*BzA liposome (a) 2/1 and (b) 1/2 embedded agarose gel.

We also investigated the possibility for writing latent images. A latent image was prewritten by using 365 nm UV light through a photo-mask on PCDA-NP spin cast glass slide (Figure 8.5B). We could not observe any noticeable image on the glass substrate after 365 nm UV irradiation. However, the latent image appeared after the photo-polymerization of PCDA-NP by using 254 nm UV light. We believe that the self-assembly diacetylene liposome rearranged to a disorder state during the cleavage of NP

133

group. As a result the disordered state prevents the acetylene monomers from photo-polymerization by chainging the distance for photopolymerization. The latent image becomes readable with good contrast when the surrounding unexposed area undergoes photo-polymerization. When 365 nm UV irradiation was applied on the this film, the cleavage of NP group in the surrounding area induces backbone purturbation of the PDA and resulted color change to red as well.
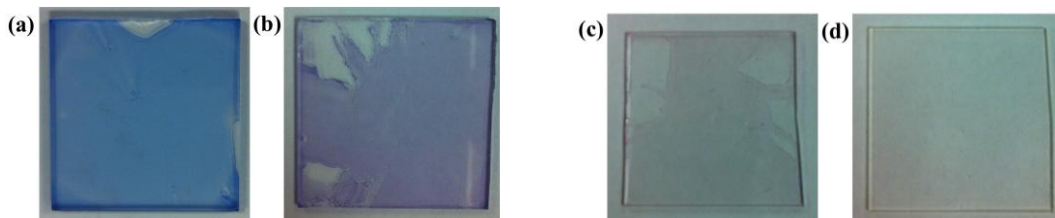
Figure 8.3. PR-PDA spin coated glass slide (a) PCDA-NP, (b) PCDA-DN, (c) PCDA-*p*BzA, (d) PCDA-pBzA-DN.
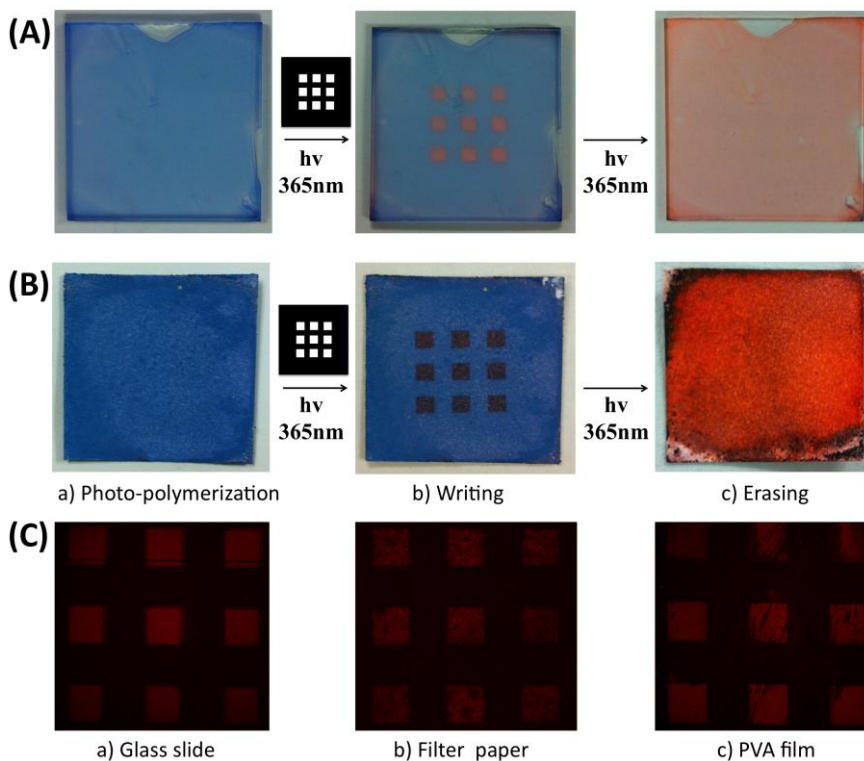
Figure 8.4. Color transition images of the PCDA-NP spin casted glass slide (A) and PCDA-NP wetted filter paper (B): a) 254 nm UV photo-polymerization. b) Writing using 365 nm UV irradiation. c) Erasing with 365 nm UV exposure. (C) Fluorescence emission image of PCDA-NP spin cast glass slide (a), wetted filter paper (b) and embedded PVA film (c)
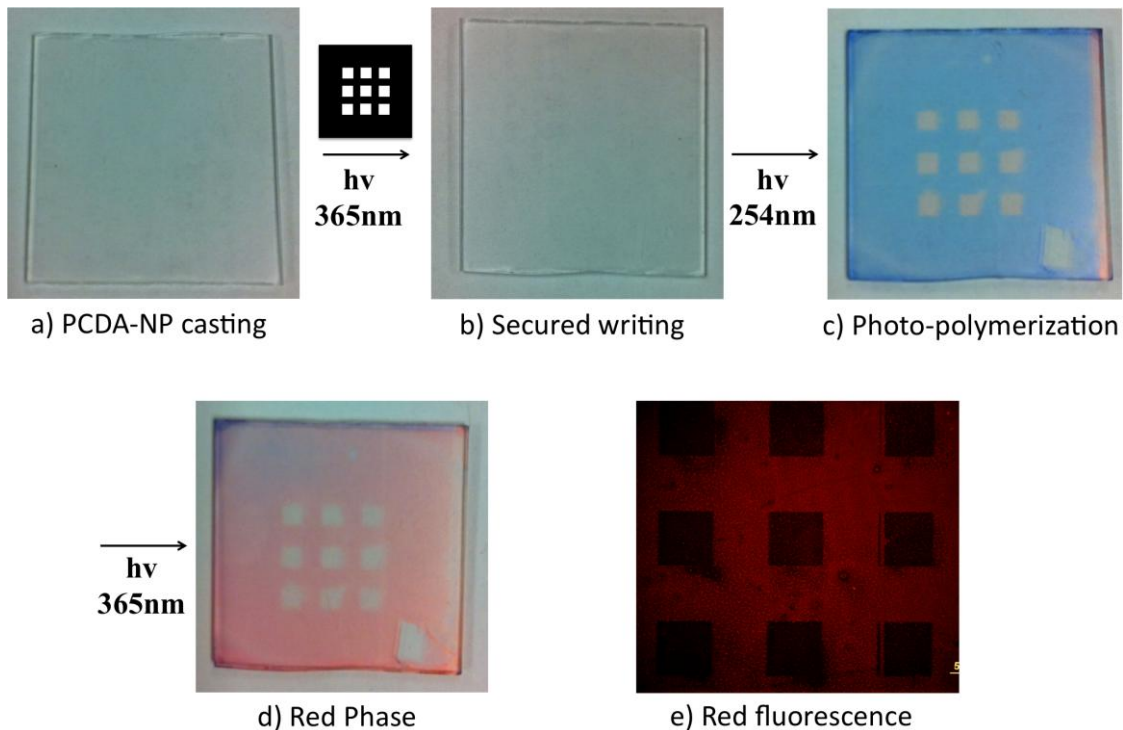
Figure 8.5. Secured writing of PCDA-NP spin casted glass slide: a) PCDA-NP spin coating. b) Secured writing with 365 nm UV light using photo mask. c) Photo-polymerization with 254 nm UV light. d) 365 nm UV irradiation on all area. e) Fluorescence emission image.

Typically PDA molecules are not quite spin castable unless the solid-substrate is chemically modified. Chemically modified glass substrates can be used to deposit PDA layers by Langmuir-Blodgett or Langmuir-Schaefer mothod.[6] Compared to these conventional methods, as can be seen in Figure 8.4A, our spin cast method and the soaking method of PCDA-NP molecule are simple and convenient because no chemical modification is required. The prepared PDA films also showed very superior optical properties such as strong blue/red color and also red emission.

8.3 Conclusions

We developed novel PR-PDA molecules having superior optical properties. The investigated PR-PDA liposomes showed rapid and also reversible response upon 365 nm

135

UV light irradiation and cooling. We also demonstrated rapid writing and erasing of an image by using UV light. The unique latent image formation was also established by pre-writing on the PR-PDA-coated substrate with 365 nm UV light and subsequently photo-polymerize the pre-written substrate.
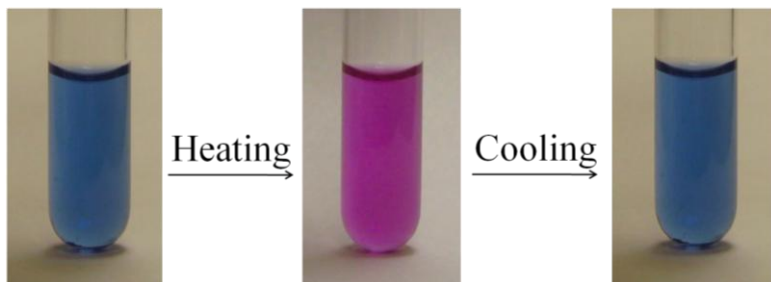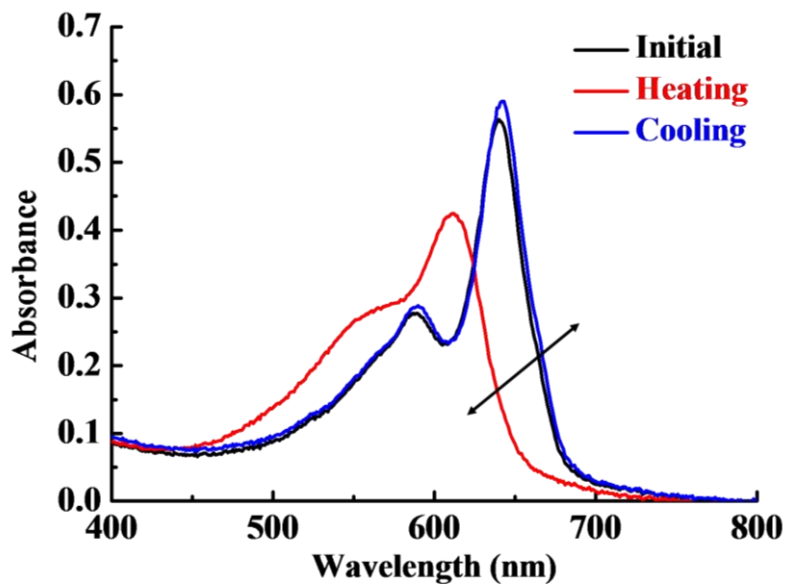
Figure 8.6. Reversible UV-vis spectrum change and an optical color change image of PCDA-*p*BzA   liposomes solution upon heating.

The easy preparation protocol of either simple spin casting or soaking is very attractive in that all processes can be done within a few minutes. The response time of the photo-polymerization of the pre-patterned PCDA-NP was less than 10 seconds and the subsequent color transition from blue to red upon 365 nm UV light was achieved within less than 3 minutes. The convenience of the fabrication protocol and the fast response of

the PR-PDA system may find a unique application in rapid and secured delivery of confidential documents.
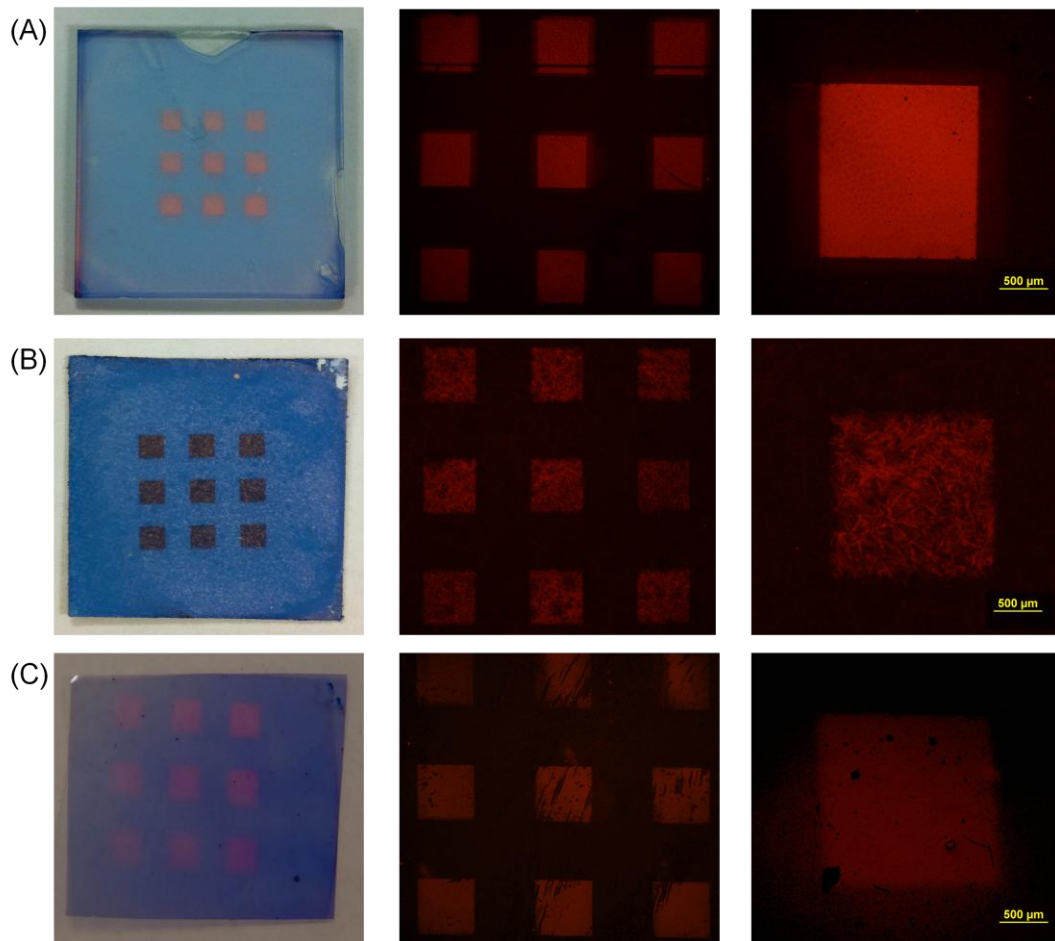
Figure 8.7. Patterned images and fluorescence of PCDA-NP spin coated glass slide (a), wetted filter paper, (b) and embedded PVA film (scale bar: 500um).

8.4 Experimental section

8.4.1. Preparation of diacetylene liposomes.

100 μl of PR-PDA (PCDA-DN, PCDA-NP and PCDA-*p*BzA-DN/PCDA-*p*BzA(2/1)) monomer solution was injected rapidly to 20 ml of 50 mM HEPES buffer pH 8.0. The suspended solution was sonicated for 20 min by probe disembrator and filtered

with 0.8 μm cellulose acetate syringe filter. The dispersed PDA liposome solution was cooled at 5 ℃ for 24 hours. The final concentration is 0.2 mM.

8.4.2. Preparation of the PR-PDA liposomes embedded agarose gel.

1ml of 0.5% agrose solution was mixed with 0.2 mM of PR-PDA liposome solution and mildly heated until the agarose completely dissolved in the solution. The result solution was cooled at 5 ℃ for 1 hour.

8.4.3. Preparation of PR-PDA spin casted glass substrate.

200 μl of PR-PDA (PCDA-DN, PCDA-NP and PCDA-pBzA-DN) in THF (10mg/1ml) was spin coated onto glass substrate at 1000rpm.

8.4.4. Preparation of PR-PDA wetted filter paper.

200 ul of PR-PDA (PCDA-DN, PCDA-NP and PCDA-pBzA-DN) molecules in THF (10mg/1ml) was dropped onto filter paper and dried.

8.4.5 Writing and erasing with UV light.

PR-PDA coated glass slide and filter paper were polymerized using 254 nm UV lamp for 10s. The resulted blue color PR-PDA coated glass slide patterned under photo-mask using 365 nm UV light for 2 minutes. The red patterned glass slide was erased with 365nm UV light for another 2 minutes.

8.4.6. Pre-writing of PR-PDA coated glass slide.

PR-PDA coated glass slide was pre-patterned under photo-mask using 365 nm UV light for 2 minutes. Pre-patterned glass slide was polymerized using 254 nm UV

lamp for 10s. The patterned glass slide was exposed to 365nm UV light for red phase color transition.

8.4.7 Synthesis and characterization.

Materials and Method. All solvents were purchased from Sigma-Aldrich Chemicals. 10,12-pentacosadiynoic acid (PCDA) was purchased from GFS Chemicals. Oxalyl chloride, thionyl chloride, 4,5-dimethoxy-2-nitrobenzyl alcohol and 4-aminobenzoic acid were purchased from Sigma-Aldrich Chemical Co. 6-nitropiperonyl alcohol was obtained from Acros Organics. UV/Vis absorption spectra were taken on a Varian Cary50 UV/Vis spectrophotometer. Fluorescence images were taken by Olympus BX51 W/DP71 fluorescent microscope.

Synthesis of PCDA Derivatives
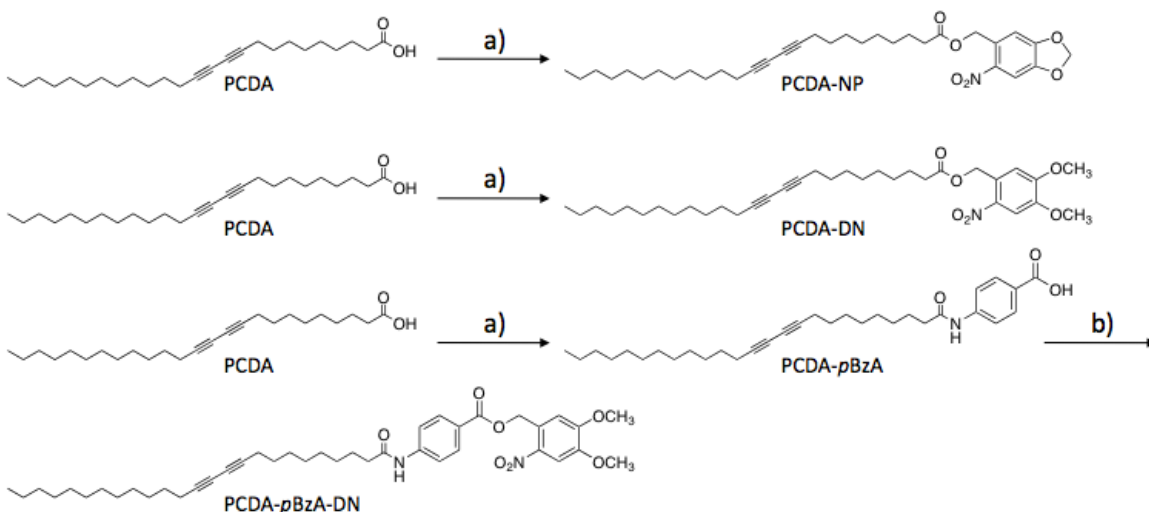
Scheme 8.2. (A) PCDA-NP synthesis: (a) oxalyl chloride, dimethylformamide, 6-nitropiperonyl alcohol, dichloromethane, 25 ℃, overnight. (B) PCDA-DN synthesis: (a) oxalyl chloride, dimethylformamide, 4,5-dimethoxy-2-nitrobenzyl alcohol, dichloromethane, 25 ℃, overnight. (C) PCDA-*p*BzA-DN synthesis: (a) oxalyl chloride, dimethylformamide, 4-aminobenzoic acid, dichloromethane, 25 ℃, overnight. (b) thioyl chloride, 4,5-dimethoxy-2-nitrobenzyl alcohol, 60 ℃, overnight.

The diacetylene monomers PCDA-NP, PCDA-DN and PCDA-*p*BzA-DN investigated in this work were synthesized through the reaction scheme (Scheme 8.2.).
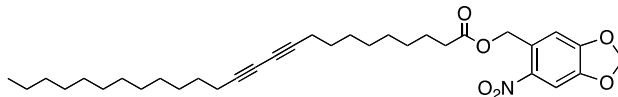
PCDA-NP To a solution of 10,12-pentacosadiynoic acid (0.50 g, 1.33 mmol) in dichloromethane (20 mL) at room temperature was added dropwise oxalyl chloride (0.51 g, 4.00 mmol). The resulting solution was stirred at room temperature for 30 min. To the solution was added a catalytic amount (one drop) of dimethylforamide and stirred for an additional hour. After concentrating in vacuo, the residue was redissolved in THF (15 mL). The resulting solution was added dropwise to the solution containing 6-nitropiperonyl alcohol (0.32 g, 1.60 mmol) and TEA (0.54 g, 5.34 mmol) in THF (15 mL). The resulting mixture was allowed to stir for overnight at room temperature, poured into the water and extracted with ethyl acetate. The organic layer was washed 3 times with water to eliminate the excess 6-nitropiperonyl alcohol, dried with $MgSO_4$ and filtered. The solvent was removed under vacuo. The residue was purified by silica gel column chromatography (hexane/ethyl acetate =5/1) to give 0.14 g (25 %) of desired diacetylene monomer **PCDA-NP** as a white solid. mp 70 ℃. ^{1}H NMR (400 MHz, DMSO-d_6): δ 0.85 (t, J =7.0 Hz, 3H), 1.23-1.55 (m, 32H), 2.26 (t, J =7.0 Hz, 4H), 2.39 (t, J =7.4 Hz, 2H), 5.32 (s, 2H), 6.26 (s, 2H), 7.18 (s, 1H), 7.71 (s, 1H). ^{13}C NMR (100 MHz, CDCl$_3$): 14.11, 19.19, 22.68, 24.84, 28.28, 28.33, 28.73, 28.87, 29.05, 29.09, 29.33, 29.46, 29.63, 31.90, 34.18, 61.79, 62.99, 76.74, 103.13, 105.88, 107.57, 109.97, 116.98, 170.95. MS (ES): Calcd, 553.7; found (M+Na)+, 576.3.
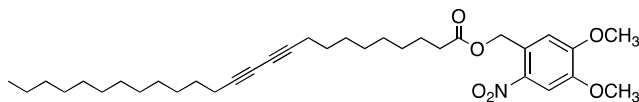
PCDA-DN To a solution of 10,12-pentacosadiynoic acid (0.50 g, 1.33 mmol) in dichloromethane (20 mL) at room temperature was added dropwise oxalyl chloride (0.51 g, 4.00 mmol). The resulting solution was stirred at room temperature for 30 min. To the solution was added a catalytic amount (one drop) of dimethylforamide and stirred for an additional hour. After concentrating in vacuo, the residue was redissolved in THF (15 mL). The resulting solution was added dropwise to the solution containing 4,5-dimethoxy-2-nitrobenzyl alcohol (0.32 g, 1.60 mmol) and TEA (0.54 g, 5.34 mmol) in THF (15 mL). The resulting mixture was allowed to stir for overnight at room temperature, poured into the water and extracted with ethyl acetate. The organic layer was washed 3 times with water to eliminate the excess 4,5-dimethoxy-2-nitrobenzyl alcohol, dried with MgSO$_4$ and filtered. The solvent was removed under vacuo. The residue was purified by silica gel column chromatography (hexane/ethyl acetate =5/1) to give 0.14 g (25 %) of desired diacetylene monomer **PCDA-DN** as a white solid. mp 70 °C. ^{1}H NMR (400 MHz, DMSO-d_6): δ 0.85 (t, J = 6.8 Hz, 3H), 1.23-1.56 (m, 32H), 2.26 (t, J = 6.8 Hz, 4H), 2.38 (t, J = 7.4 Hz, 2H), 3.89 (d, J = 6.2 Hz, 6H), 5.37 (s, 2H), 7.18 (s, 1H), 7.69 (s, 1H). ^{13}C NMR (100 MHz, CDCl$_3$): 14.11, 19.19, 22.67, 24.94, 28.26, 28.33, 28.72, 28.84, 29.08, 29.33, 29.46, 29.63, 31.90, 34.24, 56.40, 63.05, 66.66, 76.74, 108.22, 110.41, 149.54, 153.40, 191.76. MS (ES): Calcd, 569.8; found (M+Na)+, 592.4.
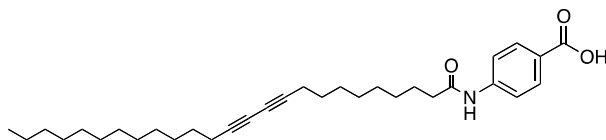
**PCDA-pBzA** PCDA-pBzA was synthesized by following the literature[1,2]. To a solution of 10,12-pentacosadiynoic acid (2.00 g, 5.34 mmol) in dichloromethane (20 mL)

at room temperature was added dropwise oxalyl chloride (2.03 g, 16.02 mmol). The resulting solution was stirred at room temperature for 30 min. To the solution was added a catalytic amount of dimethylformamide and stirred for an additional hour. After concentrating in vacuo, the residue was redissolved in THF (15 mL). The resulting solution was added dropwise to the solution containing 4-aminobenzoic acid (1.10 g, 8.01 mmol) and TEA (2.16 g, 21.36 mmol) in THF (15 mL). The resulting mixture was allowed to stir for overnight at room temperature, poured into the water and extracted with ethyl acetate. The organic layer was washed 3 times with water to eliminate the excess 4-aminobenzoic acid, dried with $MgSO_4$ and filtered. The solvent was removed under vacuo. The resulting solution was recrystallized from methyl alcohol and isopropyl alchol to give 2.20 g (83 %) of desired diacetylene monomer **PCDA-*p*BzA** as a white solid. ^{1}H NMR (400 MHz, CDCl$_3$): δ 0.85 (t, J = 6.8 Hz, 3H), 1.23-1.60 (m, 32H), 2.25-2.28 (m, 4H), 2.31-2.35 (m, 2H), 7.69 (d, J = 8.8 Hz, 2H), 7.86 (d, J = 8.8 Hz, 2H), 10.15 (s, 1H).
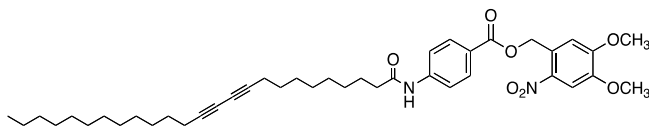
PCDA-*p*BzA-DN To a solution of PCDA-*p*BzA (1.00 g, 2.03 mmol) in dichloromethane (20 mL) at room temperature was added dropwise thionyl chloride (0.48 g, 4.05 mmol). The reaction mixture was refluxed at 60 ℃ until all of the solid were in solution. After concentrating in vacuo, the residue was redissolved in THF (15 mL). The resulting solution was added dropwise to the solution containing 4,5-dimethoxy-2-nitrobenzyl alcohol (0.60 g, 3.04 mmol) and TEA (0.62 g, 6.08 mmol) in THF (15 mL). The resulting mixture was allowed to stir for overnight at room temperature, poured into the water and extracted with ethyl acetate. The organic layer was washed 3 times with water to eliminate the excess 4,5-dimethoxy-2-nitrobenzyl alcohol, dried with $MgSO_4$

and filtered. The solvent was removed under vacuo. The residue was purified by silica gel column chromatography (hexane/ethyl acetate =3/2) to give 0.55 g (39 %) of desired diacetylene monomer **PCDA-*p*BzA-DN** as a white solid. mp 107 ℃. ^{1}H NMR (400 MHz, DMSO-d_6): δ 0.84 (t, J = 6.8 Hz, 3H), 1.22-1.58 (m, 32H), 2.26 (t, J = 5.8 Hz, 4H), 2.33 (t, J = 7.4 Hz, 2H), 3.89 (d, J = 6.4 Hz, 6H), 5.59 (s, 2H), 7.32 (s, 1H), 7.73-7.93 (m, 5H), 10.23 (s, 1H). ^{13}C NMR (100 MHz, DMSO-d_6): 13.92, 18.24, 22.08, 24.88, 27.67, 28.14, 28.29, 28.36, 28.54, 28.61, 28.69, 28.84, 28.93, 28.99, 31.28, 36.46, 56.21, 63.19, 65.32, 77.94, 111.90, 118.40, 123.14, 125.91, 130.36, 140.00, 143.98, 148.08, 153.07, 164.88, 171.91. MS (ES): Calcd, 688.9; found (M+Na)+, 711.4.

8.5 References

[1]   a)J. Lee, E. Jeong Jeong, J. Kim, *Chemical Communications* **2011**; b)J. Lee, H.-J. Kim, J. Kim, *Journal of the American Chemical Society* **2008**, *130*, 5010; c)J. Lee, H. Jun, J. Kim, *Advanced Materials* **2009**, *21*, 3674.

[2]   a)R. R. Chance, *Macromolecules* **1980**, *13*, 396; b)K. Tashiro, H. Nishimura, M. Kobayashi, *Macromolecules* **1996**, *29*, 8188; c)R. W. Carpick, D. Y. Sasaki, A. R. Burns, *Langmuir* **2000**, *16*, 1270.

[3]   a)T. Kühn, H. Schwalbe, *Journal of the American Chemical Society* **2000**, *122*, 6169; b)J. P. Casey, R. A. Blidner, W. T. Monroe, *Molecular Pharmaceutics* **2009**, *6*, 669; c)S. Murayama, M. Kato, *Analytical Chemistry* **2010**, *82*, 2186; d)M. S. Kim, S. L. Diamond, *Bioorganic & Medicinal Chemistry Letters* **2006**, *16*, 4007.

[4]   H. J. Kim, J. Lee, T. H. Kim, T. S. Lee, J. Kim, *Advanced Materials* **2008**, *20*, 1117.

[5]   a)J.-M. Kim, J.-S. Lee, H. Choi, D. Sohn, D. J. Ahn, *Macromolecules* **2005**, *38*, 9366; b)D. J. Ahn, E.-H. Chae, G. S. Lee, H.-Y. Shim, T.-E. Chang, K.-D. Ahn, J.-M. Kim, *Journal of the American Chemical Society* **2003**, *125*, 8976.

[6]   a)F. Li, E. Shishkin, M. A. Mastro, J. K. Hite, C. R. Eddy, J. H. Edgar, T. Ito, *Langmuir* **2010**, *26*, 10725; b)J. M. Kim, E. K. Ji, S. M. Woo, H. Lee, D. J. Ahn, *Advanced Materials* **2003**, *15*, 1118.

CHAPTER 9

Highly Conductive Polydiacetylene Nano Fiber for Extremely Sensitive and Selective Sensor Development

Unfinished Work

9.1 Introduction

Polydiactylenes (PDAs), a intriguing molecules having unique characteristics such as optical color change and fluorescecnne emission, have been extensively investigated for sensor applications.[1] The optical property change from blue to red by external stimuli such as temperature, pH, and ions and mechanical pressure has been utilized in potential chemosensors.[2] Sensory signals from probes and targets interaction typically have been measured by photo-luminescence device and UV-vis spectrometer. However, the fundamental detection limit of analysis device did not allow the extremely sensitive detection. Recently a lot of efforts were devoted in the amperometric sensor development because they provide a real time monitoring of target molecules as well as extremely sensitivity sensory signals compared to the conventional fluorescence and optical bio/chemosensor systems.[3] Amperometric biosensors function by the production of a current when a potential by the biological interaction event is applied between two electrodes. It has been considered that PDAs without doping is an insulator.[4] Day and Lando reported that the conductivity of PDA film is estimated to be about 10^{-11} S/cm. Also Takami reported that highly ordered PDA thin films without domain boundaries is

essential for the precise conductivity measurement.[5] They argued that a high conductivity is assumed when the measuring direction is parallel to the PDA backbone within one highly ordered crystallite. Figure 9.1 shows the value of polydiacetylene among the conductivity specified materials. In this chapter we firstly describe a novel PDA nanofibers having a high conductivity when they are highly aligned between two electrodes. It is reported that PCDA-mBzA has a reversible color transition upon heating by the strong hydrogen bondings and aromatic stacking. We simply added additional carboxylic acid group to the phenyl ring of PCDA-mBzA and generated a completely different morphology through the specific self-assembly method.
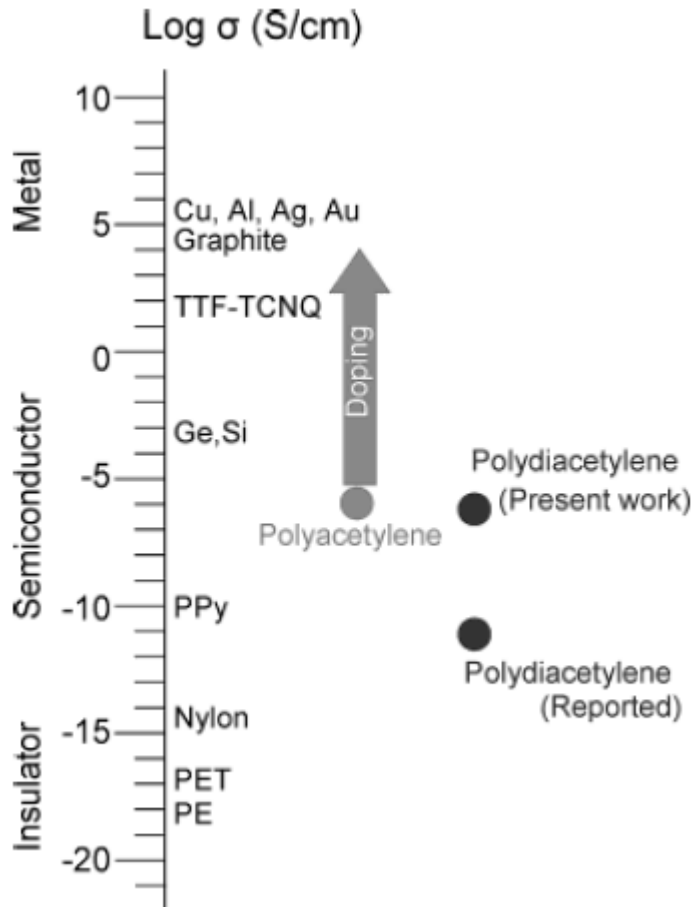

Figure 9.1 Nondoped conductivities of specified materials. Day and Lando's data,[12] Takami's data for the PDA thin films, and the value for polyacetylene[16] are also indicated. Abbreviations: TTF, tetrathiafulvalene; TCNQ, tetracyanoquinodimethane; PPy, polypyrrole; PET, poly(ethylene terephthalate); PE, polyethylene.

9.2 Result and Discussion

Lee's group reported the noncovalent organic fibers affored by two cooperating noncovalent forces.[6] We applied this method to generate the PDA nanofiber. The PCDA-IPA was readily synthesized by attaching the 5-aminoisophthalic acid to the 10,12-pentacosadyinoic acid in pyridine. PCDA-IPA nanofiber was obtained by similar method in the literature. Briefly we dissolved 1 equivalent of PCDA-IPA monomer in 2 quivalent of KOH solution by heating to 70 ^{o}C. After cooling for 3 hours the resulting solution was appeared to be viscous and opaque. UV irradiation (254nm, 1mW/cm^2) for 30 sec produced blue colored PCDA-IPA nanofibers. Figure 9.2 shows the SEM image and fluorescence microscope images of PCDA-IPA nanofiber after heating.
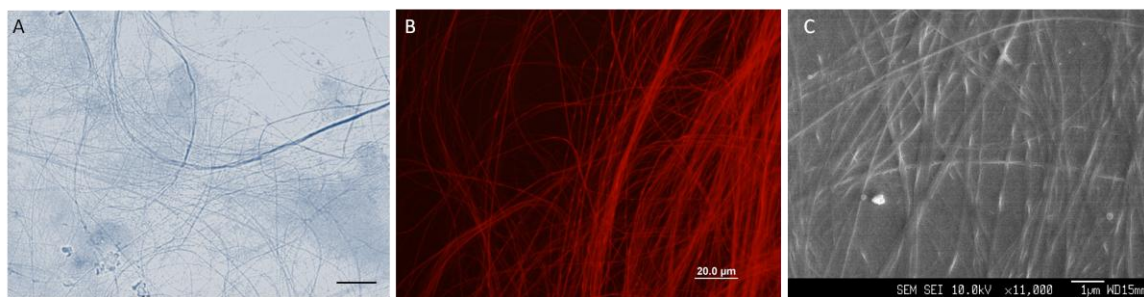
Figure 9.2 Optical (A), fluorescence (B) and SEM (C) images of PCDA-IPA nanofiber. (Scale bar: 20um)

We simply drop casted PCDA-IPA nanofiber solution onto the thouroughly cleaned glass substrate and dried under nitrogen. We subsequently deposited the aluminium electrode onto the PCDA-IPA nanofiber glass slide using thermal evaporator through a photomask method. The initial gap between electrode was 100 um and the conductivity was measured after photo polymerization. Interestingly high concurrent density was measured after photo polymerization and also the conductivity was completely disappeared after subsequent heating. As previously reported, PDAs has been considered as an insulator unless they form a highly ordered crystalline structure but our PCDA-IPA nanofiber showed extremely higher current density. We need further study for the mechanism of higher conductivity of PCDA-IPA nanofiber but we hypothesize

that the highly ordered fibrous formation of conjugated PCDA-IPA molecules is the pathway of electrons. Unfortunately, we could not generate a consistant result of high conductivity using PCDA-IPA nanofiber. We repeatedly observed a nice alignment of PCDA-IPA nanofiber without aggregation when the higher conductivity was observed.
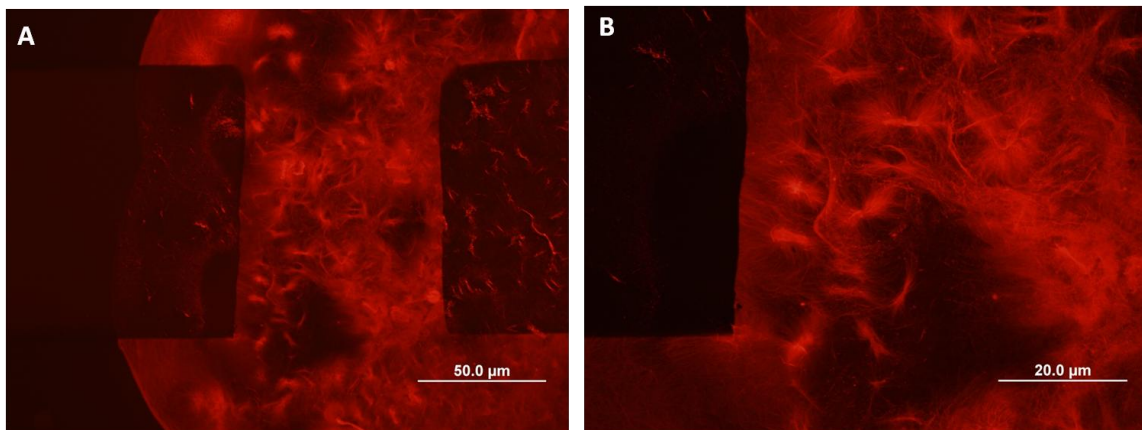

Figure 9.3 Fluorescence images of PCDA-IPA nanofiber between electrode. (Scale bar: 20um)
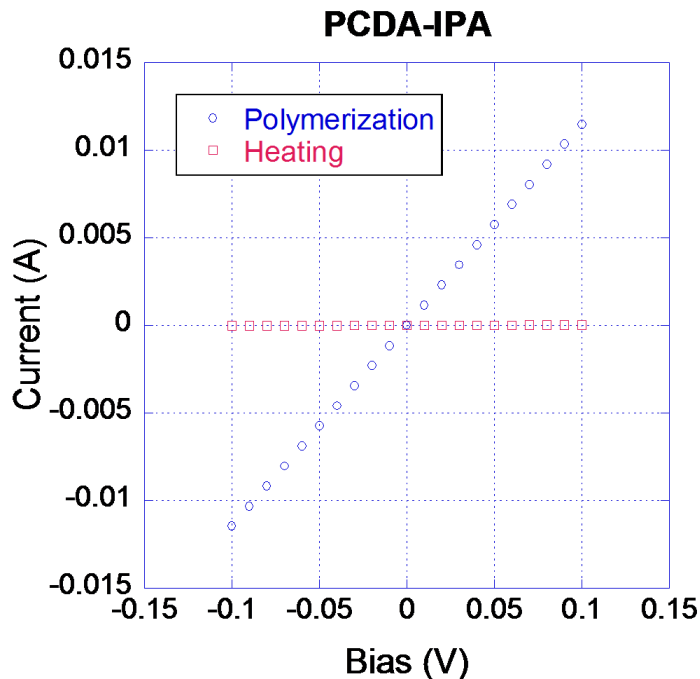

Figure 9.4 Cuurent density of PCDA-IPA nanofiber after polymerization and heating

We believed that aggregation of PCDA-IPA nanofiber might affected the consistant high conductivity generation. Conducting pathway of conjugated backbone is located in the

middle of PCDA-IPA fibers, and therefore we are not able to expect a high conductivity because the conducting layers of PCDA-IPA nanofiber will be insulated more as they arregate. Therefore we have tried to remove the aggregated PCDA-IPA nanofibers by aligning PCDA-IPA nanofibers onto glass substrate. Figure 9.5 shows a fluorescence microscope image of highly aligned PCDA-IPA nanofiber between electrodes. However, we could not continuously produce homogenously aligned PCDA-IPA nanofibers onto the glass slide using a conventional method such as spin csting and drop casting. Therefore alignment issue is still challenging to generate high conductivity of PCDA-IPA nanofiber. Once the reproducibility issue solved, we will be able to move to the fabrication of amperometric sensor by attaching biological probes onto the surface of nanofiber through a simply chemical modification.
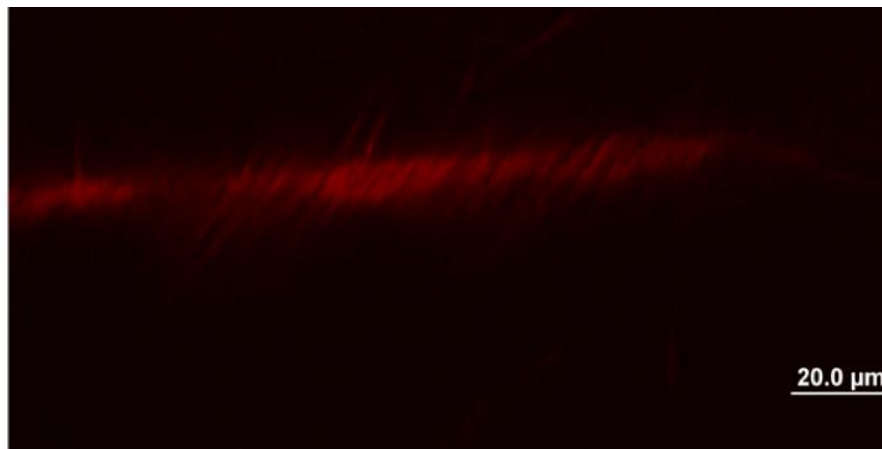
Figure 9.5 Fluorescence microscope image of highly aligned PCDA-IPA nanofiber between electrodes.

9.3 Conclusions

We proposed a novel PCDA-IPA nanofiber having high conductivity. PCDA-IPA nanofiber represented a high current density after polymerization and the conductivity was disappeared upon heating. Although the alignment issue for high conductivity is still challenging, we might able to open up a new approach for the amperometric sensory

application using PDA systems. The easy preparation protocol of highly conductive nanofiber is also very attractive in that they require no complicated self-assembly protocol. Further study for the alignment of PCDA-IPA nanofiber without any aggregation is still needed.

9.4 Experimental section

9.4.1. Preparation of PCDA-IPA nanofiber.

1eq of PCDA-IPA was dissolved in 2 eq of KOG solution. The suspended solution was stirred at 78 $^\circ$C. The dispersed PCDA-IPA solution was cooled at 5 $^\circ$C for 24 hours. The final concentration is 5 mM.

9.4.2. Preparation of PCDA-IPA nanofiber coated glass slide.

PCDA-IPA nanofiber solution was drop casted onto the thoroughly cleaned glass side. The PCDA-IPA fiber drop casted glass slide was completely dried under nitrogen flow. Aluminium electrode was deposited using photo-mask with thermal evaporator. The conductivity was measured after exposure to 254 nm UV light for 30 sec and also after heating.

9.4.3 Synthesis and characterization.

Materials and Method. All solvents were purchased from Sigma-Aldrich Chemicals. 10,12-pentacosadiynoic acid (PCDA) was purchased from GFS Chemicals. Oxalyl chloride, and 5-aminoisophthalic acid were purchased from Sigma-Aldrich Chemical Co. Fluorescence images were taken by Olympus BX51 W/DP71 fluorescent microscope.

Synthesis of PCDA Derivatives
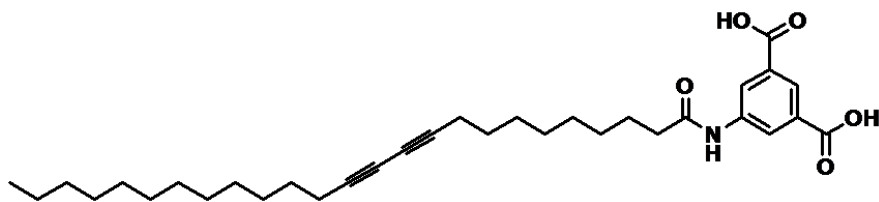
PCDA-IPA To a solution containing 1.00 g (2.67 mmol) of PCDA in 10 mL of methylene chloride was added dropwise 0.81 g (8.01 mmol) of oxalyl chloride and a catalytic amount of DMF at room temperature. The resulting solution was stirred at room temperature for 1h, concentrated in vacuo, and redissolved in 10 mL of THF. The resulting solution was added dropwise to the solution containing 0.58 g (3.20 mmol) of 5-aminoisophthalic acid in 15 mL of pyridine. The resulting mixture was stirred for 4 h at room temperature, concentrated in vacuo, and poured into cold water to yield a precipitate containing the desired diacetylene monomer PCDA-IPA as white solid (0.96 g, 67%). PCDA–IPA: mp 224 $^{\circ}$C; ^{1}H-NMR (300 MHz, DMSO-d6): δ = 0.84 (t, 3H), 1.23-1.75 (m, 36H), 2.25-2.33 (m, 6H), 8.13 (s, 1H), 8.43 (s, 2H), 10.26 (s, 1H); ^{13}C-NMR (75 MHz, DMSO-d6): δ = 13.93, 18.27, 22.09, 24.95, 27.70, 28.16, 28.33, 28.39, 28.58, 28.71, 28.87, 29.01, 31.30, 36.40, 65.34, 77.92, 123.39, 124.29, 131.64, 139.90, 166.50, 171.75; IR 1407, 1463, 1546, 1604, 1668, 1693, 2848, 2921, 3272 cm^{-1}.

9.5 References

[1]   a)J. Lee, E. Jeong Jeong, J. Kim, *Chemical Communications* **2011**; b)J. Lee, H.-J. Kim, J. Kim, *Journal of the American Chemical Society* **2008**, *130*, 5010; c)J. Lee, H. Jun, J. Kim, *Advanced Materials* **2009**, *21*, 3674.

[2]   a)R. R. Chance, *Macromolecules* **1980**, *13*, 396; b)K. Tashiro, H. Nishimura, M. Kobayashi, *Macromolecules* **1996**, *29*, 8188; c)R. W. Carpick, D. Y. Sasaki, A. R. Burns, *Langmuir* **2000**, *16*, 1270.

[3]   a)D. A. C. Brownson, C. E. Banks, *Analyst* **2011**, *136*, 2084; b)S. H. Chough, A. Mulchandani, P. Mulchandani, W. Chen, J. Wang, K. R. Rogers, *Electroanalysis (N. Y.)* **2002**, *14*, 273.

[4]   R. H. Baughman, R. R. Chance, *Annals of the New York Academy of Sciences* **1978**, *313*, 705.

[5]   K. Takami, J. Mizuno, M. Akai-kasaya, A. Saito, M. Aono, Y. Kuwahara, *The Journal of Physical Chemistry B* **2004**, *108*, 16353.

[6]   F. M. Menger, S. J. Lee, *Journal of the American Chemical Society* **1994**, *116*, 5987.

CHAPTER 10

Conclusion & Outlook

10.1 Conclusion

We have investigated the colorimetric transition and red fluorescence emission properties of polydiacetylene (PDA) supramolecules for selective and sensitive bio/chemosensor applications. We have rationally designed diacetylene molecules and have prepared PDA liposomes having functional groups that exhibit selective interactions with a variety of target molecules. We successfully developed PDA liposome based microarray sensor systems for potassium (K^+) and mercury (Hg^+) ion detection by utilizing the fact that DNA aptamers form a bulky complex upon selective binding with potassium or mercury ions. The external repulsion between these bulky complexes induces red fluorescent emission from the PDA liposome microarray, signaling a positive recognition. With the mercury ion detection system, we advanced the system towards universal application; we synthesized epoxy modified PDA molecules having superior immobilization efficacy and stability compared to the previously developed PDA liposome immobilization methods. We successfully immobilized PDA liposomes onto an amine modified glass substrate and microarryed ssDNA probe molecules for selective and sensitive detection of mercury ions. Red fluorescent emission was generated after incubation with mercury ions, demonstrating a highly versatile, sensitive and selective self-signaling sensor system.

The initial studies proved that we are able to utilize the optical chromism property of PDA liposomes as a sensor signal. Although we successfully developed a conventional-microarray sensor system, the fluorescence-based detection system requires lab scale analysis equipment and professional training on the usage of the equipment to avoid misinterpretation of sensory signals. Thus, we moved our focus to develop a colorimetric sensor system requiring no additional analysis device. Previously, we found that the detection limit of the mercury sensor was much better than that of the potassium sensor. In that system, an additional interaction between liposomes induced aggregation leading to the higher sensitivity. We believed that the extra inter liposomal aggregation might induce stronger distortion of PDA conjugated backbones, and as a result produce a solid red phase showing a complete colorimetric transition from blue to red as well as red fluorescence emission. Therefore, we applied the two interactions (intra-repulsion and inter-aggregation) to the development of a more sensitive detection system having an intra/inter molecular hydrogen bonding capability. We modified the PDA molecules with cyanuric acid because cyanuric acids are able to form multiple hydrogen bondings with melamine molecules, causing intra/inter liposomal interactions. As expected, cyanuric acid modified PDA liposomes aggregated with each other through strong inter molecular hydrogen bonding after incubation with melamine molecules. The colorimetric signal from blue to red was strong enough to be observed by naked eyes and also satisfied the world regulation level of 1.5 ppm.

We further developed the convenient and portable PDA sensor to detect nerve agents. To provide specificity, we designed PDA molecules having an oxime unit, which is an antidote to organophosphorous nerve agent gasses. We embedded these PDA

liposomes into cellulose acetate membrane filters for portable usage. The PDA liposome embedded membrane filters selectively and sensitively detected the vapor of nerve agent simulants, further exemplifying the adaptability of the PDA sensor system.

We have developed a variety of sensor systems using PDA molecules, but their application in aqueous sensor systems may have fundamental limits with regards to their dilution and long-term stability. Some PDA liposome solutions show undesired photo polymerization or aggregation after long-term storage in ambient conditions. Also, aqueous PDA liposome based sensor systems are not able to detect small amounts of dilute target molecules because the PDA liposome solution loses its blue intensity as it is diluted by the target solution. Thus, we embedded or encapsulated the PDA liposomes into solid matrices to avoid unwanted aggregation, stabilizing the sensor for long-term storage in ambient conditions. We loaded PDA liposomes into micro sized alginate particles to remove their dilution and stability problems. The PDA-loaded alginate particles showed the same blue intensity, even in a large volume of target solution, and did not exhibit aggregation after a few weeks of storage in ambient conditions. We successfully detected ppb levels of melamine, which is much better than the detection limit of the solution-based analogous. Moreover, by devising multi-phasic alginate particles having multi-component PDAs we demonstrated the multi-targeting capacity.

We expanded the application of PDA liposomes to the development of an efficient immuno-fluorescence labeling system. We synthesized a green fluorescent molecular dye, which undergoes ESIPT, and imbedded the dye molecules into the hydrophobic bilayer of the assembled PDA liposomes. The PDA liposomes having the dye have biotin molecules at the liposome surface and were able to selectively bind to the

avidin patterns on a substrate, producing a dual green/red fluorescent emission. This result represented a promising immune labeling system based on non-toxic and convenient PDA liposomes.

Although various external stimuli have been investigated to trigger the optical property change of PDA liposomes have been applied to develop a selective and sensitive sensor system, not much effort has been directed towards light as an external stimulus. We rationally designed diacetylene molecules having a photo cleavable moiety upon irriadiation with 365 nm UV light. The photo-responsive (PR) diacetylene (DA) molecules were simply spin cast on a glass substrate and polymerized using 254 nm UV light. The desired red color image was selectively and rapidly printed onto the PR-PDA film by means of a photo mask using 365 nm UV light. Alternatively, we generated a latent image on the PR-DA film by using a photomask and 365 nm UV light before photo-polymerization. The latent image was visualized after the photo-polymerization. Because the pre-exposure to 365 nm light induces the cleavage of the photo responsive group and disrupts the self-assembled diacetylene molecules, the pre-exposed area does not undergo photo-polymerization efficiently, producing a transparent image in blue background. This result may lead to a novel application of PDA molecules for latent imaging and secured communication.

In conclusion, we have developed design principles for selective, sensitive and self-signaling PDA based sensors toward a variety of target molecules such as potassium ions, mercury ions, melamine molecules and nerve agents. We have also developed a novel PDA sensor fabrication method by means of multi-phasic polymeric hydrogel particles, which enable selective and sensitive multi target detection beyond the limit of

homogeneous aqueous solution sensor systems. Strategic molecular design of diacetylene molecules by encoding intra/inter molecular hydrogen bonding and molecular recognition and the novel fabrication method based on muti-phasic hydrogel particles have demonstrated further opportunities for ultra sensitive and convenient sensor system development, immunofluorescence labeling, and latent imaging.

10.2 Outlook

Our PDA sensory systems have successfully demonstrated selective and sensitive detection of small molecular targets such as ions (potassium and mercury), organophosphates, and melamine. From these studies, we have provided design principles of intra/inter liposomal interaction for selective and sensitive small molecule detection. We believe that the proposed design principles for PDA molecules are readily applicable to the development of a variety of PDA sensor systems for small molecule detection. As a next generation of PDA sensor system, PDA systems for the detection of biological organisms would be very feasible and attractive for convenient clinical use. Numerous pathogens, bacteria, virus, protein-protein interactions and also tumor and cancer metabolisms have been studied in the interest of improving human health. By modifying the PDA molecules with a variety of well-known biological receptors, we anticipate efficient biological detection systems. To perform this research, systematic investigation of the degree of receptor and target interaction should be preceded. This will provide an answer to whether the recognition event between the biological molecules will produce large enough mechanical stress on the PDA liposome and generate appropriate sensory signal. When a large biomolecular probe is required for specificity,

devising a micro-structure of PDA molecules through various self-assembly protocols is necessary to tether the large biomolecular probe at the surface of the larger PDA structures. Therefore, additional investigation on the micro structural self-assembly of PDA molecules should be conducted to ensure compatibility with the larger receptor molecules.

Although PDA based bio/chemo sensor systems have shown selective and sensitive colorimetric/fluorometric detection of target materials, the detection level is still limited to micro molar concentrations. Recent biological diagnostics research requires femto molar concentration detection levels- especially in cancer tumor detection research. Therefore ultra sensitive detection platforms are required to satisfy these research needs. We recently generated PDA nanofibers showing high conductivity and an ampherometric on-off signal generation upon heating. They showed high conductivity after photo-polymerization but the conductivity completely disappeared after heating. We believe that the conductivity comes from the extended π-conjugated backbone. Based on the promising results, we propose amperometric sensor development using conductive PDA nanofibers. Specific biomolecular receptors can be tethered on the surface of the nanofiber and the probe PDA nanofiber is expected to change conductivity upon binding of even trace amount of target molecules. Systematic investigation on the correlation between the conductivity and molecular assembly should be conducted to achieve consistent and predictable conductivity from the PDA nanofiber for quantitative analysis.